AD-A067 785 ROCKWELL INTERNATIONAL EL SEGUNDO CA LOS ANGELES DIV F/G 11/6
FRACTURE TOUGHNESS IN TITANIUM ALLOYS.(U)
DEC 78 G R KELLER, J C CHESNUTT, F H FROES N00019-76-C-0427
UNCLASSIFIED NA-78-917 NL

1 OF 2
AD
A067 785

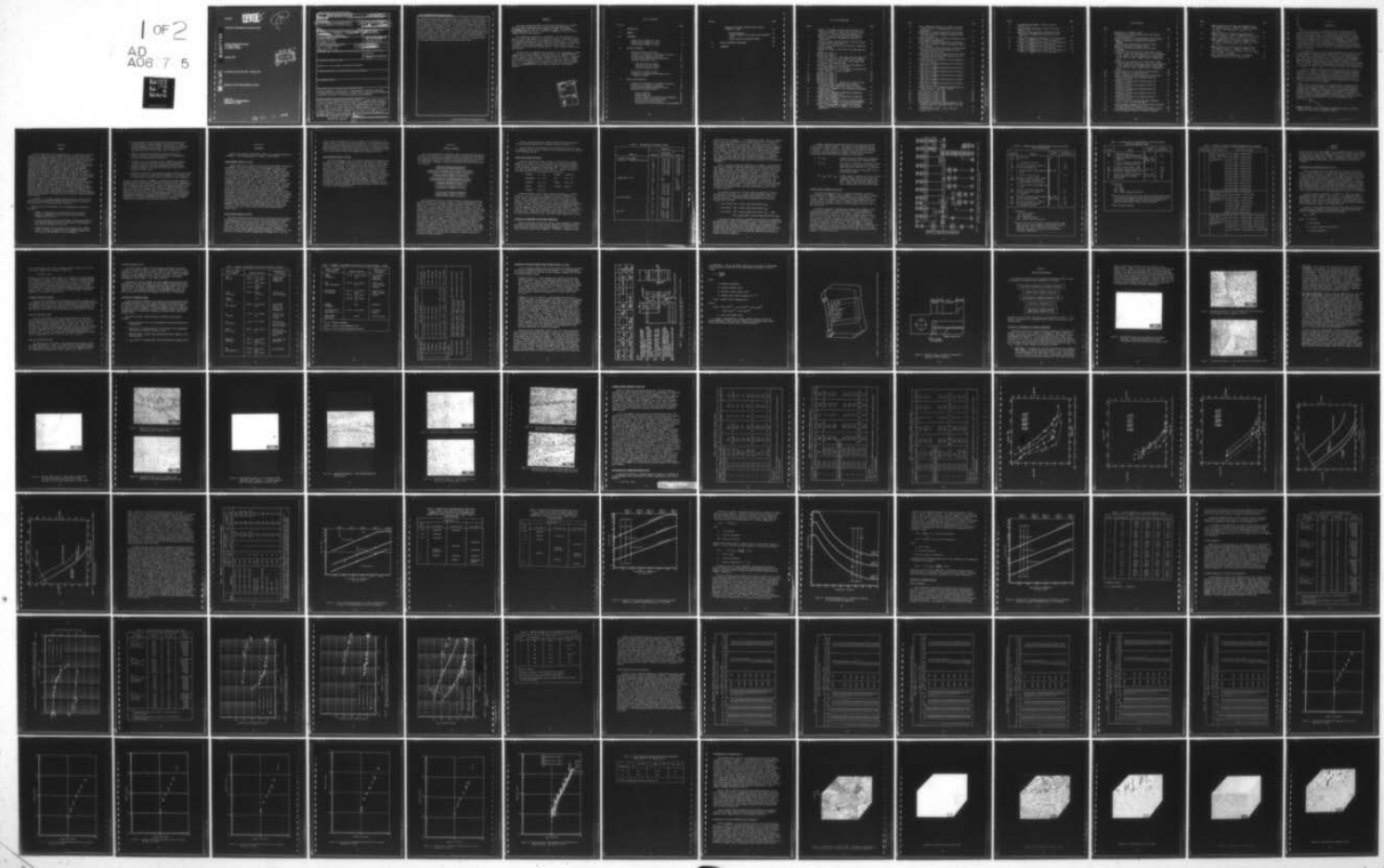

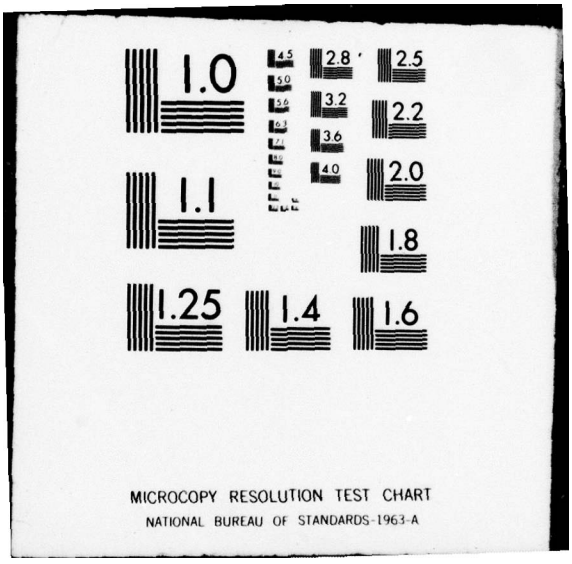
1.0
1.1
1.25
1.4
1.6
1.8
2.0
2.2
2.5
2.8
3.2
3.6
4.0
4.5
5.0
5.6
MICROCOPY RESOLUTION TEST CHART
NATIONAL BUREAU OF STANDARDS-1963-A

NA-78-917

LEVEL II

14

FRACTURE TOUGHNESS IN TITANIUM ALLOYS

Rockwell International Corporation
Los Angeles Division
Los Angeles, CA 90009

December 1978

Final Report for Period May 1976 – December 1978

Approved for public release; distribution unlimited.

Prepared for
NAVAL AIR SYSTEMS COMMAND
Washington, D.C. 20360

SECURITY CLASSIFICATION OF THIS PAGE (When Data Entered)

(14) **REPORT DOCUMENTATION PAGE**

READ INSTRUCTIONS BEFORE COMPLETING FORM

1. REPORT NUMBER: NA-78-917	2. GOVT ACCESSION NO.
3. RECIPIENT'S CATALOG NUMBER	
(6) 4. TITLE (and Subtitle): Fracture Toughness in Titanium Alloys.	(9) 5. TYPE OF REPORT & PERIOD COVERED: Final Engineering Report. 1 May [illegible]76 - 31 Dec[illegible]77,
(10) 6. AUTHOR(s): G. R. Keller, J. C. Chesnutt, F. H. Froes, [illegible], C. G. Rhodes	(15) 8. CONTRACT OR GRANT NUMBER(s): N00019-76-C-0427
9. PERFORMING ORGANIZATION NAME AND ADDRESS: Rockwell International, Los Angeles Division, El Segundo, CA 90245	10. PROGRAM ELEMENT, PROJECT, TASK AREA & WORK UNIT NUMBERS: (12) 118p.
11. CONTROLLING OFFICE NAME AND ADDRESS: Naval Air Systems Command, Code: Air-52031D, Washington, D.C., 20360	(11) 31 Dec[illegible]78
14. MONITORING AGENCY NAME & ADDRESS (if different from Controlling Office)	15. SECURITY CLASS. (of this report): Unclassified
	15a. DECLASSIFICATION/DOWNGRADING SCHEDULE

16. DISTRIBUTION STATEMENT (of this Report)

Approved for Public Release, Distribution Unlimited

17. DISTRIBUTION STATEMENT (of the abstract entered in Block 20, if different from Report)

18. SUPPLEMENTARY NOTES

19. KEY WORDS (Continue on reverse side if necessary and identify by block number)

fracture toughness, titanium alloys, thermomechanical processing, annealing time/temperature versus deformation, strength versus toughness trends, production readiness, correlation of processing/microstructures/properties

20. ABSTRACT (Continue on reverse side if necessary and identify by block number)

This is the final engineering report for a Naval Air Systems Command contract-sponsored program aimed at evaluating CORONA-5 and demonstrating the readiness of this alloy for full-scale production and implementation into aircraft hardware. CORONA-5 is a titanium alloy with a nominal composition, Ti-4.5Al-5Mo-1.5Cr, which developed under three previous NAVAIR contracts to provide a minimum plane strain fracture toughness of 100 ksi√in. (110 MPa√m) at a minimum ultimate strength of 135 ksi (930 MPa). Specific objectives established and

DD FORM 1 JAN 73 1473 EDITION OF 1 NOV 65 IS OBSOLETE

SECURITY CLASSIFICATION OF THIS PAGE (When Data Entered)

410 665

79 04 17 085

accomplished in the current program include (1) a parametric study of thermo-mechanical processing using production-simulating conditions with material from the previous contract, (2) melting of a full-scale production ingot of CORONA-5 with subsequent processing to plate also on production equipment and incorporating results of the parametric study, (3) determination of the strength versus toughness trends of CORONA-5 over the ultimate strength range of 120 to 170 ksi (830 to 1,175 MPa), (4) establishment of the amount of reduction/annealing temperature/annealing time relationship for alpha-beta ~~pro~~cessing and thermal treatment required to achieve contract goal properties, and (5) characterization of production plate and distribution of samples of the material for round-robin testing. In addition, a detailed evaluation was conducted of selected closed die forgings produced during the preceding contractual effort.

FOREWORD

This final engineering report covers the work performed on a titanium alloy development program during the period from 1 May 1976 through 31 December 1977 under NASC Contract N00019-76-C-0427. The program was accomplished under the direction of Mr. W. T. Highberger, Naval Air Systems Command technical project monitor.

This program was conducted as a team effort. The team consisted of a major user of titanium alloys in the aerospace industry, an aerospace research and development organization, and a producer of titanium alloys. The respective organizations involved in this effort were the Los Angeles Division (LAD) of Rockwell International (Rockwell), Rockwell Science Center, and Colt Industries-Crucible Materials Research Center. Overall program responsibility was with LAD.

Program effort was completed under direction of Mr. G. R. Keller, Program Manager and LAD Project Engineer, who replaced Mr. R. G. Berryman in that capacity when the latter accepted a position outside the company. Performance of the program was under the general direction of Mr. W. D. Padian, Manager, Materials and Producibility, and Mr. J. Melill, Supervisor, Materials Application. Mr. J. C. Chesnutt was the Rockwell Science Center Project Engineer, and Dr. F. H. Froes was the Crucible Materials Research Center Project Engineer.

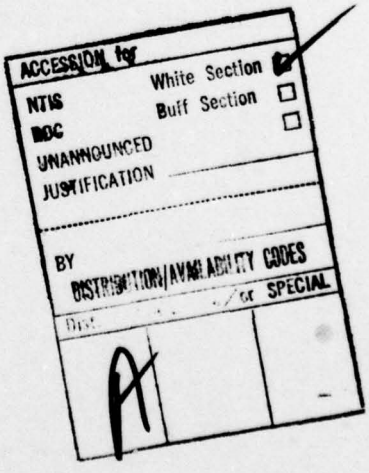

TABLE OF CONTENTS

LIST OF ILLUSTRATIONS

LIST OF TABLES

Section I

INTRODUCTION

Over the past decade, a concentrated effort has been made by both producers and aerospace users of titanium alloys to develop alloys for future aircraft applications. This effort has been motivated to a large extent by the advent of new design criteria and concepts such as fracture mechanics and design-to-cost. Ti-6Al-4V, the workhorse of titanium alloys in aircraft structures, is being pushed to its technological limits to satisfy these criteria and, in some instances, is falling short of meeting imposed requirements. A new titanium alloy, CORONA-5[a], has been developed specifically to meet the needs of aircraft applications designed to fracture mechanics criteria.

Developed over the past 3 years under sponsorship of the Naval Air Systems Command, CORONA-5, having a nominal composition of Ti-4.5Al-5Mo-1.5Cr, has been advanced to a state wherein it is ready for aircraft implementation. The salient feature of this new alloy is its very high fracture toughness at moderately high strength levels. Fracture toughness as high as 140 ksi $\sqrt{in.}$ (155 MPa$\sqrt{m}$) has been developed in this alloy at ultimate tensile strength levels of 140 ksi (965 MPa). These properties represent a two-fold increase in toughness over typical values of RA Ti-6Al-4V at equivalent strength levels.

Interest in CORONA-5 throughout the aerospace industry has resulted in distribution of samples of the alloy to interested parties for independent evaluations. In addition, so that the full potential of CORONA-5 might be realized, efforts are being conducted to establish the optimum strain/time/temperature envelope for alpha-beta processing and annealing, and also to produce the alloy at greater ultimate tensile strength levels on the order of 170 to 180 ksi (1,175 to 1,240 MPa).

This report presents results of a program aimed at demonstrating the feasibility of producing CORONA-5 on a production scale, evaluating its strength versus toughness characteristics over a wide range of producible strength levels, and making it available to investigators other than the developing agencies for their independent evaluation of its properties. In addition, results are presented herein of detailed material characterizations of selected forgings produced under a previous development contract (Reference 3).

[a]CORONA-5 from Colt Industries, Rockwell International, Naval Air Systems Command, and original alloy designation number 5.

Section II

SUMMARY

All basic objectives of the program were met. A 4,800-pound (2,180 kg) production size ingot was melted, conditioned, and forged to slab in preparation for production rolling to plate. A study was conducted at this time to establish the required parameters for final plate rolling to achieve the desired microstructures recognizing the transition from laboratory to production rolling facilities. In addition, a separate effort was conducted to establish strength versus toughness trends associated with CORONA-5. A study was also conducted to establish the amount of strain/annealing-temperature/annealing-time relationship associated with the alloy, which, together with strength versus toughness trends, defined the final heat treatments for be used for the plate produced. On completion of these tasks, approximately 3,500 pounds (1,590 kg) of bloom was rolled to 3-inch (76.2 mm) thick plate using three different thermomechanical processing sequences representing high- and low-temperature beta processing and alpha-beta processing. Samples of each of these plates were identified and transmitted to various agencies requesting material for independent evaluation. In addition, samples of two plates for each of the three processing sequences were heat treated to target strength levels of 130 ksi (900 MPa) and 145 ksi (1000 MPa), respectively. These samples were evaluated to determine the tensile properties, notched and unnotched fatigue behavior, fracture toughness, fatigue crack propagation resistance, and stress corrosion cracking resistance of the material.

In addition, six forgings, produced under the previous contract effort (Reference 3) were evaluated to determine mechanical properties similar to those determined for the production plate described.

From the results of these efforts the following general conclusions were drawn:

1. CORONA-5 is producible as a plate product from a mechanical properties standpoint using production melting and rolling equipment and facilities.

2. A strong relationship exists between amount of alpha-beta reduction and annealing temperature and time, which permits establishment of final thermal treatments for the alloy.

3. Through adjustment of microstructure and strength level, CORONA-5 exhibits an attractive combination of strength and toughness over a UTS range of 130 (900 MPa) to 170 ksi (1175MPa).

4. Through adjustment of microstructure during thermomechanical processing and heat treatment, CORONA-5 plate develops very high fracture toughness, excellent stress corrosion cracking resistance, and high unnotched fatigue strength. Notched fatigue strength is equivalent to Ti-6Al-4V at the same static strength level.

5. CORONA-5 forgings develop mechanical properties and stress corrosion cracking resistance equivalent to or exceeding plate when processed to optimize microstructure.

6. Throughout the alloy development effort, CORONA-5 has displayed excellent response to predicted behavior; good uniformity of mechanical properties; freedom from anomalous behavior during melting, forging, rolling, and evaluation; and relative ease of primary mill fabrication.

7. Based on the data bank of processing and microstructural history established for the alloy in thick sections, CORONA-5 is considered ready for application to selected fracture-controlled aircraft components.

The high fracture toughness of CORONA-5 in combination with other mechanical properties makes it an attractive candidate in fracture critical components for both airframe and engine applications. Plate and forgings look equally attractive. In addition, the alloy has the potential to find applications in the form of bar and rod for fastener stock. The processability of the alloy should also allow fabrication to sheet and coil. In the latter product form, preliminary indications are that judicious manipulation of the microstructure should promote superplastic forming of the material[11]. The high strength condition (up to 200 ksi [1,380 MPa] UTS) also looks attractive, although further data are needed to fully evaluate potential in this area.

Section III

BACKGROUND

Results of the previous contractural efforts are presented in References 1 through 3. The following presents a summary of those efforts:

NAVAIR CONTRACT N00019-73-C-0335

In April 1973, the Los Angeles Aircraft Division of Rockwell International was awarded a contract by the Naval Air Systems Command to conduct basic titanium alloy research and development in an attempt to develop alloys offering greater combinations of strength and fracture toughness than those attainable in alloys commercially available at that time. The primary goal of this effort was to develop an alloy with plane strain fracture toughness, K_{I_C}, in excess of 100 Ksi$\sqrt{in}$. (110 MPa$\sqrt{m}$) at a minimum ultimate tensile strength (UTS) of 135 ksi (930 MPa). A secondary goal of this program was to develop an alloy with moderate K_{I_C} values, on the order of 80 ksi$\sqrt{in}$. (88 MPa$\sqrt{m}$) at high UTS levels, e.g., 170 ksi (1175 MPa) minimum. This effort was conducted in two consecutive phases. During the first phase, 20-pound (9 kg) heats of 22 different alloy compositions were melted, fabricated to plate, and evaluated using tensile tests, Charpy slow-bend toughness determinations, detailed light microstructural analyses, scanning electron fractography, and transmission electron microscopy. From the results of these evaluations, two alloy compositions were selected for scale-up to 500 pound (230 kg) heats, and for detailed study in the second phase. Tests conducted during the second phase were similar to those in the first phase, but also included compact tension fracture toughness and salt-water stress corrosion. The compositions evaluated in this second phase were Ti-4.5Al-5Mo-1.5Cr, (CORONA-5), aimed at achieving the high-toughness/moderate-strength goal, and Ti-8Mo-4.5cr-2.5Al, aimed at achieving the high-strength/moderate-toughness goal.

NAVAIR CONTRACT N00019-74-C-0273

The second contractual effort was aimed at refining the alloy chemistries and processing histories of the two alloys selected for detailed evaluation in the second phase of the prior program. This second program was also conducted in two consecutive phases, and included an additional scale-up in ingot size to 800 pounds (365 kg) of each alloy. At the conclusion of the first phase of this program, the high-toughness/moderate-strength goal properties had been met by CORONA-5, while the properties of Ti8Mo-4.5cr-2.5Al fell short of meeting the high-strength/moderate-toughness goal. For this

reason, further developmental efforts on CORONA-5 were postponed to a subsequent contract, and work during the second phase of the second contractural effort was directed toward improving the properties of TI-8Mo-4.5Cr-2.5Al. Mechanical properties improvements achieved for this alloy during the second phase, however, were limited, and a decision was made to discontinue efforts at this time toward the moderate-toughness/high-strength goal alloy.

NAVAIR CONTRACT N00019-75-C-0208

The third contractual effort was aimed at evaluating the properties and microstructures of CORONA-5 using a relatively wide variety of processing parameters to produce the end configuration: a Pratt Whitney aircraft JT9D jet engine strut forging. This program included an additional scale-up in ingot size to 3,000 pounds (1,360 kg). A total of six different sets of forging parameters and two different final heat treatments were evaluated to identify effects of varying degrees of alpha-beta working on resultant microstructures and attendant mechanical properties. Preliminary evaluations of mechanical properties were made on each of the 12 different forgings to rank each in terms of combined strength and toughness. These evaluations included tensile tests, instrumented slow-bend Charpy toughness tests, metallography, and fractography. Detailed evaluation of forgings selected from the 12 conditions were performed during the current contract (NA 0019-76-C-0427) and are reported herein.

Section IV

TECHNICAL APPROACH

This section describes the production tasks associated with melting and rolling of the program plate, engineering tasks associated with the development of production processing schedules, and final evaluation of the product. The engineering evaluation of previously produced forgings (Reference 3) is also described. A schematic of these tasks presented in order of discussion is as follows:

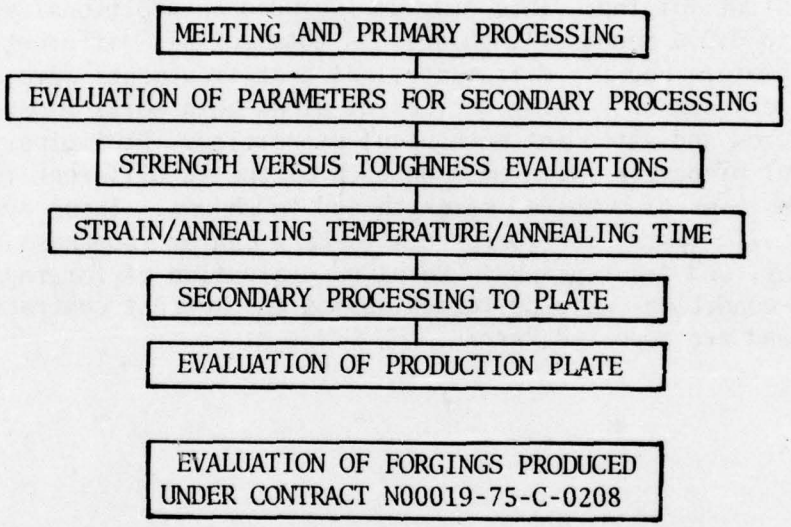

Work performed during this contract consisted of preparing and melting the first production-sized ingot of CORONA-5, weighing approximately 5,000 pounds (2,270 kilograms, followed by ingot reduction to round-corner, square (RCS) bloom. Prior to final processing of the bloom to plate, a detailed production simulating parametric study was conducted to identify any potential problems which might be encountered during actual processing of the full bloom and to understand the effect of production processing and heat treatment on microstructure of the material. Using sample material from the production-sized ingot, a study also was conducted to characterize the strength potential and attendant trends in toughness of CORONA-5. A separate effort was conducted to determine the alpha-beta processing reduction/annealing temperature/annealing time envelope for CORONA-5 and similar compositions based on strength and toughness properties. Following the parametric study, the full bloom was sectioned into three segments and each was final processed through a different thermomechanical processing (TMP) sequence to plate. Plate stock representing these TMP sequences were evaluated to establish the effect of processing schedule on microstructure, mechanical properties, and stress corrosion cracking resistance.

Finally, detailed mechanical property characterizations were made on selected forgings produced under a previous contract (Reference 3).

Specific details of the approach and work conducted within each task are presented in this section. Results of test and evaluations are presented in the following section.

MELTING AND PRIMARY PROCESSING

Using the raw materials shown in Table 1, briquettes were blended, compacted, and welded into an electrode which was then double consumable melted into a 29-inch (0.78 meter) diameter ingot weighing 4,800 pounds (2,180 kilograms), designated, Crucible Heat R52071. The beta transus of this ingot was determined to be 1,720° F(940° C). Chemical analyses of this heat resulted in the following nominal composition:

Aluminum	4.4 w/o	Hydrogen	0.0018 w/o
Molybdenum	5.1 w/o	Iron	0.20 w/o
Chromium	1.46 w/o	Carbon	0.065 w/o
Oxygen	0.183 w.o	Titanium	balance
Nitrogen	0.011 w/o		

Primary processing of this ingot consisted of soaking in a 1,950° F (1,065° C), T_B + 230° F (130° C), furnace for 6 hours, followed by a 30 percent upset and square-up operation to a 29.5-inch (0.75 m), (RCS) bloom. After minimum reheat at 1,950° F (1,065° C), the bloom was then forged to 22 by 32-inches by length (0.56 by 0.81 m by length), followed by reheat to 1,950° F (1,065° C), and final square-up and drawout operations to 13-3/4 by 23-3/4-inch by length (0.35 by 0.60 m by length) slab. The finishing temperature after this conversion was 1,500° F (815° C), T_B-220° F (120° C). The slab was then flattened on a plate placed on the bottom die of the forge press. Dimensions of the slab after cooling were 13- by 23- by 93-inches (0.33 by 0.58 by 2.36 m). The slab was then conditioned all over.

EVALUATION OF PARAMETERS FOR SECONDARY PROCESSING

Results of previous contractural efforts in the development of CORONA-5, particularly those obtained under contract N00019-75-C-0208 (Reference 3) have shown that a lenticular primary alpha morphology is necessary in this alloy to provide high-fracture toughness. In contrast, a globular primary

TABLE 1. RAW MATERIALS FOR CORONA-5 INGOT

Material	Chemistry		
	Element	Purchasing specification	Actual
Ti sponge, Mg reduced (hardness = 140 BHN/1,500 kg, max)	O	0.12 max	0.089
	C	0.03 max	0.007
	Fe	0.20 max	0.15
	Mg	0.10 max	0.029
	Mn	0.10 max	0.010
	Si	0.05 max	0.010
	N	0.025 max	0.002
	H	0.005 max	0.003
	Cl	0.15 max	0.055
Al-Mo master alloy	Al	42.0	42.2
	Mo	54.0	53.9
	Ti	---	3.69
	O	0.15 max	0.04
	N	0.010 max	0.005
	C	0.15 max	0.038
	Fe	0.50 max	0.19
	Si	0.50 max	
	Mg	0.20 max	
Cr, electrolytic	Cr	99.0 min	
	N	0.015 max	
	O	0.10 max	
	C	0.10 max	
	Fe	0.50 max	
	Si	0.20 max	
Al, shot	Al	99.0 min	
	Fe	0.40 max	
	O	0.10 max	
	S	0.25 max	

alpha results in low toughness. An interpretation of these results is offered by Hirth and Froes (Reference 4) in a separate publication. The lenticular primary alpha morphology is relatively easy to produce in small billet or plate segments under laboratory conditions. When processing large, production sized billets and plates in production facilities, however, several problems are introduced. In particular, longer furnace heating times are required to insure uniform slab heating - a major factor in avoiding curling during plate rolling. In addition, the thicker or more massive sections involved will cool much more slowly than the smaller specimens processed in a laboratory. These longer heating times and slower cooling rates promote equiaxing or spheroidization of the primary alpha, and can be detrimental to the properties of CORONA-5.

Thus, to achieve the desired microstructure in CORONA-5 using production facilities, a parametric study was required prior to final processing of the slab segments to plate. This study was carried out by forging 1-inch (25 mm) cubes of material from the preceding contract effort on a 150-ton (135 Mg) press using a strain rate of ~1 inch/sec (25 mm/sec). Forging was used rather than rolling since this deformation mode was more efficient both in material usage and time, while adequately simulating deformation by rolling. Cooling rates were retarded by placing forged cubes in vermiculite. The predominant metallographic criterion for acceptable or unacceptable TMP sequence was the shape of the primary alpha phase: lenticular being acceptable and globular being unacceptable. A second concern was to avoid formation of continuous grain boundary alpha since this could adversely affect stress corrosion resistance.

The starting microstructure for this study was equivalent to that of the slab prior to rolling, i.e., all-beta, which inherently removes from consideration any microstructural complications which might arise from previous processing. Starting with this microstructure, the following sequences were evaluated:

1. Beta annealed (βA) + primary alpha precipitation ($P_{p\alpha}$)
2. Beta worked (βW) + primary alpha precipitation ($P_{p\alpha}$)
3. Beta worked (βW) + primary alpha precipitation ($P_{p\alpha}$) + alpha-beta worked ($\alpha/\beta W$) + primary alpha precipitation ($P_{p\alpha}$)

In addition to these sequences, specimens were evaluated at intermediate processing stages so that the development of each microstructural feature could be identified as a function of processing sequence. Those microstructural features monitored throughout this study included both intergranular and transgranular alpha phase dispersion and shape, and beta grain size and shape. Primary attention was given to the transgranular alpha phase in that all previous work had indicated this to be the most influential microstructural feature on fracture toughness.

A schematic showing the processing received by each specimen involved in this study is shown in Figure 1. The purpose of investigating each set of speciments is shown in Table 2. The results of this study are presented in section V. In that those results significantly influenced the selection of secondary processing parameters, however, a summary of microstructural features for each of the three basic conditions is presented.

1. $\beta A + P_{p\alpha}$: Contains very long, needle-like transgranular alpha and continuous grain boundary alpha.

2. $\beta W + P_{p\alpha}$: Also contains lenticular, transgranular primary alpha which is discontinuous and shorter in length than that formed in $\beta A + P_{p\alpha}$ condition. Grain boundary alpha is also present, but in a semicontinuous manner.

3. $\beta W + P_{p\alpha} + \alpha/\beta W + P_{p\alpha}$: Produces range of microstructure from lenticular to equiaxed alpha; however, short-time, low-temperature anneals provide acceptable structures. Longer times and higher temperatures tend to reduce aspect ratio of primary alpha.

STRENGTH VERSUS TOUGHNESS EVALUATIONS

Following the foregoing activity, a study was conducted to establish the strength versus toughness trends in CORONA-5 over a wide range of strength levels. A total of 27 different thermomechanical processing/final heat treatment routes were employed on small plate segments produced from current contract material as shown in Table 3. Standard, round-bar tensile tests per ASTM E-8 and instrumented Charpy slow-bend toughness tests were used for this evaluation.

Ancillary to the goal of establishing strength versus toughness trends was the goal of graphically demonstrating the role that thermomechanical processing mode plays in affecting those trends - a premise used in the rationale for the initial phases of this alloy development program in 1973, that is to say, in almost any alloy, by adjusting either chemistry or final heat treatment, increases in toughness can be produced at the expense of strength or vice versa, strength at the expense of toughness and a trend line can be established for the material. True improvement in toughness performance requires an increase in static fracture toughness at equivalent or higher strength levels to maintain structural efficiency. This effect can be seen in the expression relating tensile-yield strength and static-fracture toughness to critical crack size:

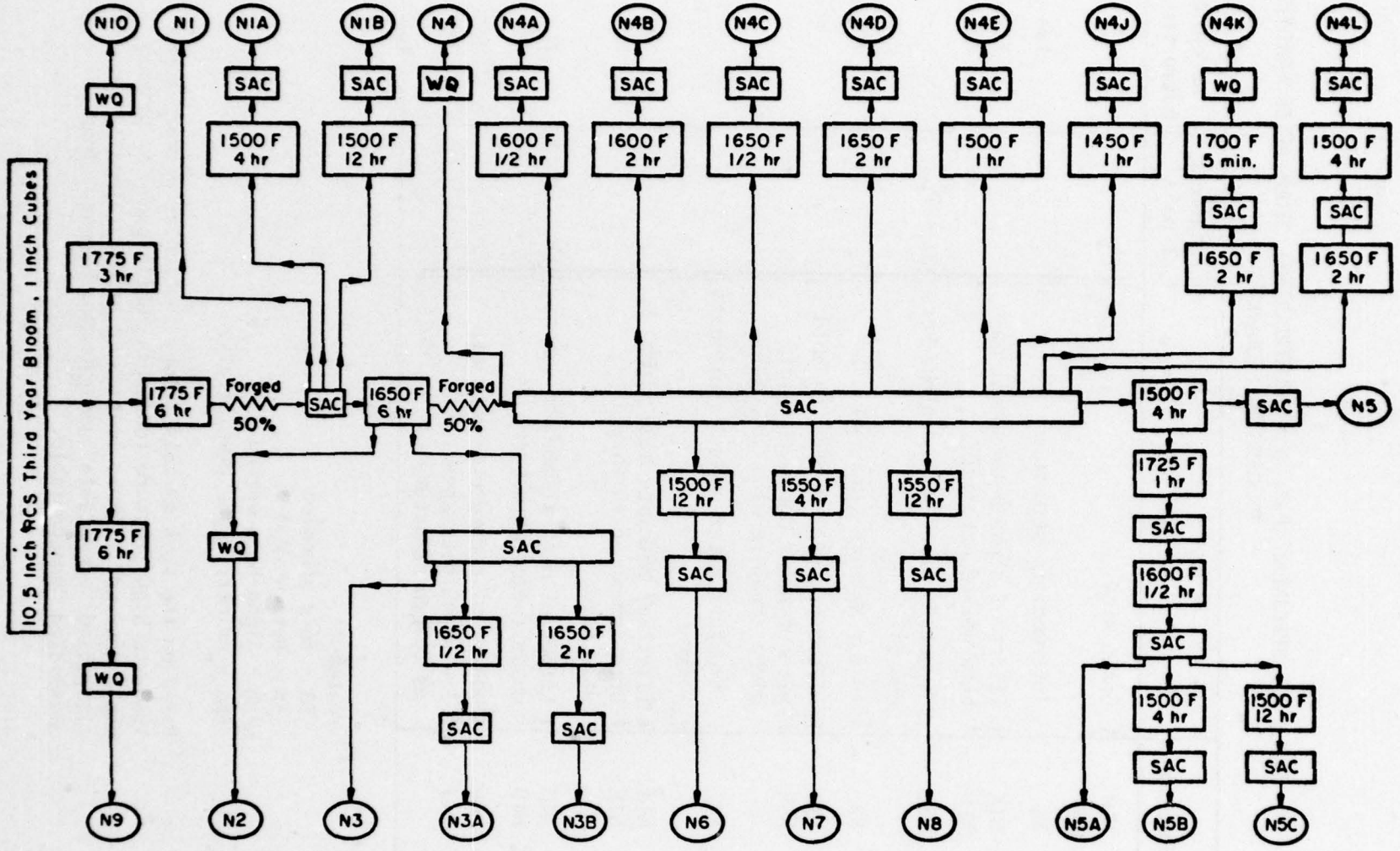

Figure 1. Schematic of specimen processing for microstructural study (beta transus ∿ 1,700° F [925° C]); WQ = water quenched, SAC = slow air cooled (in vermiculite).

TABLE 2. SPECIMENS USED IN MICROSTRUCTURAL STUDY AFTER VARIOUS PROCESSING SEQUENCES

Specimen	Purpose	Treatment Type (1)	Acceptable microstructure (2)
N10	Grain size	βA	-
N9	Grain size	βA	-
N1	Intermediate structure		Yes
N1A	Effect of alpha-beta anneal on beta-worked material		Yes
N1B	Effect of alpha-beta anneal on beta-worked material		Yes
N2	Structure after second alpha-beta anneal	βW + Ppα	-
N3	As for N2 with slow cool		Yes
N3A	Effect of 1650° F (900° C) hold without prior deformation of alpha (compare with N4C, N4D)		-
N3B	Effect of 1650° F (900° C) hold without prior deformation of alpha (compare with N4C, N4D)		-
N4	Structure after second alpha-beta forge		
N4A	Effect of moderate high alpha-beta anneal on as-forged structure		No
N4B	Effect of moderate high alpha-beta anneal on as-forged structure		No
N4C	Effect of high alpha-beta anneal on as-forged structure	βW + Ppα + α/βW + Ppα	No
N4D	Effect of high alpha-beta anneal on as-forged structure	βW + Ppα + α/βW + Ppα	No
N4E	Effect of moderate or moderate-low alpha-beta anneal on as-forged structure		Yes
N4J	Effect of moderate or moderate-low alpha-beta anneal on as-forged structure		Yes

(1) Treatment:
- βA - Beta annealed
- βW - Beta worked
- α/βW - Alpha-beta worked
- Ppα - primary alpha precipitation

(2) Based on the work on this alloy, lenticular primary alpha leads to high fracture toughness, while globular primary alpha does not. Thus, lenticular primary alpha is classified "acceptable" and globular primary alpha is classified "unacceptable."

TABLE 2. SPECIMENS USED IN MICROSTRUCTURAL STUDY AFTER VARIOUS PROCESSING SEQUENCES (CONCL)

Specimen	Purpose	Treatment Type (1)	Acceptable microstructure (2)
N4K	Show grain size N4D		-
N4L	Effect of duplex high-moderate alpha-beta anneals on as-forged structure	$\beta W + P_{p\alpha} + \alpha/\beta W + P_{p\alpha}$	Yes
N5	Effect of moderate alpha-beta anneal on as-forged structure		Yes
N5A	Effect of beta anneal + high-moderate alpha-beta anneal on structure (compare with N2, N3)	$\beta A + Pp\alpha$	Yes[c]
N5B			Yes[c]
N5C			Yes[c]
N6	Effect of moderate-high alpha-beta anneal on as-forged structure	$\beta W + Pp\alpha + \alpha/\beta W + Pp\alpha$	No
N7			No
N8			No

(1) Treatment:
- βA - Beta
- βW - Beta
- $\alpha/\beta W$ - Alpha-
- $Pp\alpha$ - Primary alpha precipitation

(2) Based on prior work on this alloy, lenticular primary alpha leads to high fracture toughness, while globular primary alpha does not. thus, lenticular primary alpha is classified "acceptable" and globular primary alpha is classified "unacceptable."

(3) Beta annealed structure.

TABLE 3. PROCESSING HISTORY OF STRENGTH/TOUGHNESS TREND SPECIMENS

Condition	Finish rolling	Final heat treatment
A	Beta rolled from 1,800° F starting at 2 in. and reducing to 1/2 in.	1,675/1 hr/WQ + 1,350/4 hr/AC
B		1,675/1 hr/WQ + 1,100/8 Hr/AC
C		1,675/1 hr/AC + 1,100/8 hr/AC
D		1,675/1 hr/WQ + 1,100/8 hr/AC
E		1,625/2 hr/WQ + 1,350/4 hr/AC
F		1,625/2 hr/WQ + 1,100/8 hr/AC
F*		1,625/2 hr/AC + 1,100/8 hr/AC
G		1,550/4 hr/WQ + 1,350/4 hr/AC
H		1,550/4 hr/WQ + 1,100/8 hr/AC
H*		1,550/4 hr/AC + 1,100/8 hr/AC
I		1,550/4 hr/WQ + 950/24 hr/AC
J		1,475/4 hr/WQ + 1,100/8 hr/AC
K		1,475/4 hr/WQ + 950/24 hr/AC
L	Alpha-beta rolled from 1,600° F after 1/2 hr soak starting at 2 in. and reducing to 3/4 in.	1,625/1 hr/WQ + 1,250/6 hr/AC
M		1,625/0.25 hr/WQ + 1,250/6 hr/AC
N		1,550/24 hr/WQ + 1,250/6 hr/AC
O		1,550/2 hr/WQ + 1,250/6 hr/AC
P		1,550/0.5 hr/WQ + 1,250/6 hr/AC
Q		1,475/48 hr/WQ + 950/24 hr/AC
R		1,475/4 hr/WQ + 950/24 hr/AC
S		Direct age at 1,100/8 hr/AC
T	Alpha-beta rolled from 1,600° F after 1/2 hr soak starting at 2 in. and reducing to 1/2 in.	1,675/1 hr/AC + 1,550/4 hr/WQ + 1,350/4 hr/AC
U		1,675/1 hr/AC + 1,550/4 hr/WQ + 1,100/8 hr/AC
V		1,675/1 hr/AC + 1,550/4 hr/WQ + 950/24 hr/AC
W		1,675/1 hr/AC + 1,475/4 hr/WQ + 950/24 hr/AC
X		1,600/4 hr/AC + 1,475/12 hr/WQ + 950/24 hr/AC
Y		1,750/1.5 hr/AC + 1,550/4 hr/WQ + 1,100/8 hr/AC

$$a_c \propto \left(\frac{K_{I_C}}{TYS}\right)^2$$

Hence, the object of a high-toughness alloy development program is to maintain or improve the critical crack length at equivalent or greater strength levels by shifting the strength versus toughness trend curve to higher levels, rather than moving along a single curve. This is accomplished by controlling the interrelationship between chemistry, processing history and final heat treatment.

STRAIN/ANNEALING TEMPERATURE/ANNEALING TIME

These interrelationships were established for a family of Ti-Mo-Cr-Al alloys including CORONA-5 in a companion study conducted during this phase of the program. Achievement of high-fracture toughness in this alloy system is highly dependent on development of an alpha phase morphology consisting of essentially primary alpha particles having a lenticular shape. If, for a given amount of deformation, the annealing time at temperature is excessive, the alpha particle phase will be globular and will tend to form a continuous grain boundary network. As has been shown for CORONA-5 (References 1 and 3), both these conditions will have an adverse effect on the toughness of the alloy. Annealing temperatures and times insufficient to cause recrystallization and produce the lenticular alpha morphology also result in low toughness.

The proper annealing temperature for CORONA-5 is within the range of approximately 1,400 to 1,600° F (760 to 870° C). For temperatures below approximately 1,400° F (760° C), times required to effect the required structural change are too long and, hence, impractical. For temperatures above approximately 1,600° F (870° C), globular alpha is produced almost immediately with any substantial amount of prior alpha-beta work.

A number of investigations and publications have shown that diffusion, tempering, creep and rupture, recrystallization, and grain growth (References 5-10) phenomena follow the rate process equation:

$$\text{Rate} = Ae^{-Q/RT}$$

where A = constant

R = gas constant

Q = activation energy for the process

T = absolute temperature

For a fixed property value, such as strength, hardness, grain size, etc, the rate process equation can be reduced to the form:

$$C = Q/2.3RT - \log t$$

Therefore, a plot of lot t (time) versus 1/T (° Rankine) for a given property value should be a straight line. Applying this equation to mechanical properties obtained on a family of Ti-Mo-Cr-Al alloys, a series of curves defining the annealing temperature-time relationship for deformations in the range of 10 to approximately 70 percent have been developed. These curves enable determination of the proper time required for annealing within the temperature range of 1,400 to 1,600° F (760 to 870° C) to achieve optimum strength and toughness for a given hot-working history.

SECONDARY PROCESSING TO PLATE

From the results obtained in the aforementioned studies, secondary processing schedules were selected and a total of approximately 3,500 pounds (1,590 kg) of bloom was converted to 3-inch (0.076 m) thick plates, through three different sequences. The sequences are identified as (1) alpha-beta processed, (2) high beta processed, and (3) low beta processed and are described as follows.

ALPHA BETA PROCESSED (α/β)

A 40-inch (1 m) length of billet weighing approximately 1,950 pounds (885 kg) was soaked for 5 hours at 1,800° F (980° C), T_B + 80° F (45° C) then rolled through an eight pass schedule from 14- (0.36 m) to 6-inch (0.15 m) thickness in 2 minutes, finishing at 1,600° F (880° C), T_B - 120° F (65° C). This plate was then cut in half and plate ends were used for trend line studies. One plate half, approximately 870 pounds (396 kg) was then soaked for 2 hours at 1,625° F (885° C), T_B - 95° F (55° C), and rolled through a nine-pass schedule from 6- (0.15 m) to 3-inch (0.076 m) thickness, finishing at a temperature of approximately 1,400° F (760° C), T_B - 320° F (175° C).

HIGH BETA PROCESSED (HIGH β)

The remaining half of the plate, also approximately 870 pounds (395 kg), was soaked for 2 hours at 1,800° F, T_B + 80° F (45° C), and rolled through a four-pass schedule from 6- (0.15 m) to 3-inch (0.076 m) thickness, finishing at a temperature of approximately 1,580° F (860° C), T_B - 140° F (75° C).

LOW BETA PROCESSED (LOW β)

A 15-inch (0.38 m) length of billet weighing approximately 825 pounds (375 kg) was soaked for 4 hours at 1,800° F (980° C) T_B + 80° F (45° C), then forged to 6- by 23- by 40-inch (0.15 by 0.58 by 1 m) slab suitable for rolling. This slab was then soaked at 1,750° F (955° C), T_B + 30° F (15° C) and rolled through a six-pass schedule to 3-inch (0.076 m) thickness, finishing at approximately 1,500° F (815° C), T_B - 220° F (120° C).

Subsequent to final processing, each plate segment was sectioned in sizes appropriate to meet the requirements of various agencies requesting material for independent evaluations. Recommendations were made, however, for specific thermal cycles to be used in obtaining the desired conditions. Table 4 presents a list of the companies involved in the independent evaluation, the quantity and condition of material shipped, and the tests to be performed.

EVALUATION OF PRODUCTION PLATES

To provide baseline information for comparison with data generated during independent evaluations, one plate segment from each of the three basic process conditions, described in the paragraph "Secondary Processing to Plate," was held for in-house evaluation. These plate segments were cut in half, and each half was given a different final heat treatment to produce two different strength levels. The actual heat treatments given these plate sections are shown in Table 5.

The material property characterizations performed on these plates included:

1. Duplicate tensile tests in the longitudinal and transverse directions of each plate.

2. Smooth (K_t = 1.0) and notched (K_t = 3.0) fatigue in the longitudinal and transverse directions of plates D and F.

3. Combined FCP/K_{Ic} (fatigue-crack-propagation/fracture toughness) tests from each plate.

4. K_{Iscc} tests in 3.5-percent NaCl in the RW direction of plates B and E.

TABLE 4. SUMMARY OF INDEPENDENT EVALUATIONS TO BE MADE ON CORONA-5

Agency or company and location	Quantity and form	Properties to be determined
AFML (Dayton)	340 lb - 6-in. slab 100 lb - 3-in. plate, high β 100 lb - 3-in. plate, α/β 20 lb - 0.063-in. sheet	Tensile, K_{Ic}[1] da/dn,[2] and formability
Alcoa (Cleveland)	200 lb - Bloom (F-15 VFS)	Tensile, K_{Ic}, and S/N fatigue
Boeing (Seattle)	low β	
GD (Fort Worth)	200 lb - 3-in. plate, low β	Air and NaCl da/dn, S/N fatigue, and weldability
GE (Evendale)	60 lb - 3-in. plate, α/β	Tensile, K_{Ic}, and low-cycle fatigue
LLL (Livermore)	40 lb - 3-in. plate	Tensile, K_{Ic}, K_{Iscc},[3] erosion, and S/N fatigue
MACAIR (St. Louis)	100 lb - 3-in. plate, α/β	Tensile, K_{Ic}, S/N fatigue, and air and NaCl da/dn
Northrop (Hawthorne)	120 lb - 3-in. plate, high β 120 lb - 3-in. plate, α/β	K_{Ic}, da/dn, and formability
NRL (Washington D.C.)	100 lb - 3-in. plate, high β 100 lb - 3-in. plate, α/β	K_{Ic} and da/dn

TABLE 4. SUMMARY OF INDEPENDENT EVALUATIONS TO BE MADE ON CORONA-5 (CONCL)

Agency or company and location	Quantity and form	Properties to be determined
NSRDC (Annapolis)	50 lb - 1/2-in. plate, low β	Air and NaCl da/dn and weldability
PWA (West Palm Beach)	100 lb - 3-in. plate, low β	Tensile, K_{Ic}, da/dn, and S/N fatigue
Rockwell/LAD (El Segundo)	100 lb - 3-in. plate, high β 100 lb - 3-in. plate, low β 100 lb - 3-in. plate, α/β	Tensile, K_{Ic}, da/dn, and S/N fatigue
Grumman (Bethpage)	low β	Weldability
G.W. University (Washington, D.C.)	50 lb - 3-in. plate	Corrosion fatigue
WYMAN-GORDON (Worcester)	Billet	Tensile and K_{Ic}

(1) K_{Ic} = fracture toughness
(2) da/dn = fatigue crack propagation rate
(3) K_{Iscc} = stress corrosion cracking resistance

TABLE 5. FINAL HEAT-TREAT PARAMETERS FOR PRODUCTION PLATE

Plate	Process Mode[1]	Final Heat Treatment[2]	Goal UTS Level
A	High beta	1,525° F/4 hr/AC + 1,300° F/6 hr/AC	130 ksi (900 MPa)
B	High beta	1,525° F/4 hr/AC + 1,050° F/8 hr/AC	145 ksi (1,000 MPa)
C	Low beta	1,525° F/4 hr/AC + 1,300° F/6 hr/AC	130 ksi (900 MPa)
D	Low beta	1,525° F/4 hr/AC + 1,050° F/8 hr/AC	145 ksi (1,000 MPa)
E	Alpha beta	1,685° F/1/2 hr/AC + 1,525° F/4 hr/AC + 1,300° F/6 hr/AC	130 ksi (900 MPa)
F	Alpha beta	1,685° F/1/2 hr/AC + 1,525° F/4 hr/AC + 1,050° F/8 hr/AC	145 ksi (1,000 MPa)

[1] Process modes:

High-beta process: Roll billet from 1,800° F (980° C) to 6-in. plate thickness; roll plate from 1,800° F (980° C) to 3-in. finish thickness

Low-beta process: Forge billet from 1,800° F (980° C) to 6-in. slab thickness; roll slab from 1,750° F (955° C) to 3-in. finish thickness

Alpha-beta process: Roll billet from 1,800° F (980° C) to 6-in. plate thickness; roll plate from 1,625° F (885° C) to 3-in. finish thickness

[2] T_B = 1,720° F (940° C)

EVALUATION OF FORGINGS PRODUCED UNDER CONTRACT N00019-75-C-0208

Six of 12 forgings produced under contract N00019-75-C-0208 were selected for detailed evaluation during the current program. The following presents the rationale used in the selection of these forgings, together with the type of testing performed on each:

Forgings 5-2 and 5-11 - These forgings were selected to evaluate the fatigue properties (S-N) of an all-beta processed forging (5-2) final heat treated to a relatively high-strength condition of 145 ksi (1,000 MPa), UTS, and an alpha-beta processed forging (5-11) final heat treated to a strength level equivalent to typical strength levels of recrystallization annealed (RA) Ti 6Al-4V alloy, i.e., 135 ksi (930 MPa). Two different stress ratios (R factor - 0.1 and 0.5) were evaluated in the latter forging to ascertain the magnitude of R factor shift in the S-N curve.

Forgings 5-1, 5-3, 5-5, and 5-12 - These forgings were selected to evaluate the effect of varying primary alpha aspect ratios on the fatigue crack propagation (FCP) and toughness (K_{Ic}) characteristics of CORONA-5. As shown in Table 3 of Reference 3, by comparing values in the platform portions of each forging, forgings 5-1, 5-3, and 5-5 were processed to an equivalent strength level of approximately 140 ksi (965 MPa), and exhibited slow-bend Charpy toughness values ranging from 142 to 162 ksi $\sqrt{\text{in.}}$ (155 to 180 MPa$\sqrt{\text{m}}$). The variations in primary alpha aspect ratio (see Figures 7, 9, and 11 of Reference 3) were produced by variations in the final forging temperature. Forging 5-1 was finished above the beta transus; 5-3 high in the alpha-beta field; and, 5-5 lower in the alpha-beta field. All three forgings had been blocked above the beta transus. Finally, forging 5-12, which had been alpha-beta blocked and finished low in the alpha-beta field, was characterized by uniform, equiaxed primary alpha, as seen in Figure 18 of Reference 3, and exhibited the least desirable combination of strength and toughness.

Three and one-half percent NaCl solution KI_{SCC} tests were performed on two of the previously described forgings, 5-1 and 5-3, to characterize the stress corrosion resistance of this alloy in the conditions representing the best combinations of strength and toughness. It should be noted that, due to the limited amount of material available in the platform sections of each forging, a special compact tension specimen was designed to allow generation of fatigue crack propagation data during normal precracking operations performed in the preparation of a fracture-toughness specimen. This specimen, shown in Figure 2, uses a modified (shortened) starter notch to provide more material for precracking. In addition, it extends the specimen width to an height/width (H/W) ratio of 0.486, as compared to the ratio of 0.6 specified

DIMENSION	B	W	W'	H	H'	H"	a	a'	L	N	D
Per Invention	$2.5\left(\frac{K_{Ic}}{Y.S.}\right)^2$	2B ± .005W	1.25W ± .01W	---	.486W ± .005W	.275W ±.005W	---	Note ③	Note ③	W/16 Max.	.25W Dia. ±.005W
Per ASTM E399	$2.5\left(\frac{K_{Ic}}{Y.S.}\right)^2$	2B ±.005W	1.25W ± .01W	.6W ±.005W	---	.275W ±.005W	Note ②	---	---	W/16 Max.	.25W Dia. ±.005W

NOTES:

1. Surfaces noted shall be perpendicular and parallel as applicable to within 0.002W TIR.
2. Per ASTM E399-72 a/W = 0.45 to 0.55 including precrack, which shall not be less than 0.05a nor less than 0.05 in.
3. L/W = 0.2 or less and a'/W = 0.3 ± 0.01 at start of FCP test. Also a'/W = 0.50 to 0.55 at conclusion of FCP test
4. The points of intersection of the crack starter tips with two specimen surfaces shall be equally distant from either pin hole center to within 0.005 W.
5. Basic notch geometry per ASTM E399

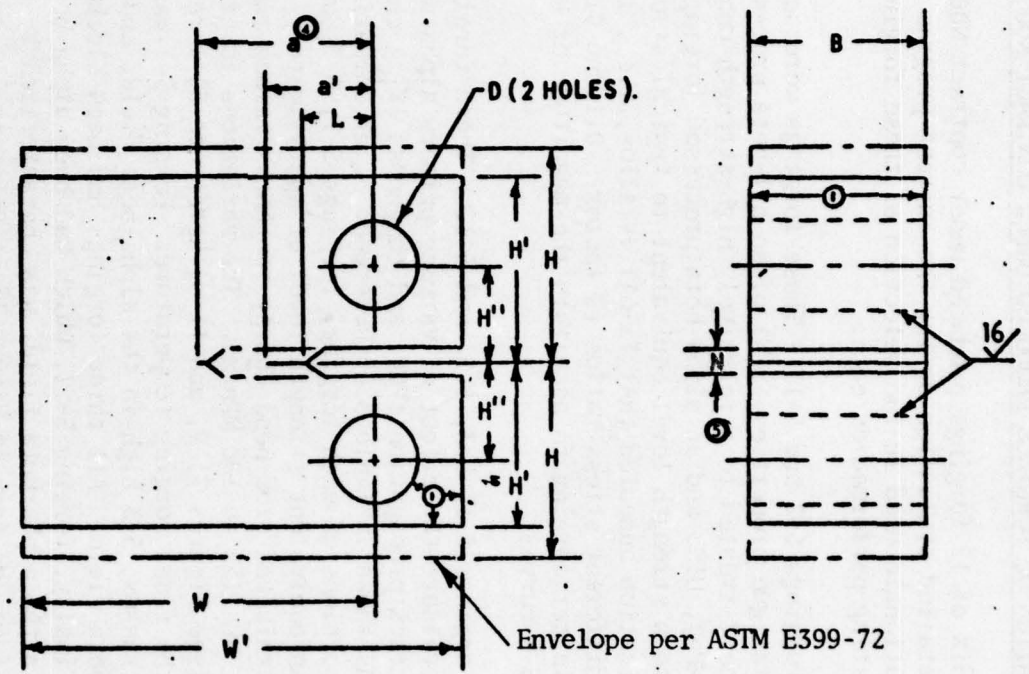

Figure 2. Comparison of compact tension specimen developed for current contract with configuration specified per ASTM E399-72.

per ASTM E399-72. Due to the change in H/W ratio, the formula for determining stress intensity per ASTM E399-72 has been modified (Reference 5) to be as follows:

$$K = \frac{Pf(a/w)}{BW^{1/2}}$$

where

P = maximum load (pounds)

B = specimen thickness (inch)

W = effective specimen length (inch)

K = maximum stress intensity (pounds inch $^{-3/2}$)

f(a/w) = geometry factor (dimensionless),

given by

$$f(a/w) = 30.96\ (a/w)^{1/2} - 195.8\ (a/w)^{3/2} + 730.6\ (a/w)^{5/2} - 1186.5\ (a/w)^{7/2} + 754.6\ (a/w)^{9/2}$$

a = total crack length (inch)

A schematic representation of FCP/K_{Ic} specimen locations within the forging platform is shown in Figure 3, while K_{Iscc} specimen location within the as-tested FCP/K_{Ic} specimen half is shown in Figure 4.

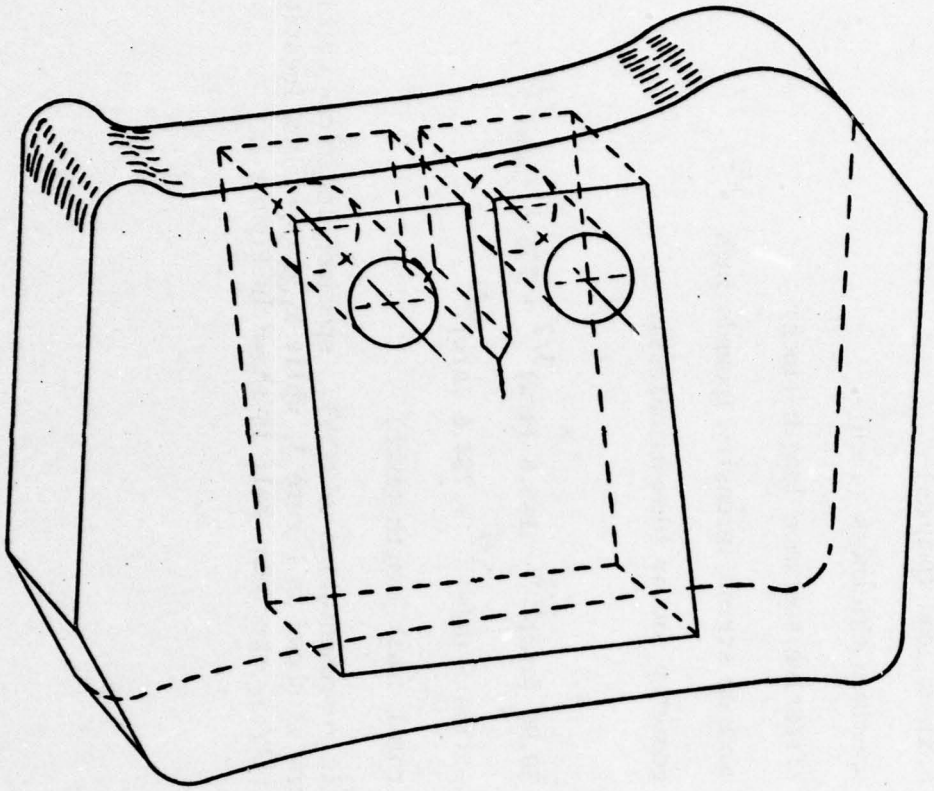

Figure 3. Location of compact tension specimen in typical forging (platform section only shown).

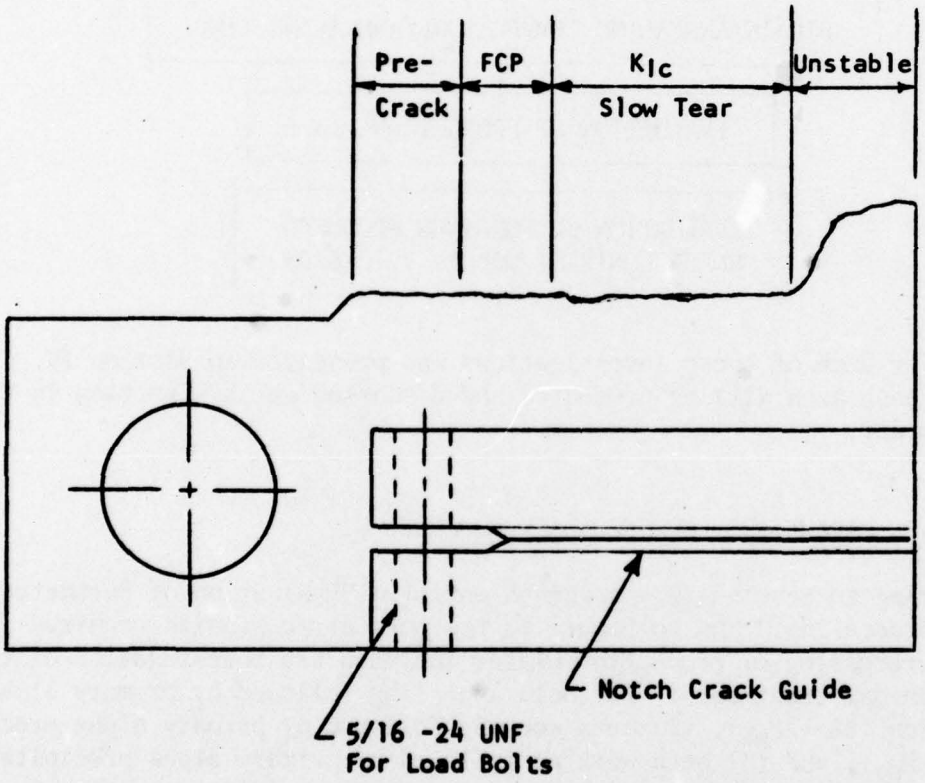

Figure 4. Location of K_{Iscc} specimen in failed half of combination FCP/K_{Ic} specimen.

Section V

RESULTS AND DISCUSSION

The results recorded during this program were generated from five areas of engineering investigation shown schematically as follows:

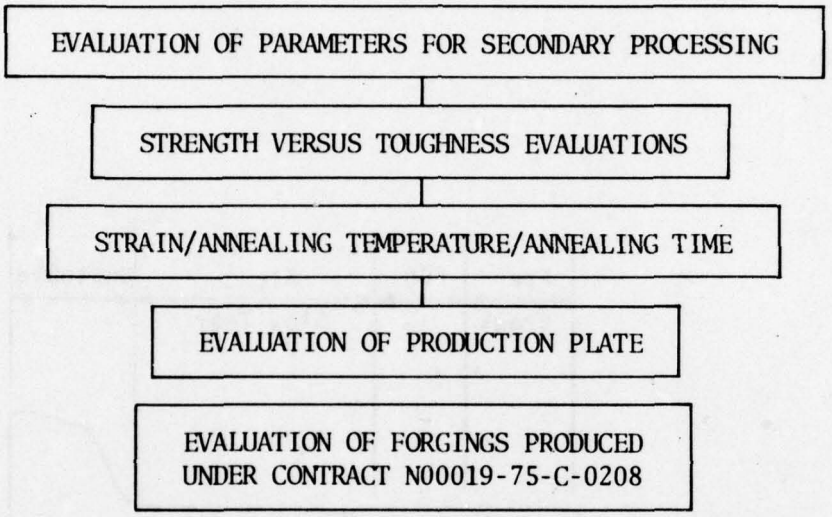

Rationale for each of these investigations was presented in Section IV. Test results in each area will be presented and discussed in this section in the preceding order.

EVALUATION OF PARAMETERS FOR SECONDARY PROCESSING

Referring to Section IV, paragraph entitled "Evaluation of Parameters for Secondary Processing," and to Figure 1, the parametric studies required for secondary processing of production plates included the investigation of three thermomechanical treatments: (1) beta annealing followed by primary alpha precipitation ($\beta A + P_{p\alpha}$), (2) beta working followed by primary alpha precipitation ($\beta W + P_{p\alpha}$), and (3) beta working followed by primary alpha precipitation plus alpha-beta working followed by primary alpha precipitation ($\beta W + P_{p\alpha} + \alpha/\beta W + P_{p\alpha}$). Results of these studies are presented as follows:

1. $\boxed{\beta A + P_{p\alpha}}$: Five samples (N9, N10, N5A, N5B, and N5C) were studied in this category. N9 and N10 were merely samples of the bloom following primary breakdown and beta annealing for 6 and 3 hours, respectively, at 1,775° F (970° C), T_B + 55° F (30° C), followed by a water quench. In that grain growth differences between the 3- and 6-hour hold times

were not significant, the 6-hour cycle was chosen to insure homogenization. Samples N5A, B, and C were evaluated to determine the effects of beta annealing followed by duplex and triplex annealing treatments on primary alpha morphology after a two-step conventional forging process, the first above and the second below the beta transus. These three samples demonstrated typical $\beta A + P_{p\alpha}$ structures with very long, needle-like transgranular alpha and a continuous alpha structure present at the grain boundaries (Figures 5, 6, and 7). Both the transgranular and grain boundary alpha particles tend to thicken with increasing time at subtransus annealing temperatures.

Figure 5. Specimen N5A (Figure 1) beta anneal plus high alpha-beta hold. Note extremely high aspect ratio of transgranular alpha and continuous grain boundary alpha.

Figure 6. Specimen N5B (Figure 1). Note coarsening of both transgranular and intergranular alpha compared to Figure 5.

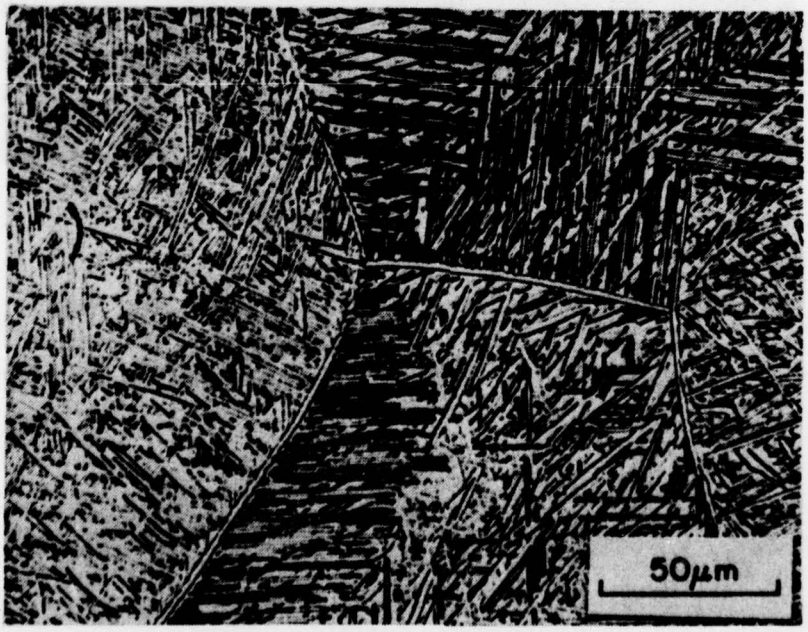

Figure 7. Specimen N5C (Figure 1). Note coarsening of grain boundary alpha.

2. $\boxed{\beta W + P_{p\alpha}}$: Seven specimens (N1, N1A, N1B, N2, N3, N3A, and N3B) were evaluated in this category. All specimens exhibited a lenticular, transgranular primary alpha with semicontinuous primary alpha at the grain boundaries. The lenticular primary alpha formed during this processing mode is substantially different from that formed during $\beta A + P_{p\alpha}$ treatments, where long needles form. In the present case, discontinuous needles form which are much shorter in length. (Compare Figures 8 through 11 with Figures 5 through 7.) Aging for 8 hours at 1,650° F (900° C) does little to change either the lenticular nature of the transgranular primary alpha or the semicontinuous morphology of the grain boundary alpha (Figure 8). This observation is in direct contrast with the observations made in material after the alpha-beta working plus alpha-beta annealing discussed as follows.

3. $\boxed{\beta W + P_{p\alpha} + \alpha/\beta W + P_{p\alpha}}$: Thirteen different samples (N4, N4A, N4B, N4C, N4D, N4E, N4J, N4K, N4L, N5, N6, N7, and N8) were evaluated in this category. Sample N4 shows that the effect of the alpha-beta working on the primary alpha is that of distorting or deforming the primary alpha (compare Figure 12, specimen N4, with Figures 9 and 10, specimens N2 and N3). Specimen N4A through N4J and N5, N6, N7, and N8 illustrate that increasing time and temperature during alpha-beta annealing tends to drive the deformed, lenticular, transgranular alpha toward an undesirable, globular morphology. Only the short-time, low-temperature anneals yield acceptable primary alpha morphologies (e.g., Figures 13 and 14, specimens N4E and N4J). Longer time, high-temperature treatments tend to promote reduction of primary alpha aspect ratios to approximately 1:1 (Figures 15 and 16, specimens (N4C and N4D). The 1,650° F (900° C) 2-hour treatment (Figure 16, specimen N4D) produces an almost spherical primary alpha, in marked contrast to the shape observed without alpha-beta deformation (Figures 8 and 11, specimens N3A and N3B). A similar effect is noted with the grain-boundary alpha, wherein this phase is discontinuous along the grain boundaries.

   As shown in Figure 16 (specimen N4D), alpha-beta working plus annealing high in the alpha-beta field results in "cell" formation between the globular primary alpha particles. Flash annealing above the beta transus (specimen N4K) revealed these "cells" to be subgrains rather than small, recrystallized grains. The structure exhibited by specimen N4D, suggested an alternate heat treatment to produce an acceptable microstructure after $\beta W + P_{p\alpha} + \alpha/\beta W + P_{p\alpha}$, wherein an additional, lower temperature anneal has been added to the treatment (Figure 17, specimen N4L) to produce lenticular primary alpha within the subgrain structure.

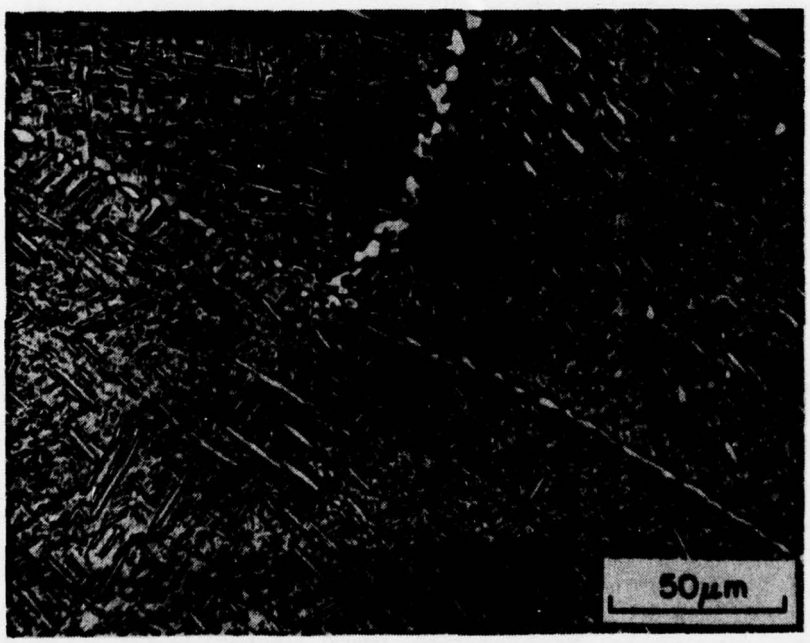

Figure 8. Specimen N3B (Figure 1). Beta forge plus high alpha-beta hold with additional 1650°F (900°C) 2-hour treatment. Note lenticular morphology of primary alpha.

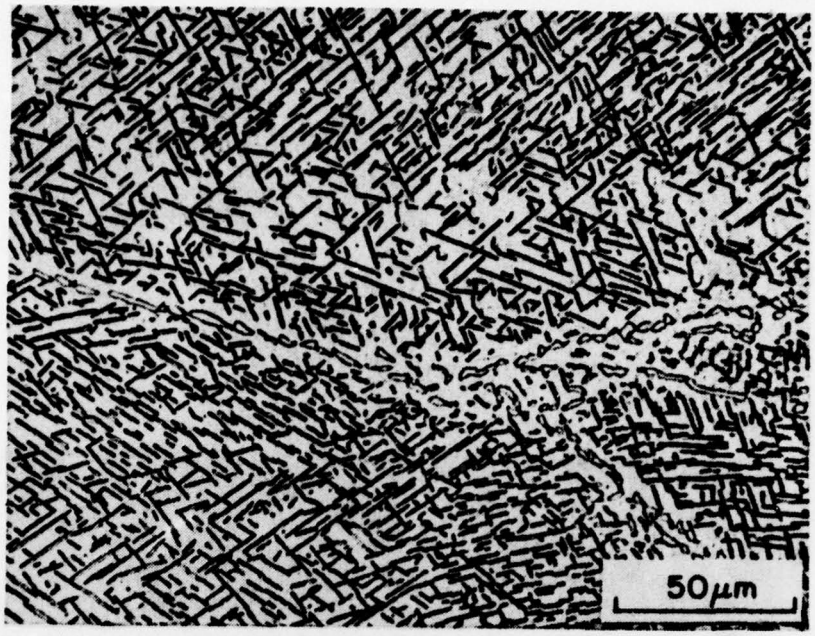

Figure 9. Specimen N2 (Figure 1), lenticular primary alpha, semicontinuous grain boundary alpha.

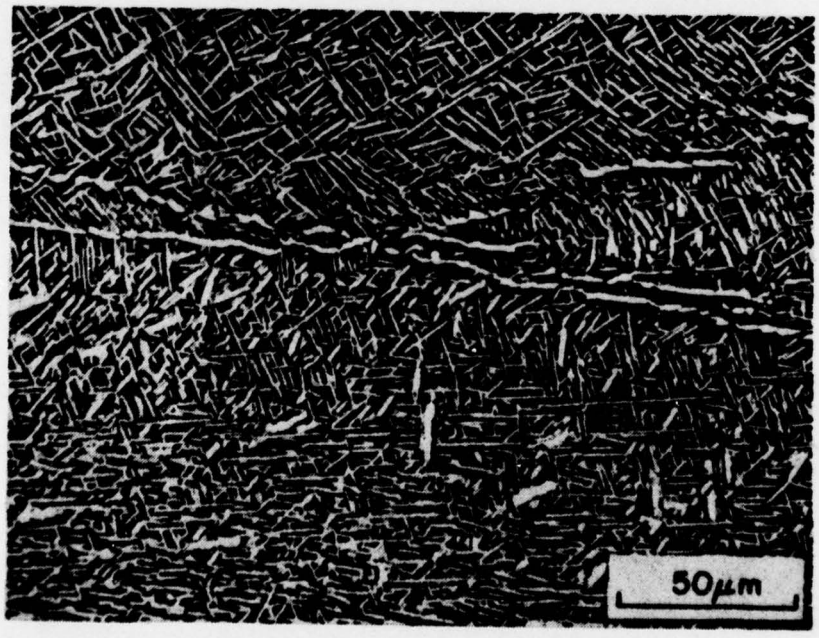

Figure 10. Specimen N3 (Figure 1) as for Figure 9 with addition of fine alpha background from slow cool.

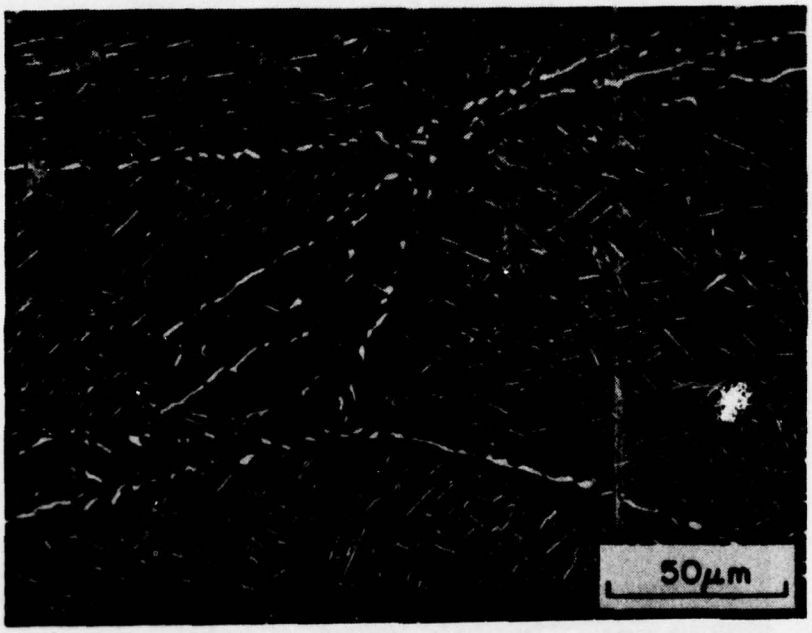

Figure 11. Specimen N3A (Figure 1), as for Figure 10 with additional 1650° F (900° C) - 1/2-hour treatment. Note lenticular morphology of primary alpha.

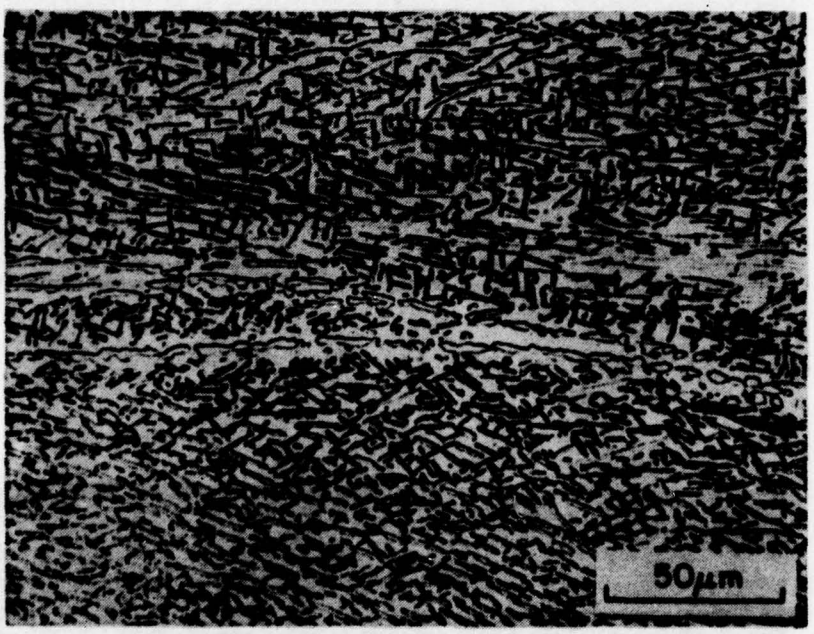

Figure 12. Specimen N4 (Figure 1). Note deformed lenticular primary alpha.

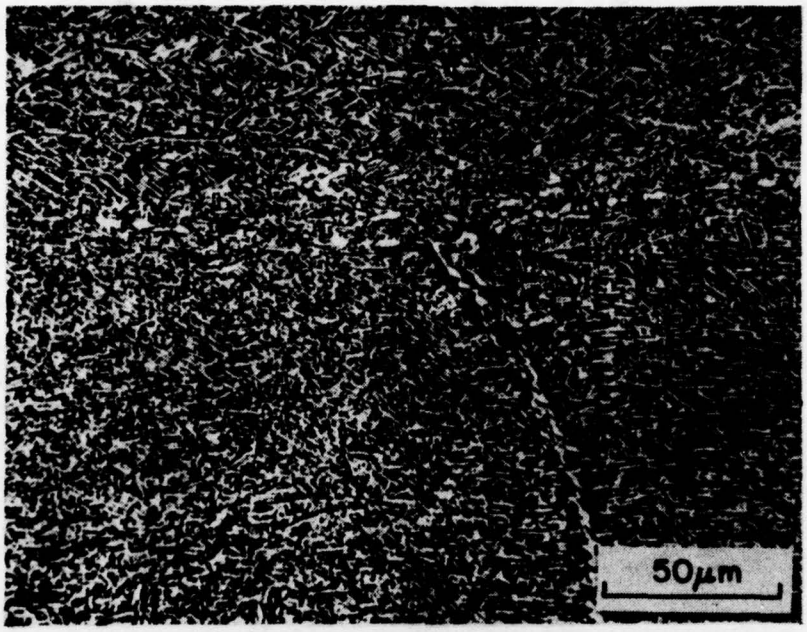

Figure 13. Specimen N4E (Figure 1). Note distorted primary alpha.

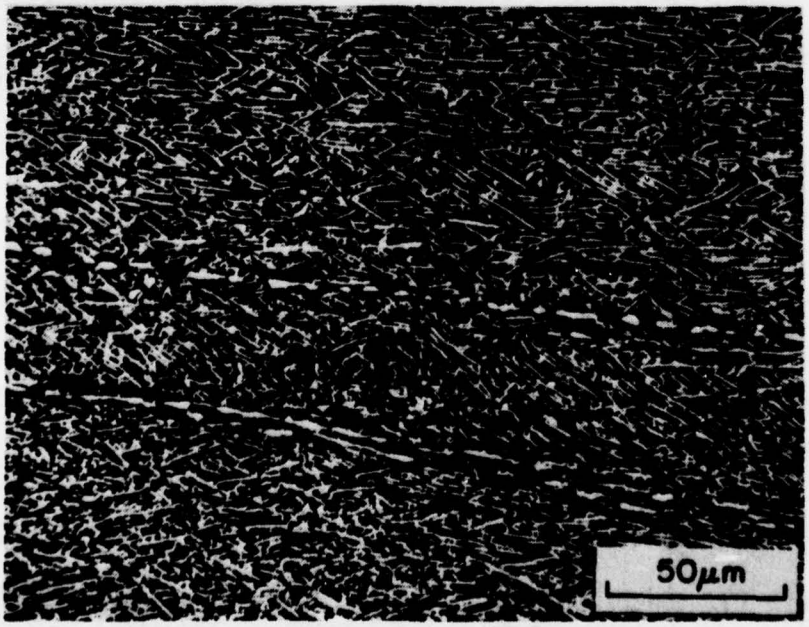

Figure 14. Specimen N4J (Figure 1). Note distorted primary alpha of relatively high aspect ratio.

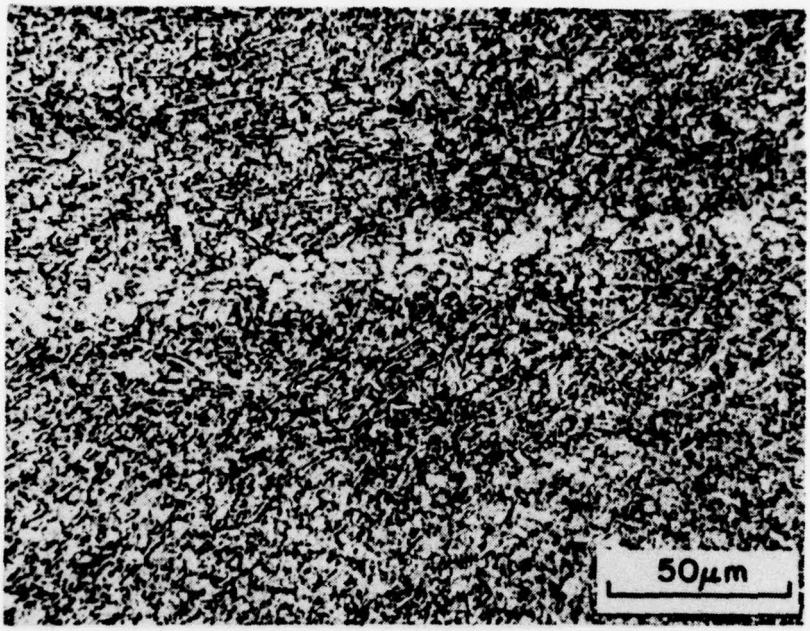

Figure 15. Specimen N4C (Figure 1). Note globular primary alpha compared to preceding figures.

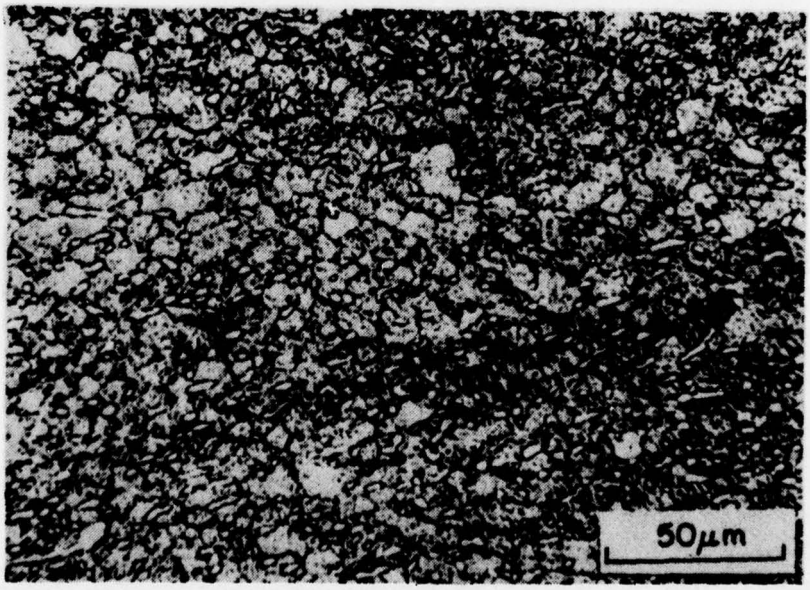

Figure 16. Specimen N4D (Figure 1). Note almost spherical primary alpha and sub grain structure between these particles.

STRENGTH VERSUS TOUGHNESS EVALUATIONS

Results of duplicate instrumented Charpy-type, slow-bend toughness specimens and single standard tensile specimens in longitudinal and transverse testing directions are presented for 27 plate segments in Table 6. Each plate segment was subjected to a different thermomechanical processing/final heat-treatment sequence, as described in Table 3, in order to establish. strength versus toughness trends of CORONA-5 over a wide range of strength levels. Data are presented over the UTS range of 140 to 210 ksi (965 to 1,450 MPa) and are also plotted in Figures 18, 19, and 20 which distinguish the three primary processing modes: beta finished and alpha-beta annealed, alpha-beta finished and alpha-beta annealed, and alpha-beta finished and duplex annealed.

In that the toughness results shown in the aforementioned tables and figures were obtained from instrumented Charpy-type, slow-bend tests, caution must be exercised in drawing conclusions based on absolute magnitudes of these toughness values. These results do, however, provide guidelines wherein qualitative comparisons can be made. For example, a comparison of Figures 18, 19, and 20 indicate a higher level of toughness obtained from beta processed and alpha-beta annealed material than from either of the two processing modes over the entire strength range. These results are summarized in Figures 21 and 22, combining plots of the three processing modes using transverse strength and toughness data only. The higher toughness is associated with processing sequences which, as determined in the earlier work, result in a lenticular alpha-phase morphology and greater resistance to crack propagation in the microstructure. A discontinuous alpha grain-boundary network is also produced which is desirable from the $K_{I_{SCC}}$ standpoint. The uniformity of data evident in the plots suggest good reproducibility of strength/toughness combinations for given microstructural conditions. It is also clear that by adjustment of thermomechanical processing sequences and heat treatment, shifts in the trend lines can be produced as desired. As discussed earlier, to fully exploit higher toughness characteristics of a material a corresponding increase in strength is desirable. As noted in Figures 21 and 22, a baseline is constructed for an alloy exhibiting a K_{I_C} of 70 ksi $\sqrt{in}$ (77 MPa $\sqrt{m}$) at a TYS of 120 ksi (828 MPa) shown as a reference, $K_{I_C} = 0.583$ TYS, which describes the increase in TYS (and corresponding UTS) required to maintain a constant strength/toughness relationship and, hence, a constant critical flaw size. As seen in these figures, the trend line shift necessary to accomplish this is achievable in CORONA-5 by altering processing mode together with subsequent heat treatment.

STRAIN/ANNEALING TEMPERATURE/ANNEALING TIME

As discussed previously, a separate study was conducted to establish the strain/temperature/time relationship for CORONA-5 employing the rate process equation:

$$C = Q/2.3\,RT - \log t$$

TABLE 6. MECHANICAL PROPERTIES OF CORONA-5 PLATE

Condition[1]	Direction[2]	(K_Q (ksi$\sqrt{in}$)	UTS (ksi)	TYS (ksi)	Elong (%)	RA (%)	E (10^6 psi)
Beta finished and alpha-beta annelaed							
A	LT & L	74.4-77.4	152.3	143.7	16	29.9	15.2
	TL & T	73.5-77.5	157.3	147.6	13	23.0	15.6
B	LT & L	31.1-32.8	196.4-206.4	183.4-192.4	6	11.6	16.0-16.6
	TL & T	34.0-39.4	209.4	194.8	3	--	16.7
C	LT & L	52.9-54.4	167.3	148.8	13	29.3	16.4
	TL & T	ND[3]	ND	--	--	--	--
D	LT & L	88.5-91.3	151.3	135.3	18	38.9	16.2
	TL & T	ND	ND	--	--	--	--
E	LT & L	87.1-87.3	146.3	137.1	20	39.5	16.2
	TL & T	79.5-85.7	150.7	143.1	14	22.0	15.5
F	LT & L	37.4-49.7	180.9-185.4	162.3-171.9	10 - 14	16.6-17.4	16.3
	TL & T	38.7-42.0	191.9	174.3	7	7	16.5
F	LT & L	ND	167.8	148.8	12	25.9	16.4
	TL & T	ND	169.8	153.3	12	20.2	17.1
G	LT & L	93.3-97.3	142.3	131.4	18	40.1	14.7
	TL & T	87.6	146.9	138.5	18	33.6	15.9
H	LT & L	52.5-53.5	173.8-175.9	150.3-154.2	10 - 12	17.4-21.6	16.6-17.5
	TL & T	54.5-55.8	175.9	158.1	12	12	16.9

(1) See Table 3.

(2) LT and TL refer to toughness test specimen orientation, L and T to tensile specimen orientation.

(3) ND - no data generated.

TABLE 6. MECHANICAL PROPERTIES OF CORONA-5 PLATE (CONT)

Condition (1)	Direction	K_Q (ksi$\sqrt{in}$)	UTS (ksi)	TYS (ksi)	Elong (%)	RA (%)	E (10^6 psi)
H	LT & L	ND	163.3	145.8	16	23.9	16.3
	TL & T	ND	168.6	153.3	12	16.8	16.9
I	LT & L	36.5-40.0	183.6-184.3	165.7-166.0	8	14.6-14.9	16.7-18.2
	TL & T	39.3-44.0	191.1	165.7	4	8.2	17.9
J	LT & L	55.5-60.6	164.8	147.3	12	26.7	17.2
	TL & T	61.8-66.4	165.8	152.7	10	16.8	16.6
K	LT & L	42.8-44.1	175.9	154.8	10	19.6	16.9
	TL & T	44.6	185.6	162.9	8	9.1	17.2
Alpha-beta finished and alpha-beta annealed							
L	LT & L	57.6-61.4	151.3	147.9	16	51.7	15.5
	TL & T	42.4-46.1	162.1	159.1	16	46.9	16.6
M	LT & L	46.8-55.2	151.8	147.3	16	46.1	16.2
	TL & T	33.5-33.8	163.3	156.9	14	45.5	17.1
N	LT & L	61.9-66.4	145.3	139.2	18	43.1	15.9
	TL & T	51.2-52.4	154.9	149.4	20	45.9	18.0
O	LT & L	49.2-56.7	145.3-146.3	140.7-141.3	18 - 22	41.9-44.9	16.0-16.1
	TL & T	43.2-44.4	153.6-156.0	153.6-156.0	16 - 20	43.1-48.9	17.2-17.3
P	LT & L	54.7-59.9	144.3	141.3	20	43.1	15.2
	TL & T	25.1-30.7	159.5	156.9	18	49.5	17.3

(1) See Table 3.
(2) LT and TL refer to toughness test specimen orientation, L and T to tensile specimen orientation.
(3) ND - no data generated.

TABLE 6. MECHANICAL PROPERTIES OF CORONA-5 PLATE (CONCL)

Condition[1]	Direction	K_Q (ksi$\sqrt{in}$)	UTS (ksi)	TYS (ksi)	Elong (%)	RA (%)	E (10^6 psi)
Q	LT & L	23.0	177.9	156.6	10	18.2	16.4
	TL & T	21.2-22.5	189.4	177.7	14	27.9	15.7
R	LT & L	22.1-23.6	179.4	165.0	10	21.0	16.5
	TL & T	19.5	192.4	184.6	8	18.2	17.6
S	LT & L	54.8	162.8	156.3	14	43.1	15.7
	TL & T	21.8-24.5	ND	--	--	--	--
Alpha-beta finished and duplex annealed							
T	LT & L	64.5-66.2	139.3	132.9	20	43.7	15.2
	TL & T	54.9-75.7	146.5	141.3	20	51.3	15.6
U	LT & L	31.0	172.5	163.0	12	29.6	17.8
	TL & T	29.1	178.4	171.3	14	24.4	16.9
V	LT & L	21.3-27.2	185.1-185.4	168.7-170.4	8 - 10	17.1-18.8	16.3-16.5
	TL & T	17.4-25.6	192.4-195.4	175.6	6 - 10	13.0-17.4	17.2-17.3
W	LT & L	31.2	168.3	153.3	10	18.8	16.2
	TL & T	ND	179.4	165.9	14	22.4	17.2
X	LT & L	20.8-22.7	185.4	165.9	10	15.2	16.2
	TL & T	21.3-27.8	188.9	173.1	8	20.2	20.4
Y	LT & L	50.1-50.4	172.9	156.0	4	6.4	16.3
	TL & T	50.1-59.7	171.1	155.4	4	4.0	16.7

(1) See Table 3.

(2) LT and TL refer to toughness test specimen orientation, L and T to tensile specimen orientation.

(3) ND - no data generated.

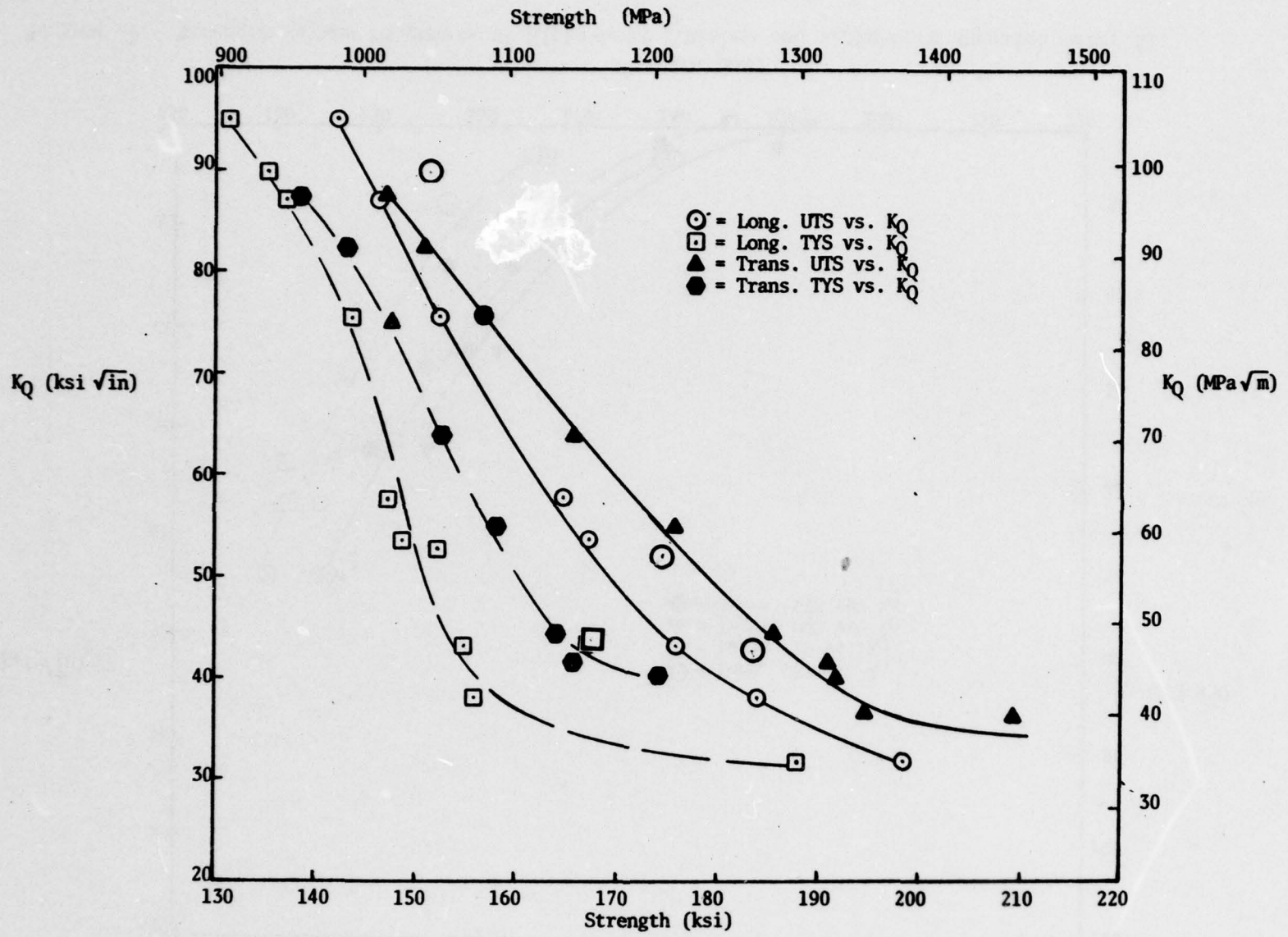

Figure 18. Strength versus toughness of beta finished and alpha-beta annealed material.

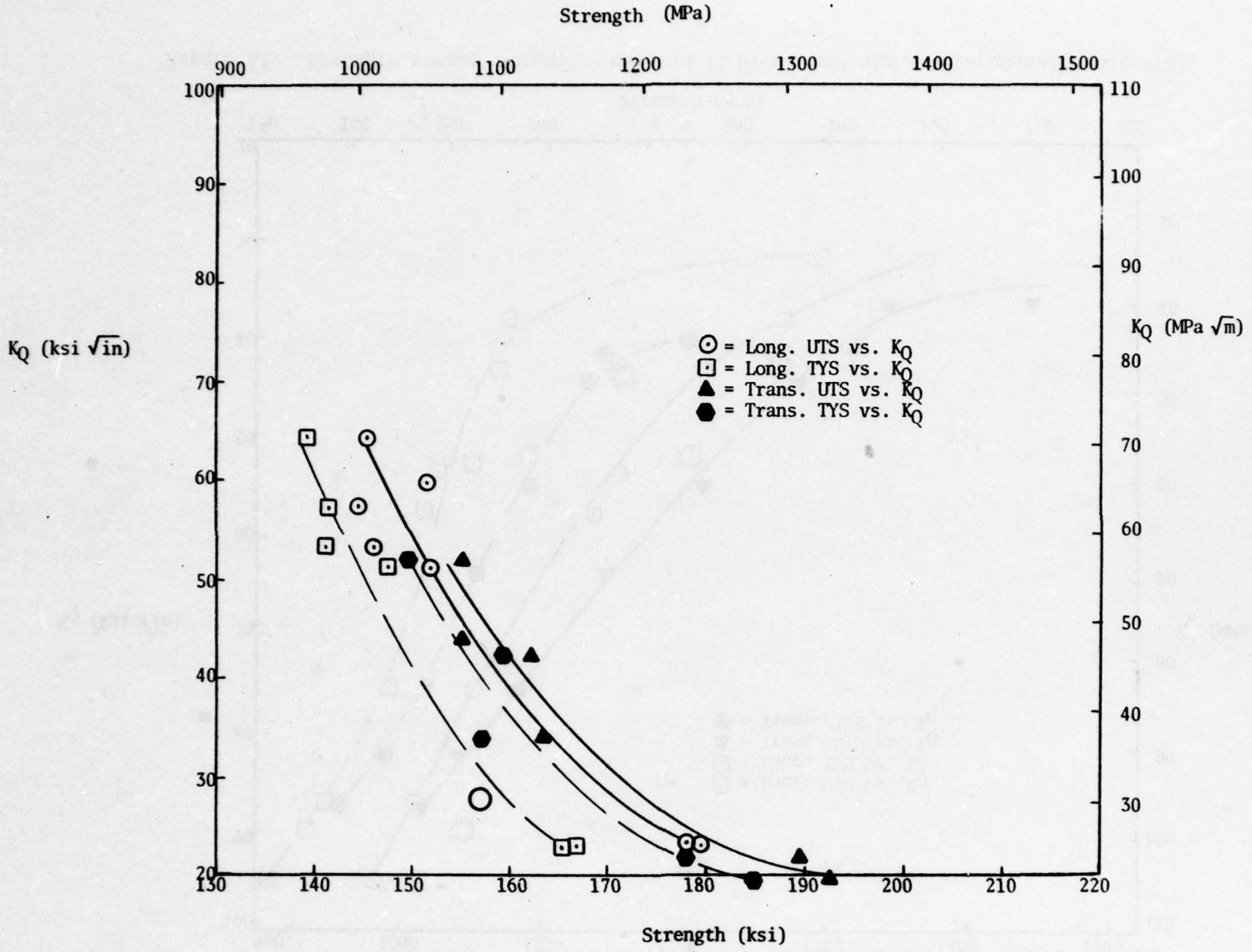

Figure 19. Strength versus toughness of alpha-beta finished and alpha-beta annealed material.

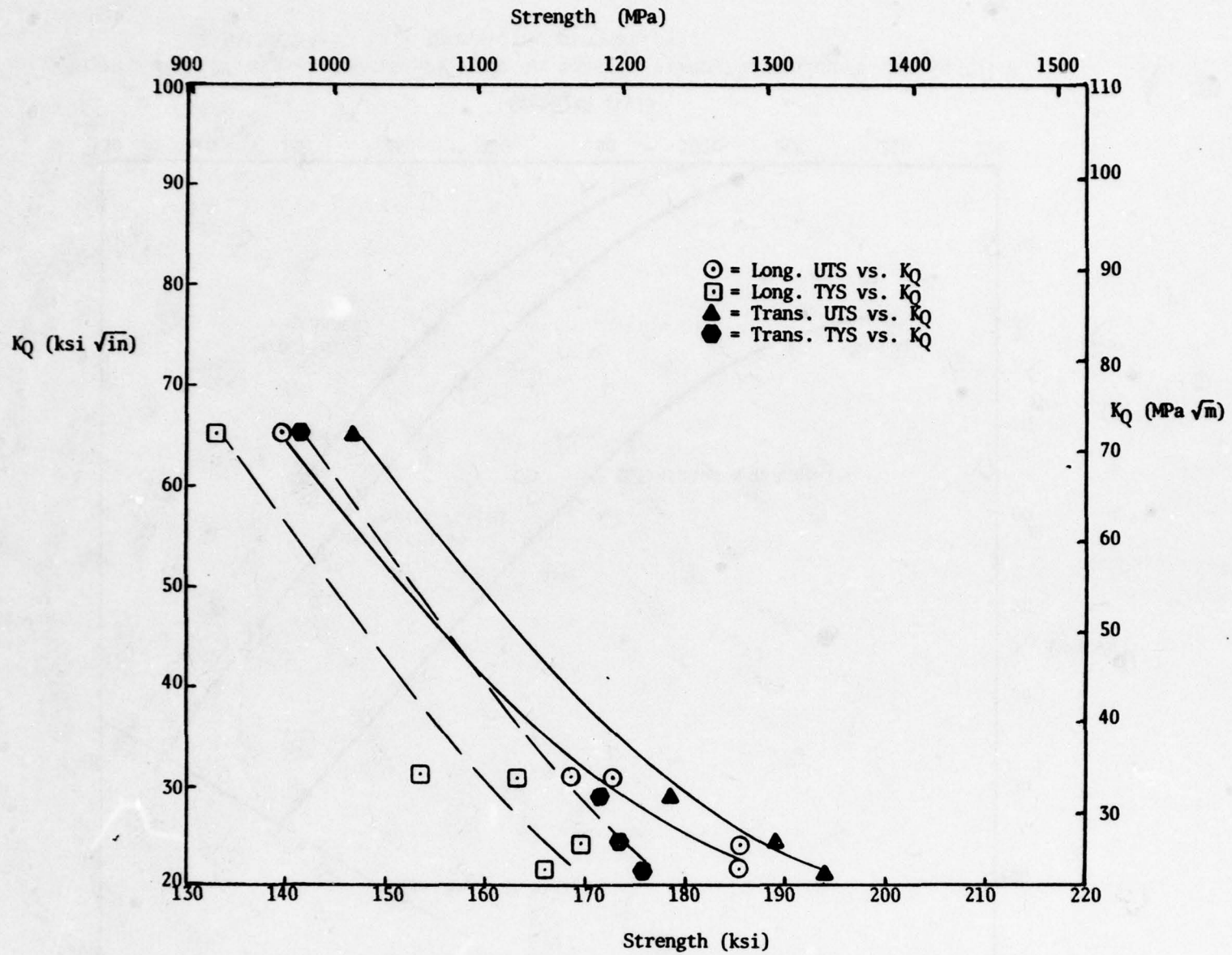

Figure 20. Strength versus toughness of alpha-beta finished and duplex annealed material.

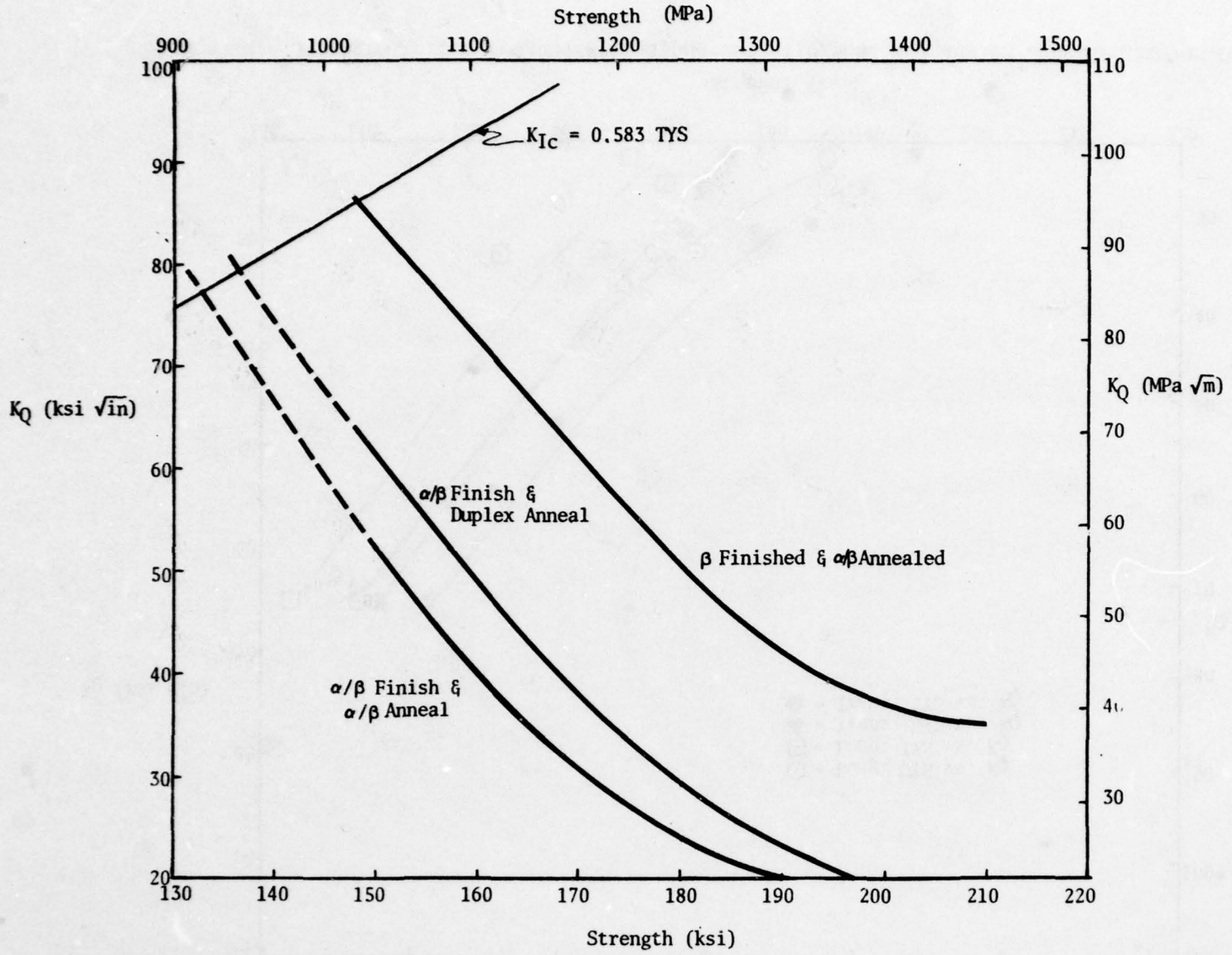

Figure 21. Effect of processing mode on tensile strength/toughness combinations in CORONA-5 (all transverse properties).

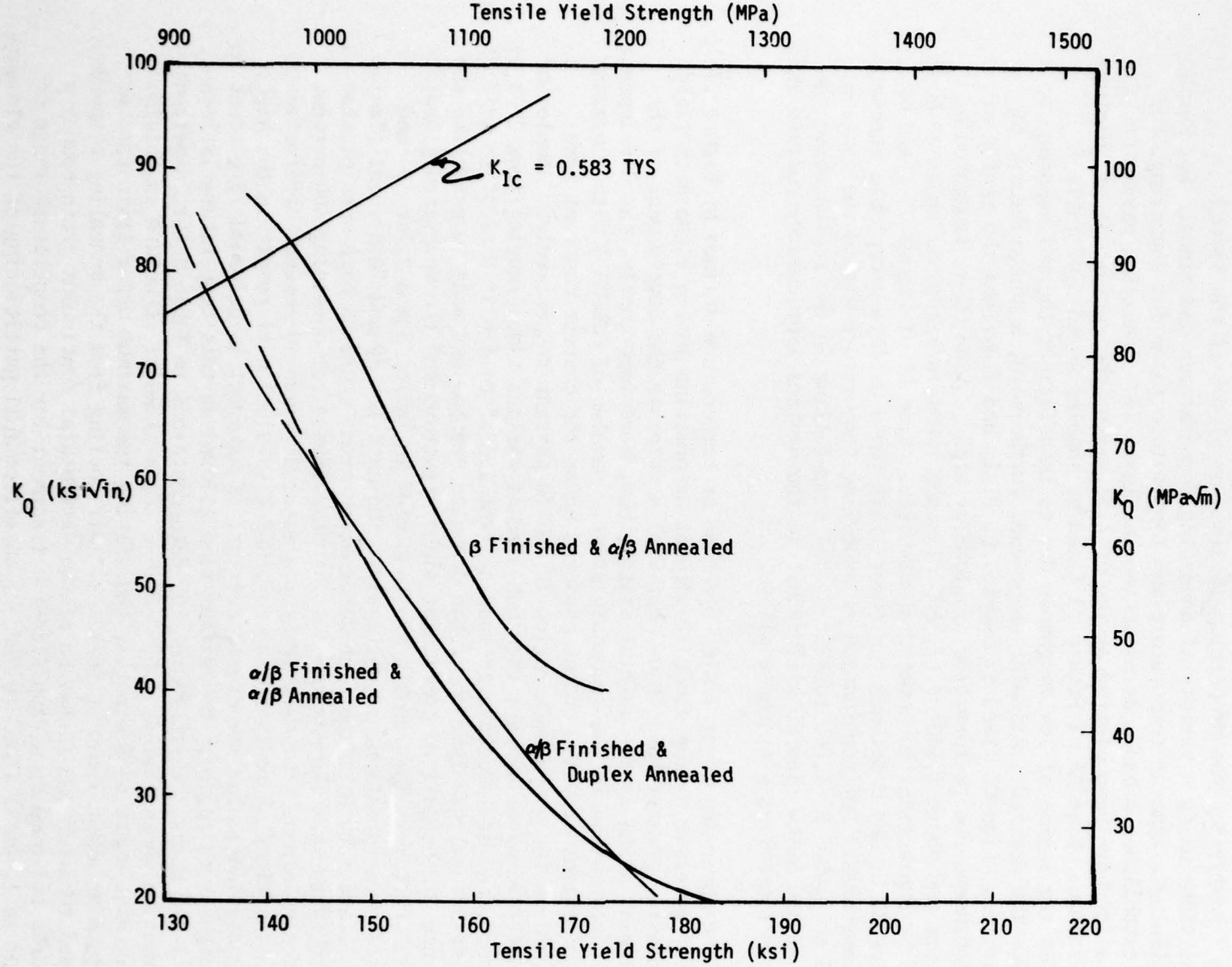

Figure 22. Effect of processing mode on tensile yield strength/toughness combinations in CORONA-5 (all transverse properties).

Table 7 summarizes the properties obtained on alloys of the listed compositions using a variety of annealing temperatures and times. For purposes of defining a time-at-temperature and temperature range for annealing, the data establishes a band, as presented in Figure 23. Annealing parameters for each alloy have been plotted as log of time versus the reciprocal of absolute temperature. Line AA of Figure 23 fixed by samples A and C of Table 7 defines the region of low toughness due to insufficient thermal exposure to produce the desired lenticular shape and, furthermore, a nonuniformity of properties. Line CC fixed by samples E, F, I, and J defines the region of low toughness due to formation of globular alpha. Line CC is truncated at 80 hours and above 1,400° F (1,760° C) since times in excess of about 80 hours would be impractical in commercial practice. Line BB of Figure 23 fixed by samples B, D, and H defines the lower limit for a uniform acceptable strength and toughness. Any combination of annealing temperature within the range of 1,400 to 1,600° F (1,760 to 870° C) and time falling in the region above the line BB and below line CC will result in the desired lenticular structure and uniform properties with these alloys.

The upper and lower limits for time at temperature defined by Figure 23 are for material having about 10 percent deformation in the alpha-beta field. Deformation greater than 10 percent will accelerate the development of the lenticular alpha in the initial stages, but, more importantly, the development of globular alpha in the secondary stage. Samples of CORONA-5 with a nominal oxygen content of 0.18 percent produced under the current contract were deformed in the alpha-beta region 30 and 70 percent respectively. Samples of the deformed material were then annealed at various times ranging from 0.08 to 24 hours, and at temperatures ranging from 1,475° to 1,625° F (800° to 885° C). Microstructural examination of the annealed samples was made to establish the presence of the desired lenticular alpha structure and the undesired globular alpha structure. The results are tabulated in Tables 8 and 9 for 30- and 70-percent deformation, respectively. The data for 30 and 70 percent (Tables 8 and 9), and for the 10-percent deformation from Figure 23 have been plotted in Figure 24 to show the maximum time at temperature for obtaining 100 percent lenticular alpha. For example, for a material given 10-percent deformation, annealing times up to 15 hours at 1,600° F (870° C) will result in the high-toughness lenticular structure, whereas, if material is deformed 70-percent in the alpha-beta region, the maximum time allowed at this temperature is less than 1-1/2 hours. Furthermore, the data contained in Table 9 for 70-percent deformation shows that at 1,625° F (885° C) a globular structure is obtained at times as short as 5 minutes, thus fixing the maximum upper limit for temperature at about 1,600° F (870° C). Air cooling from the annealing temperature is used to avoid the formation of the detrimental continuous grain boundary networks followed by a stabilization treatment for the temperature range of 1,000° to 1,400° F (535° to 760° C) to effect full partitioning of the elements and thermal stress relief.

TABLE 7. PROPERTIES OF Ti-Mo-Cr-Al ALLOY FOR VARIOUS HEAT TREATMENTS

Sample	Composition	Anneal Cycle		Tensile Strength		K_Q Toughness[1]	
		Temp (°F)	Time (hr)	Direction	UTS, (ksi)	Direction	(ksi$\sqrt{in.}$)
A	Ti-5.2Mo-1.7Cr-4.6Al-0.110$_2$	1,525	4	L	137-138	RW	90-97
				T	138	WR	66-69
B	Ti-5.2Mo-1.7Cr-4.6Al-0.110$_2$	1,525	8	L	139	RW	113-115
					136-141	WR	113-118
C	Ti-5.2Mo-1.7Cr-4.6Al-0.110$_2$	1,450	8	L	139-140	RW	127-129
				T	141	WR	84-89
D	Ti-5.2Mo-1.7Cr-4.6Al-0.110$_2$	1,450	16	L	142-143	RW	104-118
				T	140-142	WR	110-123
E	Ti-5Mo-1Cr-4.5Al	1,475	48	T	135	WR	50-44
F	Ti-3Mo-1Cr-4.5Al	1,600	72	L	143	RW	73
				T	142	WR	65
G	Ti-5.8Mo-1.2Cr-3.8Al-0.0750$_2$	1,525	16	L	125	RW	169
				T	128	WR	179
H	Ti-5Mo-1.5Cr-4.5Al	1,575	4	L	141	RW	99
				T	143	WR	85
I	Ti-8Mo-5.5Al	1,600	48	L	144	RW	41
				T	141	WR	34
J	Ti-8Mo-4.5Al-4Zr	1,500	72	L	139	RW	82
				T	146	WR	81

[1] K_Q values calculated from precracked Charpy samples using the relationship: $K_Q^2 = W/A \times E/2(1-\nu^2)$, refer to Ronald, T.M.F., Hall, J.A., and Pierce, C.M., "Some Observations Pertaining to Simple Fracture Toughness Screening Tests for Titanium," Technical Report AFML-TR-70-311, March 1971

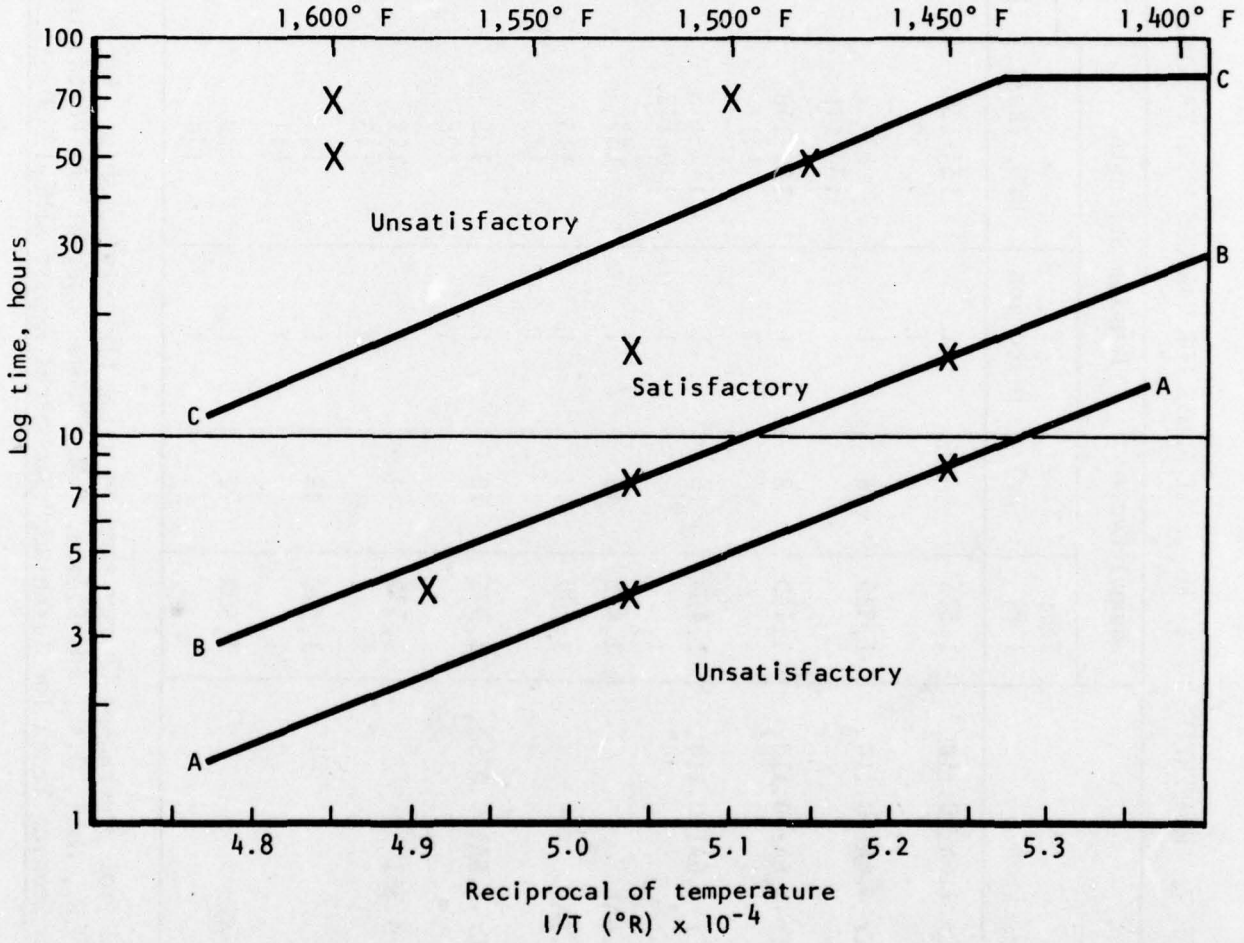

Figure 23. Plot of annealing parameters for Ti-Mo-Cr-Al alloys listed in Table 7, with approximately 10 percent deformation.

TABLE 8. DESCRIPTION OF MICROSTRUCTURE FOR INGOT R52071, 4.4%Al, 5.1%Mo, 1.46%Cr AND 0.18% OXYGEN, GIVEN A 30% DEFORMATION IN THE ALPHA-BETA FIELD AND ANNEALED FOR VARIOUS TIMES IN THE 1,475° TO 1,625° F (800° TO 885° C) TEMPERATURE RANGE

	Temperature, ° F		
Time, 4 hr	1,625 (885° C)	1,550 (845° C)	1,475 (800° C)
0.08	Lenticular	Lenticular	-
0.25	Lenticular	-	-
0.50	Lenticular	-	-
1	-	-	Lenticular
2	-	Lenticular	-
4	Globular/ lenticular	-	Lenticular
8	Globular	Lenticular	Lenticular
24	-	Globular	Lenticular/ globular

TABLE 9. DESCRIPTION OF MICROSTRUCTURE FOR INGOT R52071, 4.4%Al, 5.1%Mo, 1.46%Cr AND 0.18% OXYGEN, GIVEN A 70% DEFORMATION IN THE ALPHA-BETA FIELD AND ANNEALED FOR VARIOUS TIMES IN THE 1,475° TO 1,625° F (800° TO 885° C) TEMPERATURE RANGE

Temperature, ° F			
Time, hr	1,625 (885° C)	1,550 (845° C)	1,475 (800° C)
0.08	Globular	-	-
0.25	Globular	Lenticular	-
0.50	Globular	-	-
1	-	-	Lenticular
2	-	Globular/ lenticular	-
4	Globular	-	Globular/ lenticular
8	-	Globular	-
24	-	-	Globular

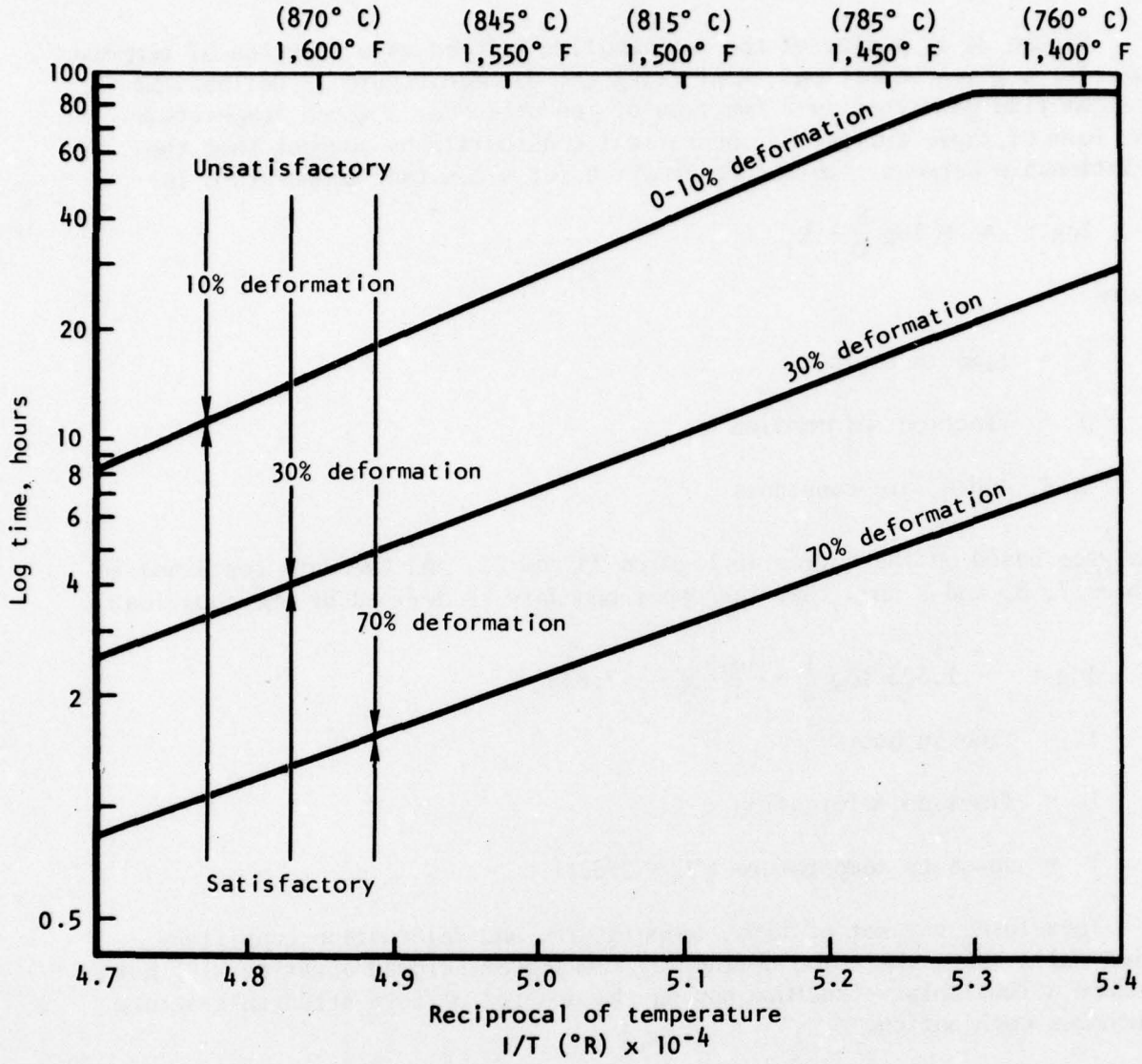

Figure 24. Maximum time at annealing temperature for obtaining lenticular alpha over a range of deformation from 10 to 70 percent.

Figure 24 is a plot of the maximum time allowed as a function of temperature for a given reduction. Replotting the data in Figure 25 defines the maximum time permitted as a function of reduction for a given temperature. The form of these curves and theoretical considerations suggest that the relationship between time and deformation for a constant temperature is:

$$\log t = M \log \frac{K}{D} + K_1$$

where

t = time in hours

D = fraction deformation

M, K, and K_1 are constants.

Analyses based on the curves in Figures 24 and 25, and the data contained in Tables 7, 8, and 9 show that the upper boundary is defined by the equation:

$$\log t = 1.323 \log \frac{1}{D} + \frac{40,522}{4.575T} - 7.838$$

t = time in hours

D = fraction deformation

T = absolute temperature (°C + 273.1)

Therefore, any set of time, temperature, and deformation conditions which falls above the curve defined by the abovementioned equation will not produce a lenticular structure having the desired uniform strength-fracture toughness combination.

The above-mentioned equation defines the maximum or upper limit for time, deformation, and temperature for achieving the desired structure and properties. Figure 23 defines the lower limit, line BB, for material given approximately 10-percent deformation in the alpha-beta temperature region. Increasing the amount of deformation will accelerate the development of lenticular alpha in the initial stages. For example, Figure 23 shows that material given approximately 10-percent deformation and heated for 4 hours at 1,550° F (845° C) will not have the desired lenticular structure and uniformity of properties. However, as shown in Table 8, material given 30-percent deformation in the alpha-beta temperature region shows a full lenticular structure after 2 hours at 1,550° F (845° C). This acceleration by deformation is further evident from examination of the data for material deformed

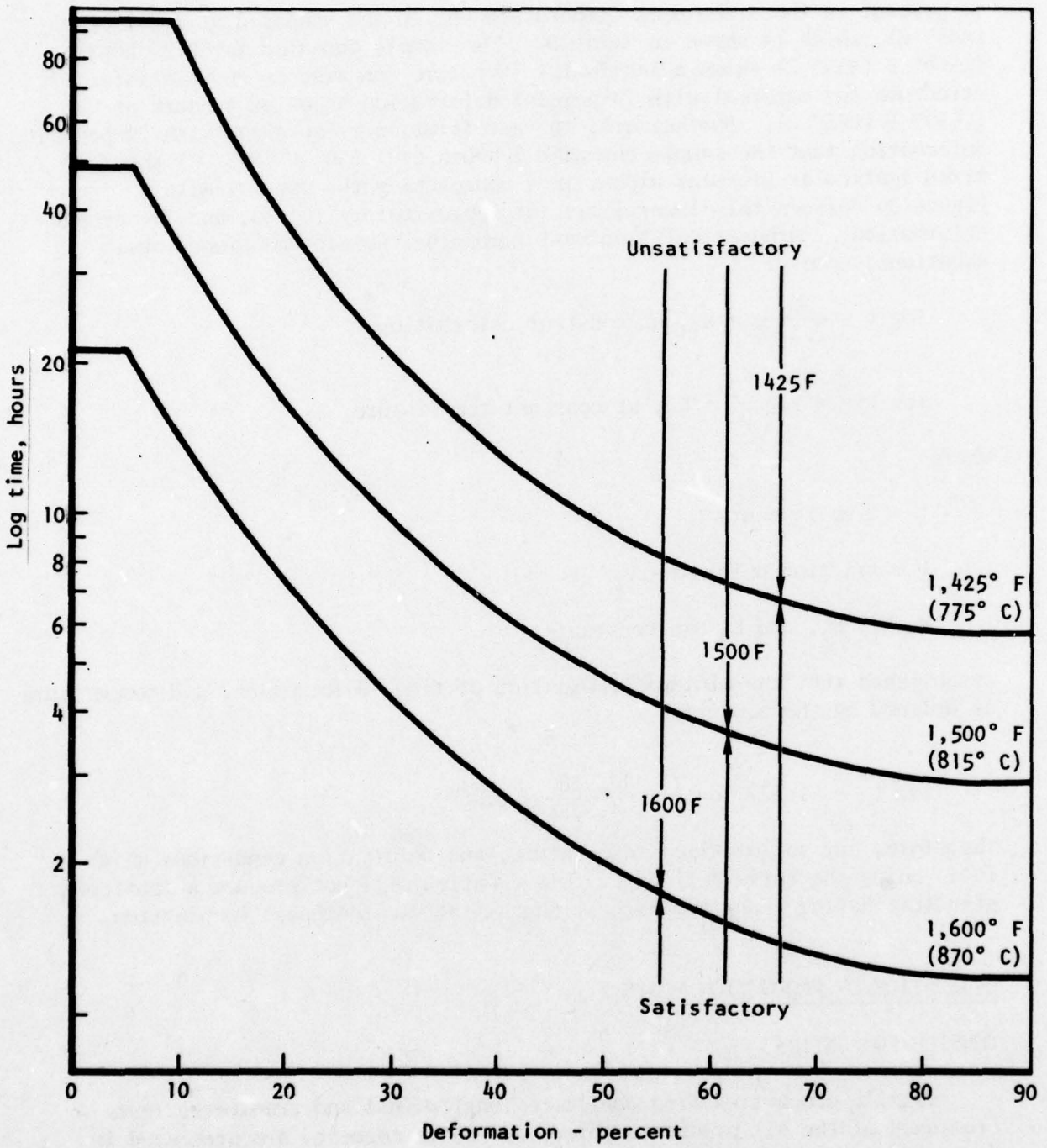

Figure 25. Maximum annealing time as a function of reduction for a given annealing temperature.

70-percent in the alpha-beta temperature region and annealed at 1,550° F (845° C), which is shown in Table 9. The sample annealed for 0.25 hour at 1,550° F (845° C) shows a lenticular structure compared to an unsatisfactory structure for material with 10-percent deformation annealed 4 hours at 1,550° F (845° C). Furthermore, the acceleration is so great with 70-percent deformation that the sample annealed 2 hours at 1,550° F (845° C) shows a mixed lenticular-globular alpha, thus approaching the upper limit. Figure 26 defines this lower limit for approximately 10, 30, and 70-percent deformation. Mathematical treatment combining the aforementioned basic equations; namely:

$$\log t = \frac{Q}{2.3\ RT} + K_1, \text{ at constant deformation}$$

$$\log t = M \log \frac{K_2}{D} + K_3, \text{ at constant temperature}$$

where

t = time in hours

D = fraction deformation

M, K_1, K_2, and K_3 are constants

establishes that the minimum combination of time, deformation, and temperature is defined by the equation:

$$\log t = 1.323 \log \frac{1}{D} + \frac{42,920}{4.575T} - 8.969$$

therefore, any set of time, temperature, and deformation conditions which falls below the curve defined by this equation will not produce a lenticular structure having a uniform high strength-fracture toughness combination.

EVALUATION OF PRODUCTION PLATE

TENSILE PROPERTIES

Tensile properties from duplicate longitudinal and transverse tests from each of the six production processed plate segments are presented in Table 10. As seen from Table 5, all test results met the target goals of 130 ksi (900 MPa) or 145 ksi (1,000 MPa) UTS depending upon heat treatment. Good uniformity of ultimate and yield strength is observed in each test direction and also when comparing test directions, particularly for the high beta processed material. A 3 to 5-ksi (20 to 35 MPa) range typifies the strength variation with a few exceptions. A 10 to 11-ksi (70 to 75 MPa)

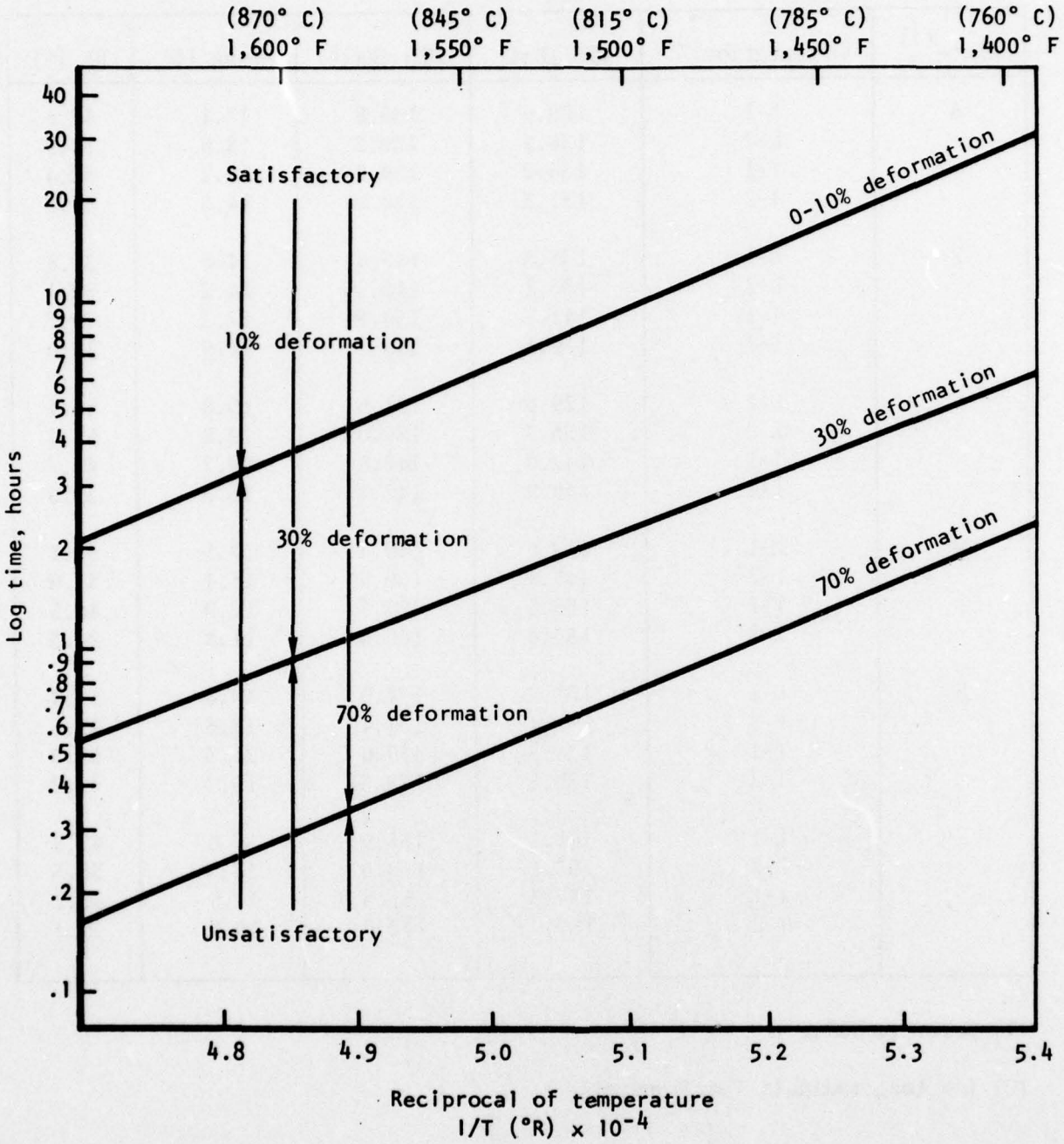

Figure 26. Minimum time at annealing temperature for obtaining lenticular alpha over a range of deformation from 10 to 70 percent.

TABLE 10. TENSILE PROPERTIES OF 3-INCH-THICK PRODUCTION PLATE

Plate[1]	Orientation[2]	TYS (ksi)	UTS (ksi)	Elong (%)	RA (%)
A	L-1	129.9	135.8	17.1	47.8
	L-2	128.9	136.2	18.0	38.9
	T-1	135.2	139.5	16.2	32.4
	T-2	131.8	138.9	14.5	34.2
B	L-1	136.3	146.4	14.6	37.8
	L-2	136.2	145.3	14.2	30.4
	T-1	141.7	150.8	14.2	29.7
	T-2	139.1	149.2	11.9	24.0
C	L-1	129.6	131.6	19.8	66.1
	L-2	136.7	139.0	19.8	53.4
	T-1	142.0	142.5	19.2	40.2
	T-2	140.9	142.4	16.3	39.6
D	L-1	142.6	149.4	17.5	51.1
	L-2	147.4	156.5	14.4	33.6
	T-1	153.5	157.5	12.9	46.5
	T-2	153.8	160.8	11.8	24.3
E	L-1	132.9	134.9	19.8	59.4
	L-2	135.4	137.4	18.8	49.5
	T-1	138.5	139.0	21.3	58.0
	T-2	139.8	140.8	15.2	42.2
F	L-1	148.1	155.9	15.0	47.9
	L-2	153.1	159.6	13.6	38.5
	T-1	157.3	161.8	12.9	45.1
	T-2	157.0	162.0	10.9	29.2

(1) Refer to Table 5

(2) L = Longitudinal; T = Transverse

difference between longitudinal and transverse properties for the low-beta and alpha beta processed plate represented the maximum variation noted. This is not considered excessive for production processed material.

As expected, somewhat wider variation in tensile ductility resulted, particularly reduction of area values. Nevertheless, good to excellent ductility was obtained for all material at this strength level.

At the higher aging temperature, no significant difference in strength level is evident as a function of process mode, although some improvement in ducility appears to result with lower temperature processing. At the lower aging temperature, a 5 to 15 ksi (35 to 105 MPa) increase in strength results with lower temperature processing, with tensile ductility also showing some improvement.

FATIGUE PROPERTIES

Smooth (K_T = 1.0) and notched (K_T = 3.0) round-bar axial tension fatigue curves were generated for production plate D [low-beta processed and heat treated to 145 ksi (1,000 MPa), UTS] and plate F [alpha-beta processed and heat treated to 145 ksi (1,000 MPa), UTS] at a stress ratio of +0.05. The results of these tests are shown in Table 11 and Figures 27 and 28. Properties in the longitudinal and transverse directions were seen to be essentially equivalent to each other in both plates. Furthermore, there was essentially no difference between the fatigue properties from plate-to-plate. Consequently, all four sets of data have been replotted in Figure 29, wherein comparisons are made with typical properties for Ti-6Al-4V in the RA condition. It can be seen from this figure that the unnotched fatigue strength of CORONA-5 is substantially greater than that of Ti-6Al-4V condition RA, while notched fatigue strength (K_T = 3.0) of the two alloys are essentially equivalent.

FRACTURE TOUGHNESS AND FATIGUE CRACK PROPAGATION

Fracture toughness results of WR, combined FCP/K_{IC} tests sampled from each of the six production processed plate segments are presented in Table 12. Test specimen was identical to that shown in Figure 21. The results indicate the influence of both hot working and heat treatment. Higher fracture toughness tends to be obtained following high-temperature processing employed to obtain the lenticular primary alpha morphology. Substantial alpha-beta processing, although resulting in higher strength, produces comparatively low values of toughness due to formation of globular alpha. For a given hot-working process, toughness also tends to be lower at higher yield strength levels reflecting the influence of matrix strengthening heat treatments on the alloy.

TABLE 11. FATIGUE PROPERTIES OF PRODUCTION PLATE

Plate and test condition	Max stress (ksi)	Max stress (% Ftu)	Cycles to failure
Plate D (1)	91.8	60	10,000,000 NF
Kt = 1, R = 0.05	114.8	75	4,622,000
Longitudinal	116.3	76	3,056,000
Ftu = 153.0 ksi	118.6	77.5	1,781,000
	119.3	78	98,000
	122.4	80	1,358,000
	122.4	80	139,000
	125.5	82	15,000
Plate D	100.2	63	10,137,000 NF
Kt = 1, R = 0.05	106.5	67	2,853,000
Transverse	111.3	70	4,633,000
Ftu = 159.0 ksi	116.1	73	3,090,000
	119.3	75	834,000
	123.2	77.5	955,000
	127.2	80	1,417,000
	127.2	80	1,115,000
	135.1	85	20,000
Plate D	29.1	19	10,000,000 NF
Kt = 3, R = 0.05	30.6	20	8,468,000
Longitudinal	38.3	25	390,000
Ftu = 153.0 ksi	41.3	27	220,000
	45.9	30	79,000
	61.2	40	28,000
	76.5	50	12,000
	91.8	60	7,000
Plate D	30.3	19	10,000,000 NF
Kt = 3, R = 0.05	35.0	22	702,000
Transverse	38.2	24	210,000
Ftu = 159.0 ksi	39.7	25	10,000,000 NF
	44.6	28	94,000
	47.7	30	61,000
	55.7	35	45,000
	63.6	40	15,000

(1) Low-beta processed, heat treated: 1,525° F/4 hr/AC + 1,050° F/8 hr/AC

(2) Alpha-beta processed, heat treated: 1,525° F/4 hr/AC + 1,050° F/8 hr/AC

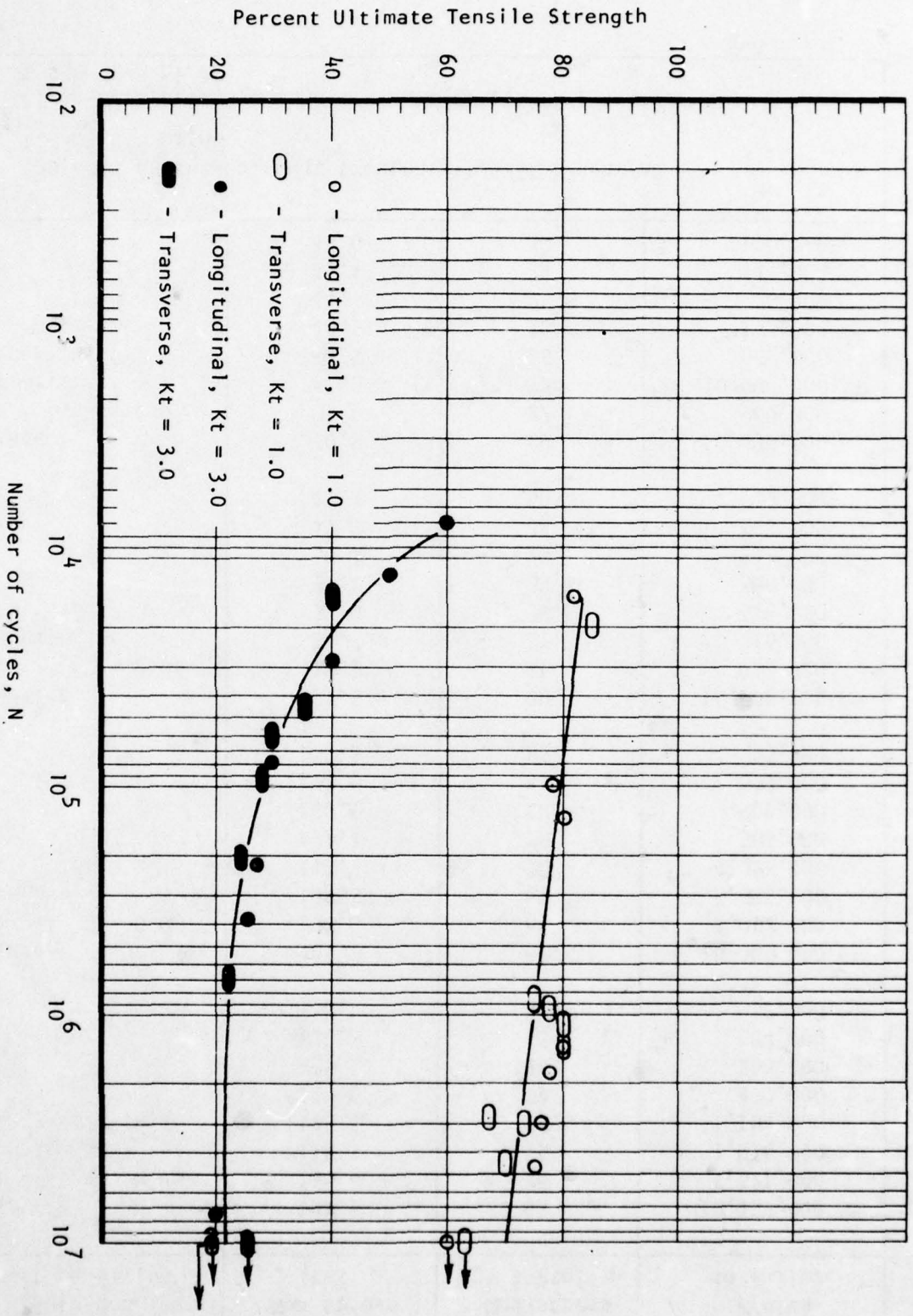

Figure 27. Smooth and notched fatigue properties of cond. D plate (low beta processed and heat treated to 145 ksi (1,000 MPa) UTS) (R = 0.05).

TABLE 11. FATIGUE PROPERTIES OF PRODUCTION PLATE (CONCL)

Plate and test condition	Max stress (ksi)	Max stress (% Ftu)	Cycles to failure
Plate F[2]	102.5	65	10,139,000 NF
Kt = 1, R = 0.05	110.4	70	1,521,000
Longitudinal	118.3	75	1,016,000
Ftu = 157.7 ksi	122.2	77.5	1,104,000
	124.6	79	479,000
	126.1	80	265,000
	129.3	82	84,000
	130.1	82.5	52,000
Plate F	101.2	62.5	10,000,000 NF
Kt = 1, R = 0.05	103.6	64	4,052,000
Transverse	108.5	67	3,395,000
Ftu = 161.9 ksi	113.3	70	4,285,000
	121.4	75	583,000
	129.5	80	709,000
	133.6	82.5	339,000
	137.8	85	43,000
Plate F	31.5	20	10,000,000 NF
Kt = 3, R = 0.05	33.1	21	950,000
Longitudinal	34.7	22	216,000
Ftu = 157.7	35.6	22.5	118,000
	37.1	23.5	366,000
	39.4	25	313,000
	44.2	28	123,000
	47.3	30	35,000
Plate F	30.8	19	10,000,000 NF
Kt - 3, R = 0.05	35.6	22	909,000
Transverse	37.3	23	10,000,000 NF
Ftu = 161.9	40.5	25	632,000
	40.5	25	173,000
	44.5	27.5	78,000
	45.4	28	47,000
	48.6	30	136,000

(1) Low-beta processed, heat treated: 1,525° F/4 hr/AC + 1,050° F/8 hr/AC

(2) Alpha-beta processed, heat treated: 1,525° F/4 hr/AC + 1,050° F/8 hr/AC

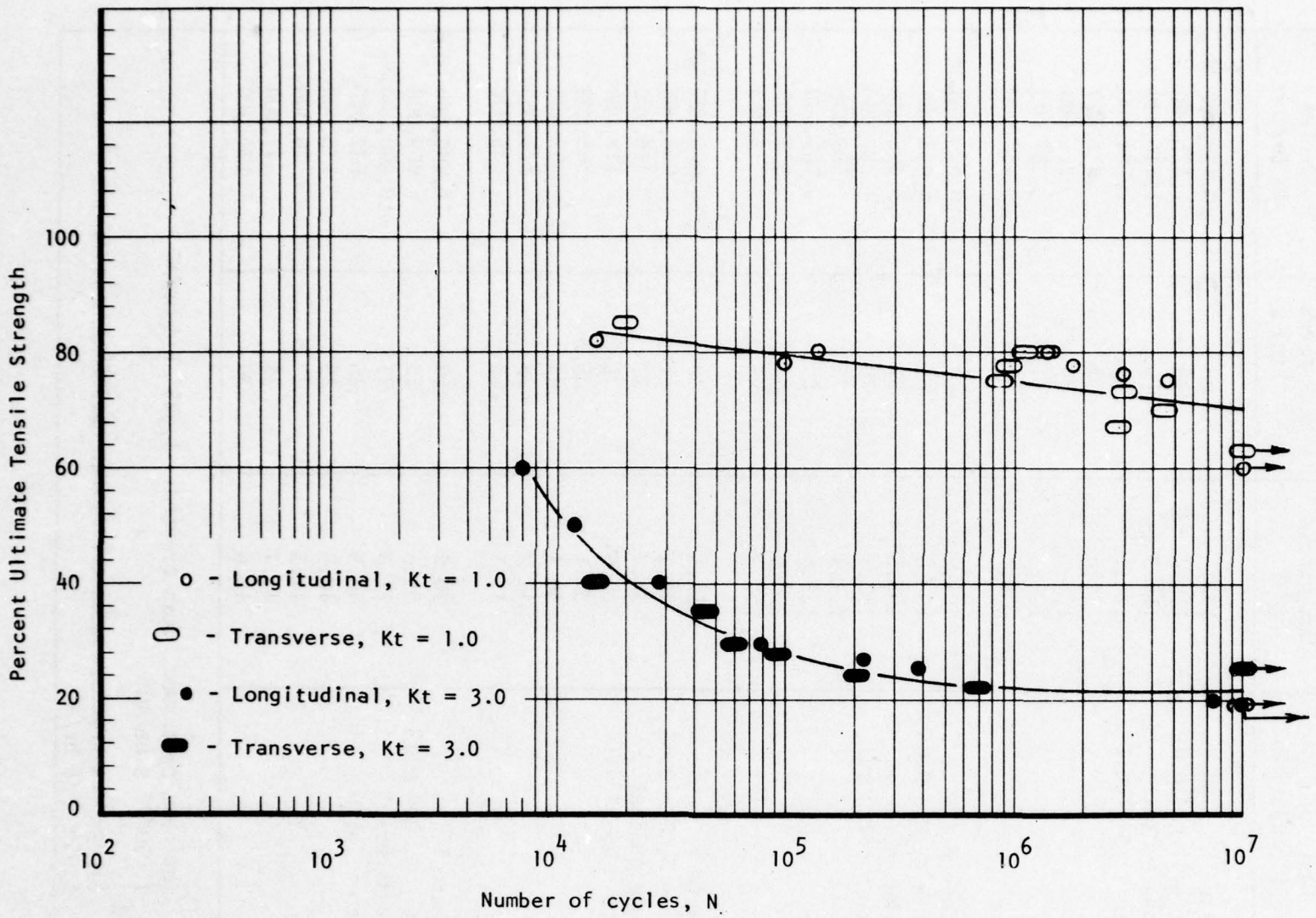

Figure 27. Smooth and notched fatigue properties of cond. D plate (low beta processed and heat treated to 145 ksi (1,000 MPa) UTS) (R = 0.05).

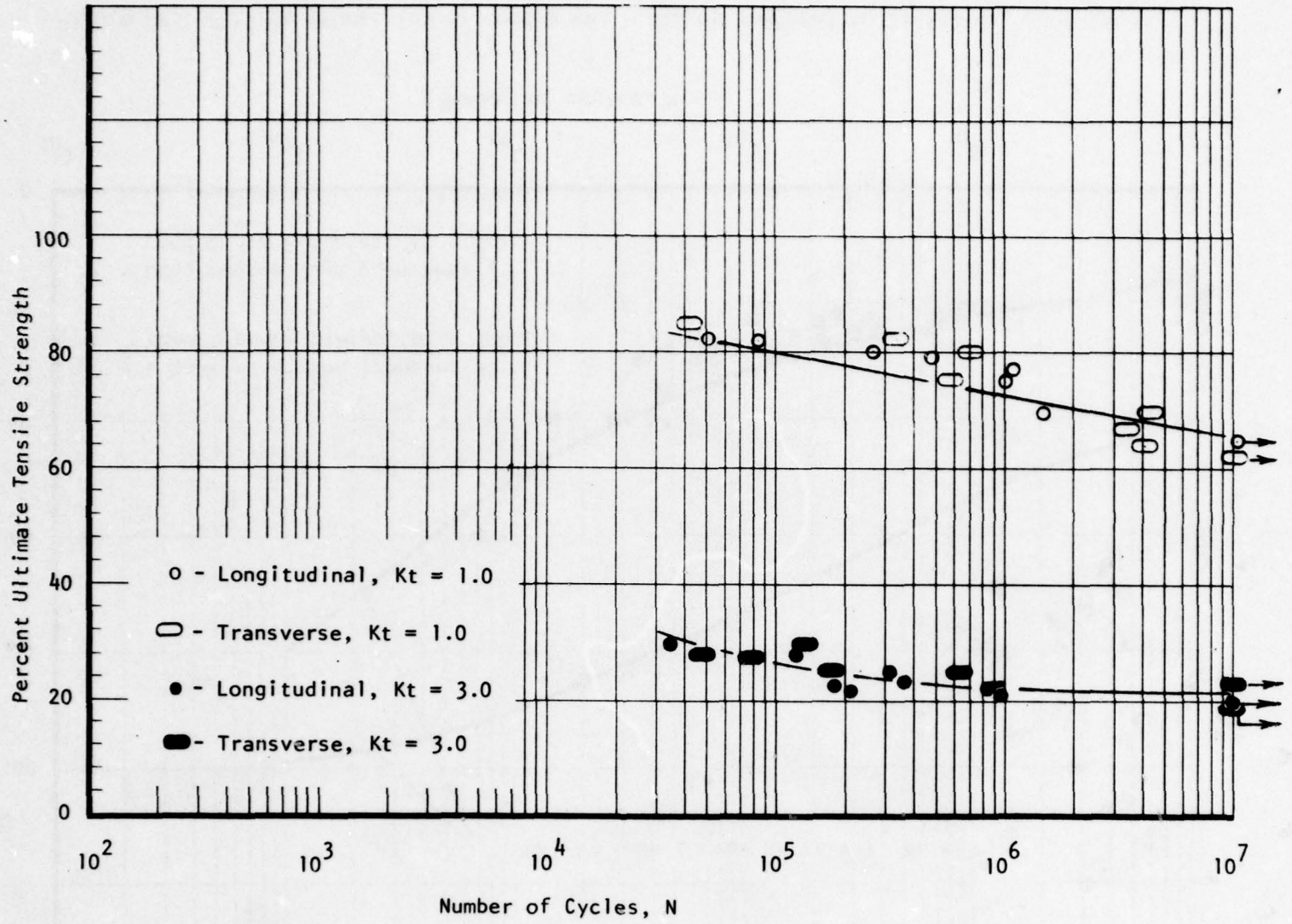

Figure 28. Smooth and notched fatigue properties of cond. F plate (alpha-beta processed and heat treated to 145 ksi (1,000 MPa) UTS) (R = 0.05).

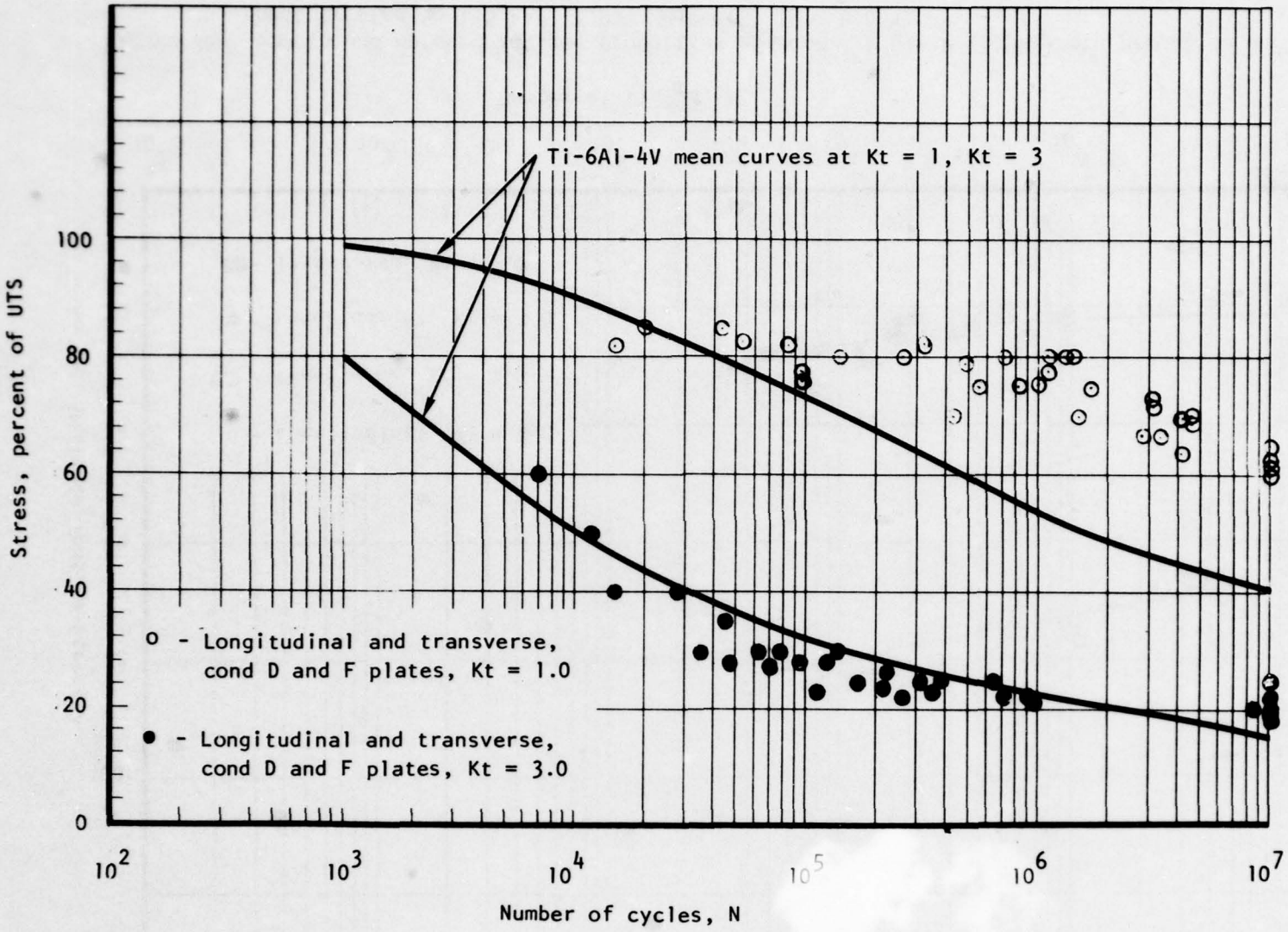

Figure 29. Fatigue properties of cond B and F plates compared to Ti-6Al-4V, cond RA, (Reference 14).

TABLE 12. FRACTURE TOUGHNESS DATA FOR PRODUCTION PROCESSED PLATE

Plate[1]	Orientation	TYS[2] (ksi)	K_{Ic} (K_Q) (ksi $\sqrt{in.}$)
A	WR	133.5	124.1
B	WR	140.4	(112.3)[3]
C	WR	141.5	76.3
D	WR	153.7	(60.0)[4]
E	WR	139.2	88.6
F	WR	157.2	53.6

[1] Refer to Table 5

[2] Average of duplicate long transverse test specimens

[3] Failed precrack shape requirement of ASTM E399-74

[4] Failed during precracking; value estimated from fracture surface and precrack loading

Fatigue crack propagation results are presented in Tables 13 through 18 and Figures 30 through 35 for production plates A through F. For comparison purposes, the data are replotted in Figure 36 and contrasted with a scatter band of data reported in References 1 and 2. Greater scatter is exhibited by the production plate over the entire range of delta K evaluated than is shown for plates previously produced. Curves for forgings presented in a later section of this report also fall within this scatter band of prior data. The effects of processing and heat treatment are both evident in the production plate data. Plates A and, particularly, B rolled from the higher soaking temperature result in growth rates slower than the lower temperature processed plates. Plate B exhibited a growth rate on the low side of the prior data scatter band over the entire range of delta K evaluated. Plates E and F rolled from the lower soaking temperatures exhibited the fastest growth rates yet encountered for the alloy. Plates C and D were intermediate in behavior.

STRESS CORROSION CRACKING RESISTANCE

Results of stress corrosion cracking tests conducted on specimens sampled from production plates B and E are presented in Table 19. One hundred-hour tests were performed on samples machined from plates B and E compact tension specimens using a bolt-loaded, double cantilever beam specimen configuration (Reference 13). The specimens were fatigue precracked and loaded with the crack tips in contact with 3.5-weight percent NaCl solution to an initial stress intensity of 0.8 K_{I_C} and the specimens immersed in solution for 100 hours. On completion of the 100-hour soak the specimens were unloaded and broken open under cyclic loading to expose the fracture surfaces. From these surfaces the final crack position was measured using an optical microscope. Plates B and E were selected for testing to evaluate the most favorable toughness and fatigue crack-growth-rate conditions representing the two processing extremes. Plate B was high-beta processed and heat treated to 145 ksi ultimate strength goal while plate E was alpha-beta processed and heat treated to 130 ksi ultimate strength goal. The data indicate no significant difference as a function of processing history, and when expressed as a percent of K_{I_C} compare favorably with cond RA Ti-6Al-4V for which a 60-percent K_{I_C} value of $K_{I_{SCC}}$ in synthetic sump tank water (a less aggresive environment) is considered nominal (Reference 15), under 1000-hour testing conditions.

TABLE 13. TABULATION OF FATIGUE CRACK PROPAGATION DATA FOR PRODUCTION PLATE A

5NWR, CORONA-5 Plate, LA, RT, R = 0.08, W = 5.805, H = 2.818, B' = 2.898								
	A	B	DA	DN	Max LD	Min LD	DA/DN (10^{-6} in./CY)	Delta K ksi $\sqrt{in.}$
1	1.810	1.850						
2	1,830	1.875	0.025	28,000	11,500	920	0.82	10.37
3	1,850	1.890	0.015	23,750			0.76	10.44
4	1.895	1.930	0.040	38,030			1.13	10.55
5	1.950	2.000	0.070	42,040			1.50	10.76
6	2.010	2.050	0.050	14,380	13,850	1,100	3.82	13.24
7	2.045	2.090	0.040	10,140			3.75	13.47
8	2.115	2.170	0.080	16,630			4.51	13.75
9	2.150	2.195	0.025	4,030	16,100	1,300	7.44	16.30
10	2.200	2.245	0.050	8,340			5.60	16.53
11	2.250	2.285	0.040	6,580			6.84	16.83
12	2.300	2.335	0.050	3,480	19,050	1,500	14.4	20.33
13	2.345	2.380	0.045	3,440			13.1	20.71
14	2.405	2.430	0.050	4,080			12.3	21.08
15	2.450	2.450	0.020	1,860	22,500	1,800	18.8	25.31
16	2.500	2.495	0.045	1,960			24.5	25.69
17	2.550	2.550	0.055	2,260			23.5	26.18
18	2.600	2.600	0.050	1,540	25,500	2,050	32.5	30.27
19	2.650	2.660	0.060	1,508			36.5	30.91
20	2.700	2.700	0.040	1,120			40.2	31.53
21	2.750	2.765	0.65	727	32,000	2,550	79.8	40.41
22	2.805	2.805	0.040	698			68.8	41.34
23	2.855	2.855	0.050	577			86.7	42.18

TABLE 14. TABULATION OF FATIGUE CRACK PROPAGATION DATA FOR PRODUCTION PLATE B

5NWR, CORONA-5 Plate, LA, RT, R = 0.08, W = 5.831, H = 2.821, B = 2,910								
	A	B	DA	DN	Max LD	Min LD	DA/DN (10^{-6} in./CY)	Delta K ksi $\sqrt{in.}$
1	1.750	1.750						
2	1.780	1.820	0.070	9,270	11,500	920	5.40	10.03
3	1.840	1.840	0.020	50,660			0.79	10.19
4	1.860	1.845	0.025	23,830			0.97	10.31
5	1.905	1.870	0.025	36,570			0.96	10.38
6	1.920	1.885	0.015	32,340			0.46	10.47
7	1.945	1.920	0.035	42,480			0.71	10.55
8	2.005	2.005	0.085	37,590	13,850	1,100	1.94	12.95
9	2.050	2.055	0.050	28,370			1.69	13.23
10	2.115	2.100	0.045	24,860			2.21	13.50
11	2.165	2.160	0.060	12,890	16,100	1,300	4.27	15.99
12	2.200	2.185	0.025	7,910			3.79	16.25
13	2.245	2.240	0.055	9,130			5.48	16.49
14	2.300	2.300	0.060	6,410	19,050	1,500	9.05	19.96
15	2.360	2.360	0.060	5,510			10.9	20.41
16	2.400	2.400	0.040	4,480			8.92	20.80
17	2.450	2.440	0.040	2,950	22,500	1,800	15.3	24.92
18	2.515	2.505	0.065	3,600			18.1	25.40
19	2.560	2.560	0.055	2,650			18.9	26.04
20	2.600	2.605	0.045	1,642	25,500	2,050	26.2	30.02
21	2.655	2.650	0.045	1,509			33.1	30.58
22	2.700	2.700	0.050	1,504			31.9	31.13
23	2.760	2.760	0.060	979	32,000	2,550	61.3	39.98
24	2.800	2.810	0.050	774			58.1	40.88
25	2.850	2.860	0.050	785			63.7	41.69

TABLE 15. TABULATION OF FATIGUE CRACK PROPAGATION DATA FOR PRODUCTION PLATE C

5NWR, CORONA-5 Plate, LA, RT, R = 0.08

W = 5.809, H = 2.816, B = 2.908

	A	B	DA	DN	Max LD	Min LD	DA/DN (10^{-6} in./CY)	Delta K ksi $\sqrt{in.}$
1	1.750	1.860						
2	1.805	1.890	0.043	39,100	11,500	920	1.10	10.27
3	1.850	1.915	0.035	25,160			1.39	10.41
4	1.920	1.945	0.050	38,120			1.31	10.57
5	1,960	1,985	0.040	9,480	13,850	1,100	4.22	12.95
6	2.010	2.030	0.048	9,920			4.84	13.10
7	2.065	2.075	0.050	11,530			4.34	13.38
8	2.100	2.110	0.035	6,690			5.23	13.60
9	2.165	2.155	0.055	6,560	16,100	1,300	8.38	16.07
10	2.200	2.195	0.038	4,130			9.20	16.35
11	2.245	2.230	0.040	4,270			9.37	16.58
12	2,320	2,315	0.080	4,610	19,050	1,500	17.4	20.13
13	2.350	2.340	0.028	2,010			13.9	20.55
14	2.405	2.395	0.055	2,970			18.5	20.87
15	2,465	2.450	0.058	2,060	22,500	1,800	28.2	25.14
16	2.510	2.480	0.038	1,210			31.4	25.60
17	2.565	2.540	0.058	2,020			28.7	26.08
18	2.610	2.585	0.045	947	25,500	2,050	47.5	30.14
19	2.660	2.625	0.045	821			54.8	30.68
20	2.710	2.670	0.048	814			59.0	31.25
21	2.765	2.720	0.053	267	32,000	2,550	198.5	40.04
22	2.810	2.740	0.033	220			150.0	40.76
23	2.865	2.780	0.048	232			206.8	41.44

TABLE 16. TABULATION OF FATIGUE CRACK PROPAGATION DATA FOR PRODUCTION PLATE D

5NWR, CORONA-5 Plate, LA, RT, R = 0.08 W = 5.802, H = 2.818, B = 2.908								
	A	B	DA	DN	Max LD	Min LD	DA/DN (10^{-6} in./CY)	Delta K ksi $\sqrt{in.}$
1	1.780	1.750						
2	1.800	1.785	0.028	19,600	11,500	920	1.40	10.11
3	1.850	1.835	0.050	34,000			1.47	10.25
4	1.900	1.910	0.063	32,800			1.91	10.45
5	1.950	1.950	0.045	26,100			1.72	10.66
6	2.000	1.990	0.045	9,900	13,850	1,100	4.55	13.03
7	2.055	2.045	0.055	12,800			4.30	13.27
8	2.120	3.095	0.058	13,720			4.20	13.56
9	2.150	2.130	0.033	4,160	16,100	1,300	7.81	16.05
10	2.215	2.185	0.060	6,850			8.76	16.34
11	2.255	2.230	0.043	5,310			8.00	16.65
12	2.305	2.285	0.053	3,740	19,050	1,500	14.0	20.08
13	2.350	2.335	0.048	3,440			13.8	20.47
14	2.405	2.385	0.053	2,990			17.6	20.86
15	2.450	2.430	0.045	1,950	22,500	1,800	23.1	25.08
16	2.500	2.475	0.048	1,750			27.1	25.52
17	2.550	2.525	0.050	1,630			30.7	26.02
18	2.610	2.580	0.058	1,151	25,500	2,050	50.0	30.06
19	2.655	2.630	0.048	856			55.5	30.70
20	2.700	2.675	0.045	784			57.4	31.26
21	2.760	2.725	0.055	306	32,000	2,550	179.7	40.06
22	2.805	2.765	0.043	179			237.4	40.89
23	2.855	2.820	0.053	168			312.5	41.71

TABLE 17. TABULATION OF FATIGUE CRACK PROPAGATION DATA FOR PRODUCTION PLATE E

5NWR, CORONA-5 Plate, LA, RT, R = 0.08 W = 5.801, H = 2.819, B = 2.906								
	A	B	DA	DN	Max LD	Min LD	DA/DN (10^{-6} in./CY)	Delta K ksi $\sqrt{in.}$
1	1.765	1.740						
2	1.785	1.800	0.060	30,790	11,500	920	1.30	10.09
3	1.820	1.830	0.030	29,290			1.03	10.23
4	1.870	1.895	0.065	34,350			1.69	10.39
5	1.920	1.945	0.050	32,240			1.55	10.59
6	1.960	1.975	0.030	18,910			1.85	10.76
7	2.020	2.030	0.055	11,050	13,850	1,100	5.25	13.19
8	2.050	2.075	0.045	7,230			5.26	13.41
9	2.100	2.125	0.050	9,990			5.01	13.64
10	2.130	2.155	0.030	3,520	16,100	1,300	8.52	16.07
11	2.150	2.180	0.025	2,480			9.27	16.24
12	2.200	2.220	0.040	4,970			9.05	16.44
13	2.250	2.265	0.045	5,030			9.54	16.79
14	2.300	2.305	0.040	2,740	19,050	1,500	16.4	20.19
15	2.350	2.355	0.050	3,160			15.8	20.57
16	2.400	2.410	0.055	2,750			19.3	20.97
17	2.450	2.455	0.045	1,550	22,500	1,800	31.0	25.21
18	2.515	2.530	0.075	2,110			33.2	25.78
19	2.570	2.575	0.045	1,550			32.3	26.39
20	2.605	2.620	0.045	646	25,500	2,050	61.9	30.43
21	2.650	2.660	0.040	910			47.3	30.93
22	2.700	2.710	0.050	936			53.4	31.51
23	2.755	2.760	0.050	324	32,000	2,550	163.6	40.41
24	2.805	2.815	0.055	360			147.2	41.31
25	2.855	2.855	0.040	259			173.8	42.17

TABLE 18. TABULATION OF FATIGUE CRACK PROPAGATION DATA FOR PRODUCTION PLATE F

5NWR, CORONA-5 Plate, LA, RT, R = 0.08

W = 5.804, H = 2.819, B = 2.908

	A	B	DA	DN	Max LD	Min LD	DA/DN (10^{-6} in./CY)	Delta K ksi $\sqrt{in.}$
1	1.700	1.775						
2	1.720	1.785	0.010	10,440	11,500	920	1.44	9.98
3	1.750	1.800	0.015	8,130			2.83	10.03
4	1.775	1.830	0.030	18,430			1.52	10.14
5	1.845	1.880	0.050	39,550			1.52	10.30
6	1.880	1.900	0.020	19,490			1.44	10.46
7	1.945	1.945	0.045	29,810			1.85	10.61
8	2.020	2.015	0.070	15,360	13,850	1,100	4.75	13.09
9	2.045	2.030	0.015	5,490			3.64	13.31
10	2.080	2.070	0.040	6,150			6.18	13.47
11	2.100	2.090	0.020	4,470			4.47	13.61
12	2.160	2.155	0.065	8,270	16,100	1,300	7.62	16.05
13	2.200	2.190	0.035	4,440			8.56	16.36
14	2.250	2.240	0.050	5,570			8.98	16.62
15	2.300	2.295	0.055	3,090	19,050	1,500	17.2	20.11
16	2.355	2.340	0.045	3,160			15.8	20.50
17	2.400	2.390	0.050	2,560			18.8	20.88
18	2.450	2.435	0.045	1,561	22,500	1,800	30.8	25.07
19	2.495	2.480	0.045	1,301			34.6	25.52
20	2.550	2.530	0.050	1,431			37.0	26.01
21	2.595	2.575	0.045	728	25,500	2,050	61.8	30.03
22	2.650	2.620	0.045	799			62.6	30.62
23	2.700	2.680	0.060	920			59.8	31.24
24	2.820	2.780	0.100	377	32,000	2,550	292	40.57
25	2.855	2.825	0.020	67			418	41.76

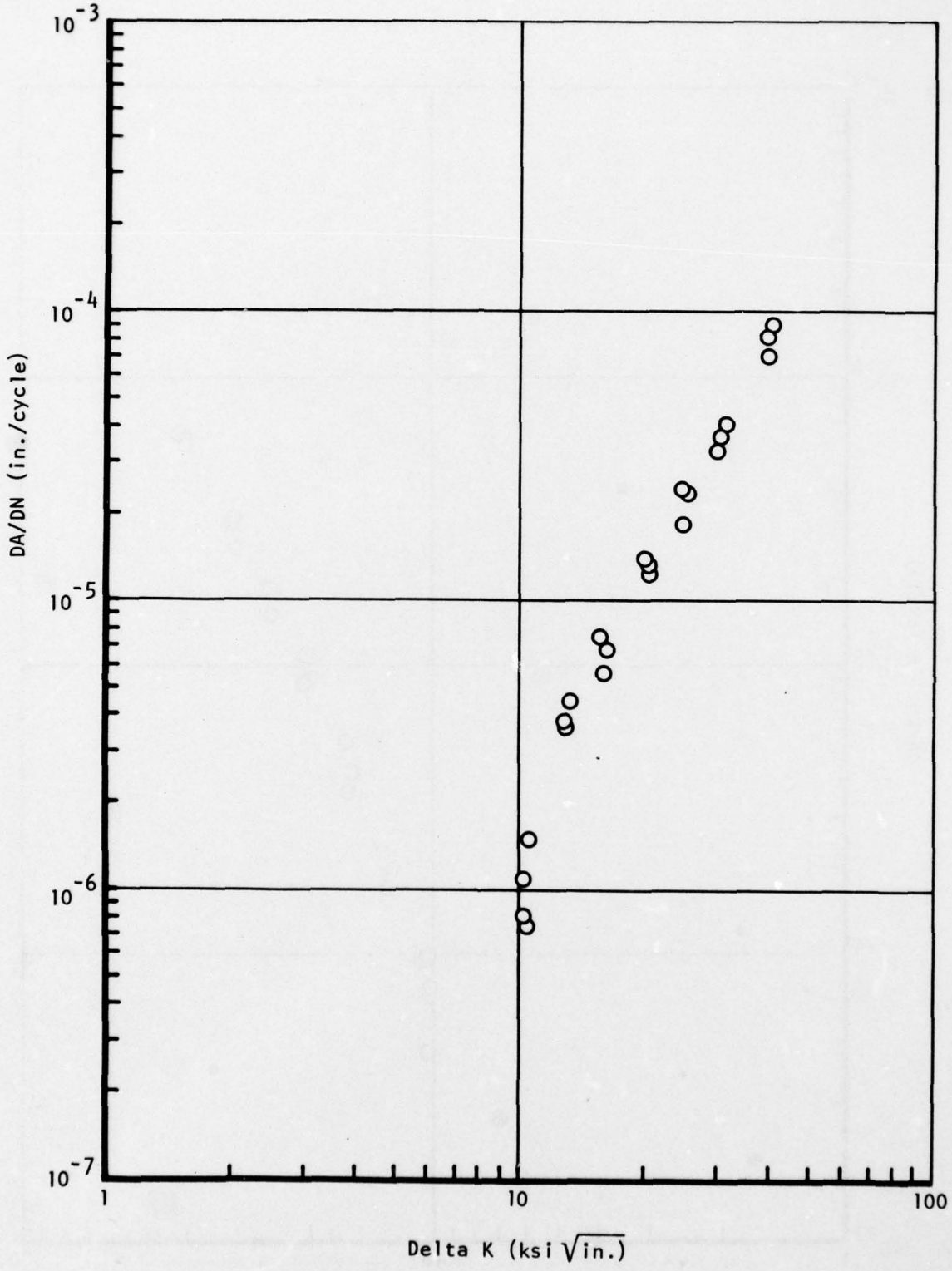

Figure 30. Fatigue crack propagation characteristics of plate A (WR, LHA, R = 0.08).

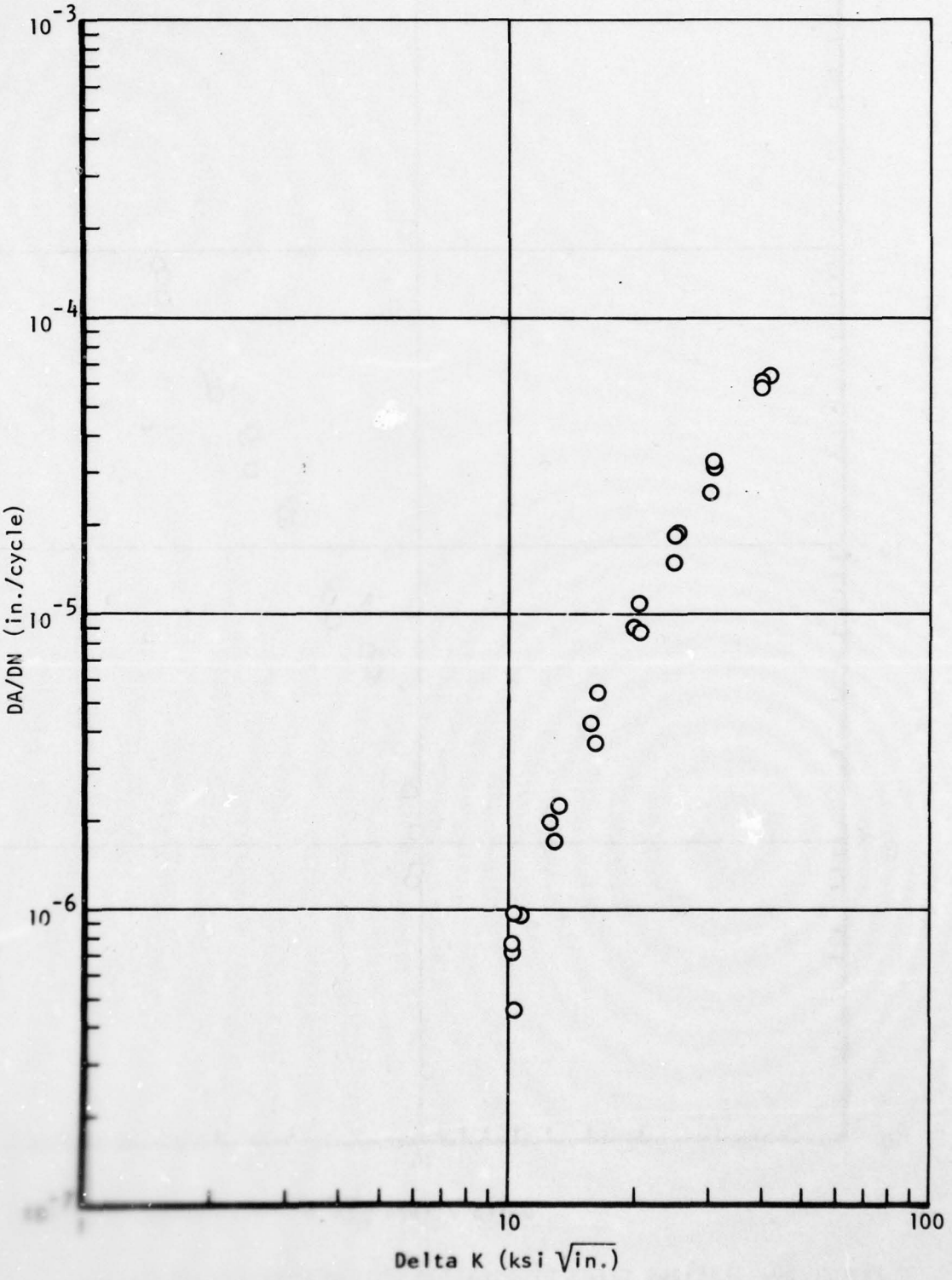

Fatigue crack propagation characteristics of plate B (BB, LHA, R = 0.08).

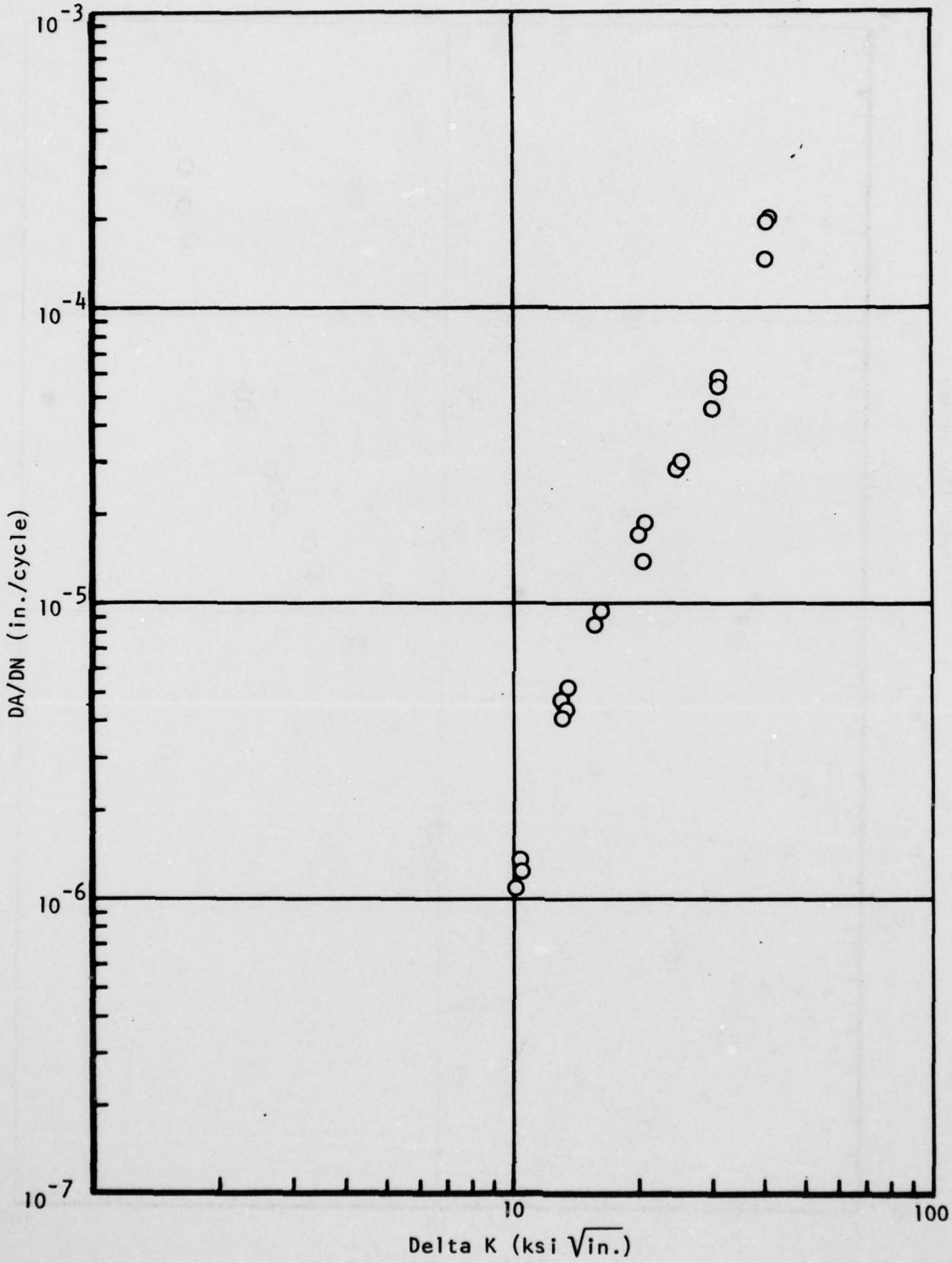

Figure 32. Fatigue crack propagation characteristics of plate C (WR, LHA, R = 0.08).

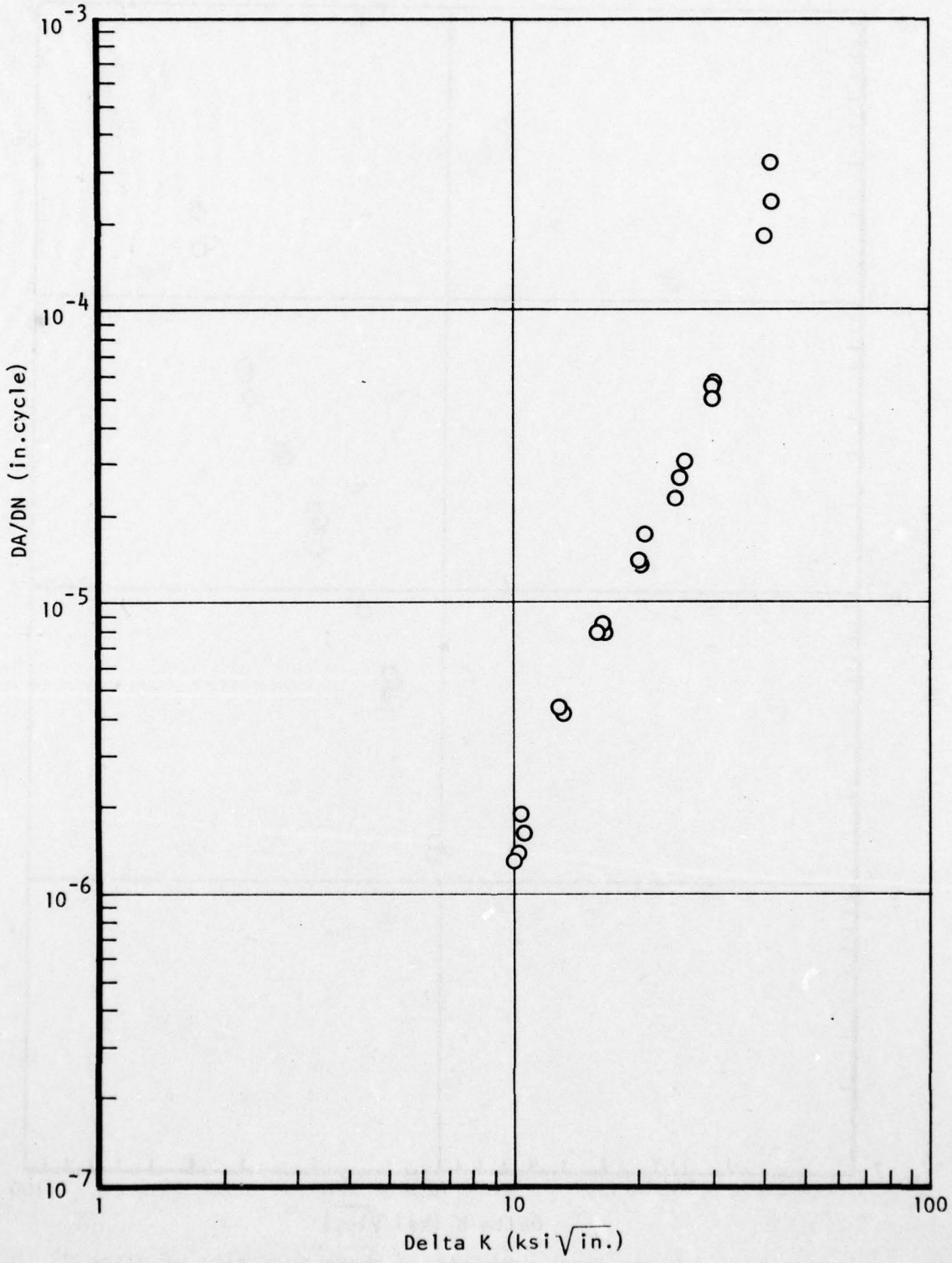

Figure 33. Fatigue crack propagation characteristics of plate D (WR, LHA, R = 0.08).

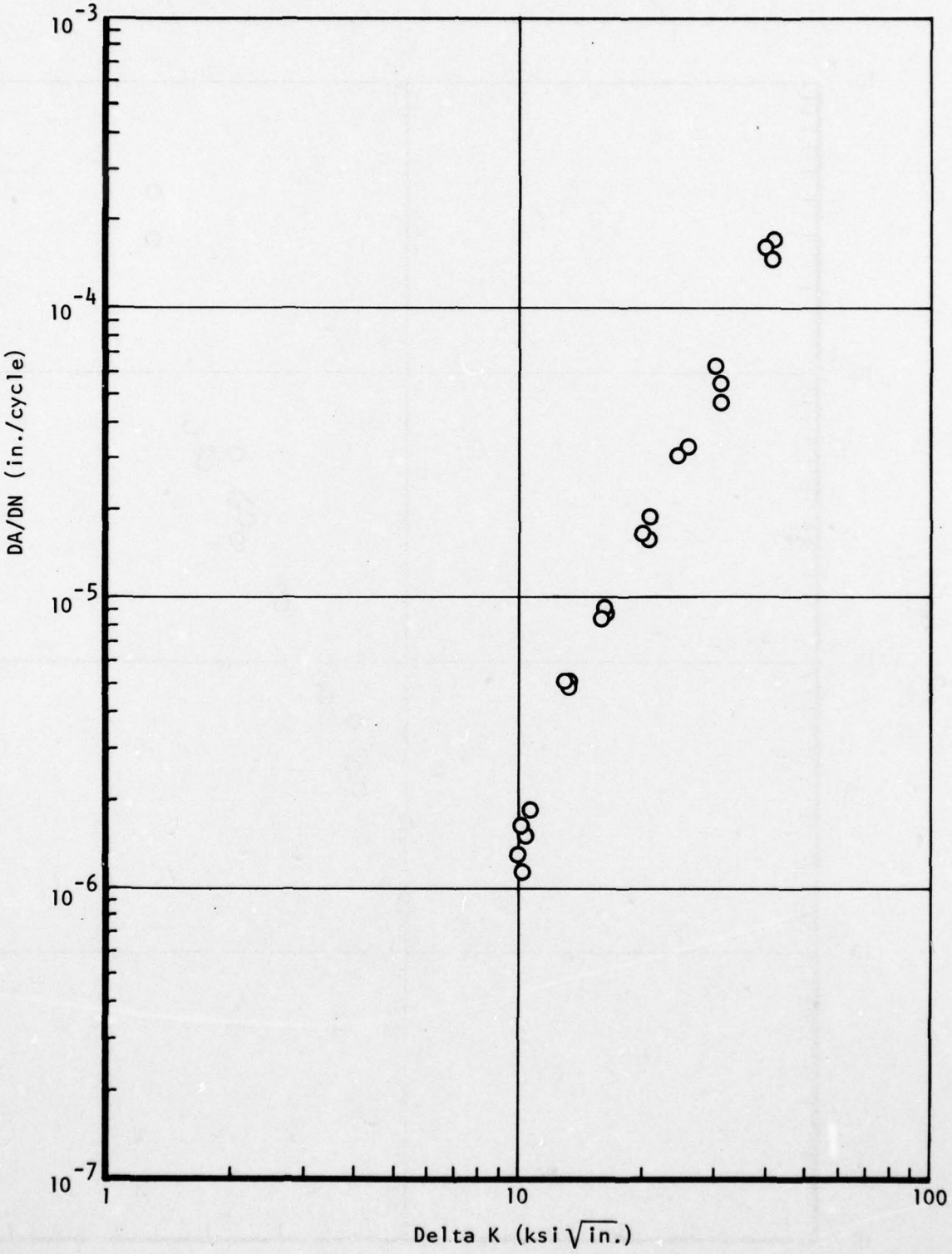

Figure 34. Fatigue crack propagation characteristics of plate E (WR, LHA, R = 0.08).

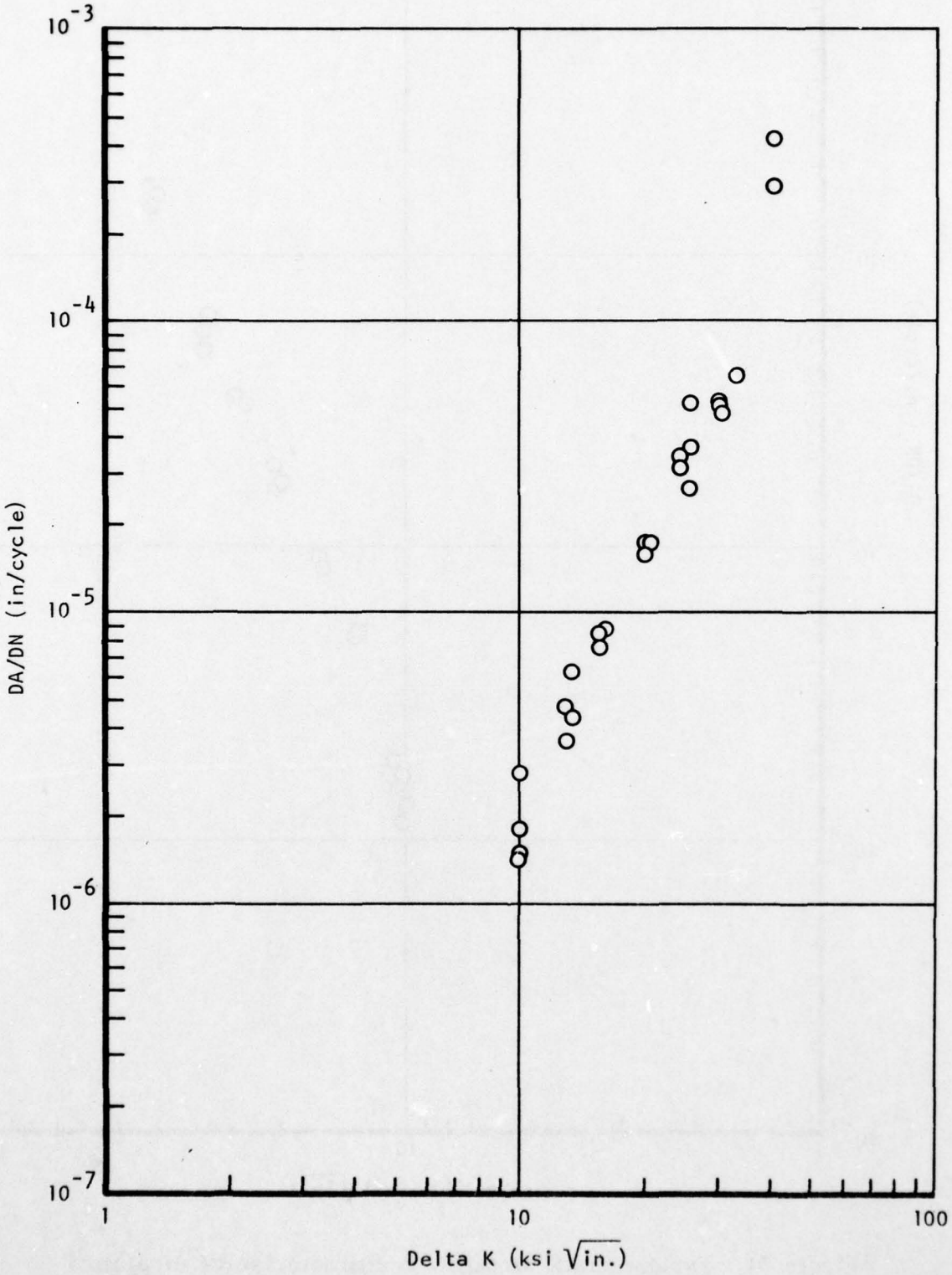

Figure 35. Fatigue crack propagation characteristics of plate F (WR, LHA, R = 0.08).

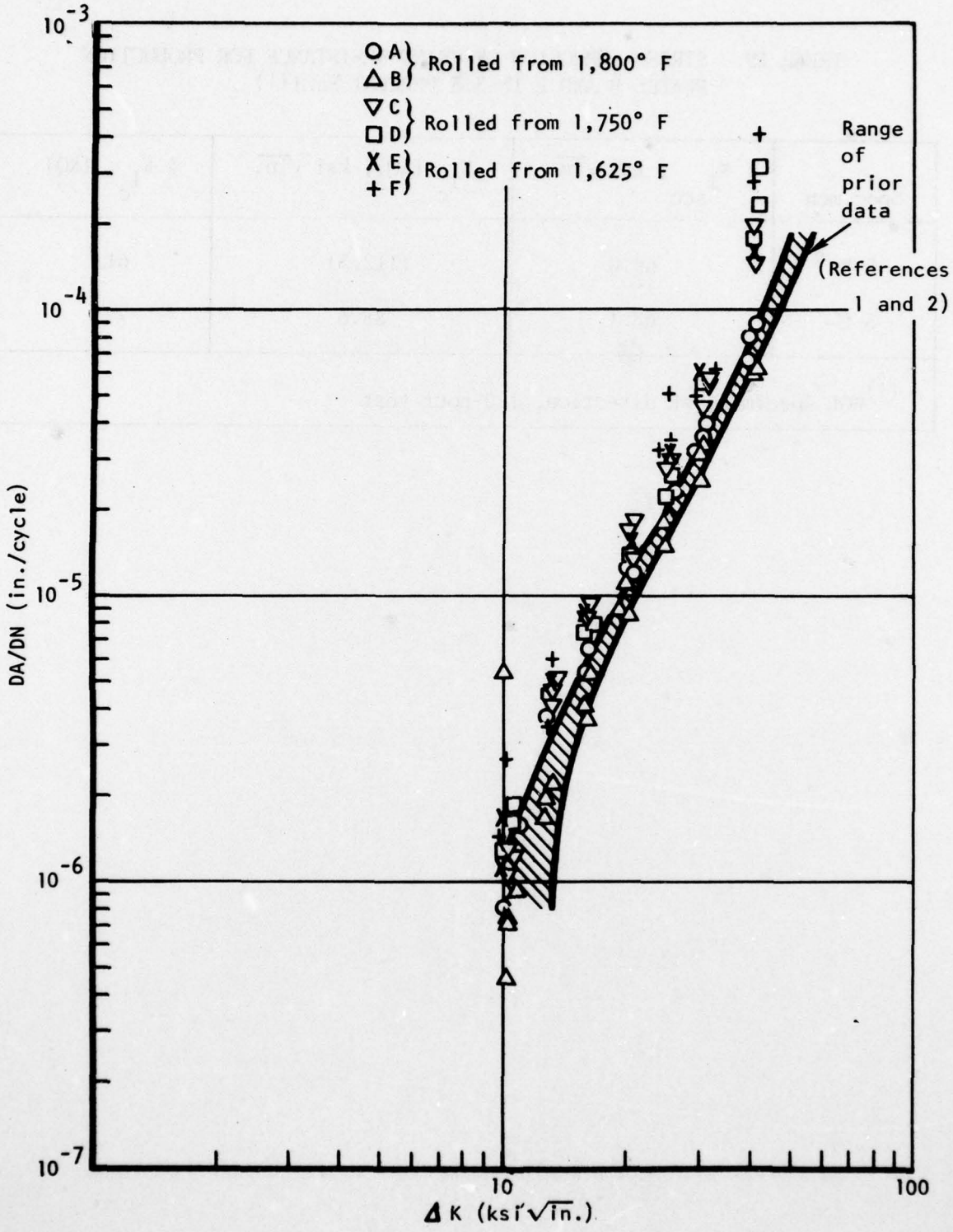

Figure 36. Combined fatigue crack propagation characteristics of production plate. (WR, LHA, R = 0.08).

TABLE 19. STRESS CORROSION CRACKING RESISTANCE FOR PRODUCTION PLATES B AND E IN 3.5 PERCENT NaCl[1]

Specimen	$K_{I_{scc}}$, ksi $\sqrt{in.}$	K_{I_c} (KQ), ksi $\sqrt{in.}$	% K_{I_c}, (KQ)
5-B	69.0	(112.3)	61
5-E	68.1	88.6	77

[1] WOL specimen, WR direction, 100-hour test

MICROSTRUCTURAL CHARACTERIZATION

The microstructure of each of six production processed plate segments is shown in Figures 37 through 42. The orientation of the micrograph, with respect to the plate direction, is indicated in Figure 37 using the convention of ASTM E399-74 where L is parallel to the rolling direction, T parallel to the transverse direction and S parallel to the through-thickness direction. Plates A and B have microstructures which are characteristic of material rolled at temperatures above the beta transus. These microstructures, Figures 37 and 38, consist of coarse, acicular primary alpha plates with an extensive network of alpha phase along the prior beta grain boundaries. The acicular alpha plates, which form by nucleation and growth, have a high-aspect ratio. The microstructures of both plates are quite similar in appearance and differ generally only by the nature of the fine alpha precipitation in the regions between the alpha plates. The effect of the final aging temperature on this fine precipitation reaction and the resulting effect on mechanical properties have been well documented by a study of CORONA-5 forgings (References 3 and 12).

Plates C and D (Figures 39 and 40) have microstructures which result from rolling that starts at a temperature above the beta transus and finishes at a temperature in the alpha-beta phase field. This microstructure consists of primary alpha which has an acicular morphology but with a smaller aspect ratio than the beta-processed material. As in the case of plates A and B, the microstructural difference between plates C and D is found in the transformed beta regions. Plate D has a finer dispersion of precipitated alpha which appears as a darker etching in Figure 40 than the transformed beta of plate C in Figure 39.

Finally, plates E and F, which were rolled starting at a temperature below the beta transus, have microstructures which consist of slightly elongated primary alpha particles in a transformed beta matrix.

CORRELATION OF FRACTURE PROPERTIES AND FRACTOGRAPHY

Fracture toughness, K_{I_C}, and 100-hour stress corrosion cracking threshold, $K_{I_{SCC}}$, results for a production processed plate are repeated in Table 20 together with average transverse tensile properties for the plates produced. The fracture toughness trends for the plate were similar to those for forged material (References 3 and 12) in that the highest toughness values were obtained for material which had been beta processed and that low-temperature aging, which produced higher strength for plate of similar processing history, also produced a commensurate loss in fracture toughness (compare plates A and B, C and D, E and F). For plates C, D, E, and F no significant fracture toughness trend could be established (other than the aging temperature effect); the effect of higher aspect ratio primary alpha in plate C and D is non-

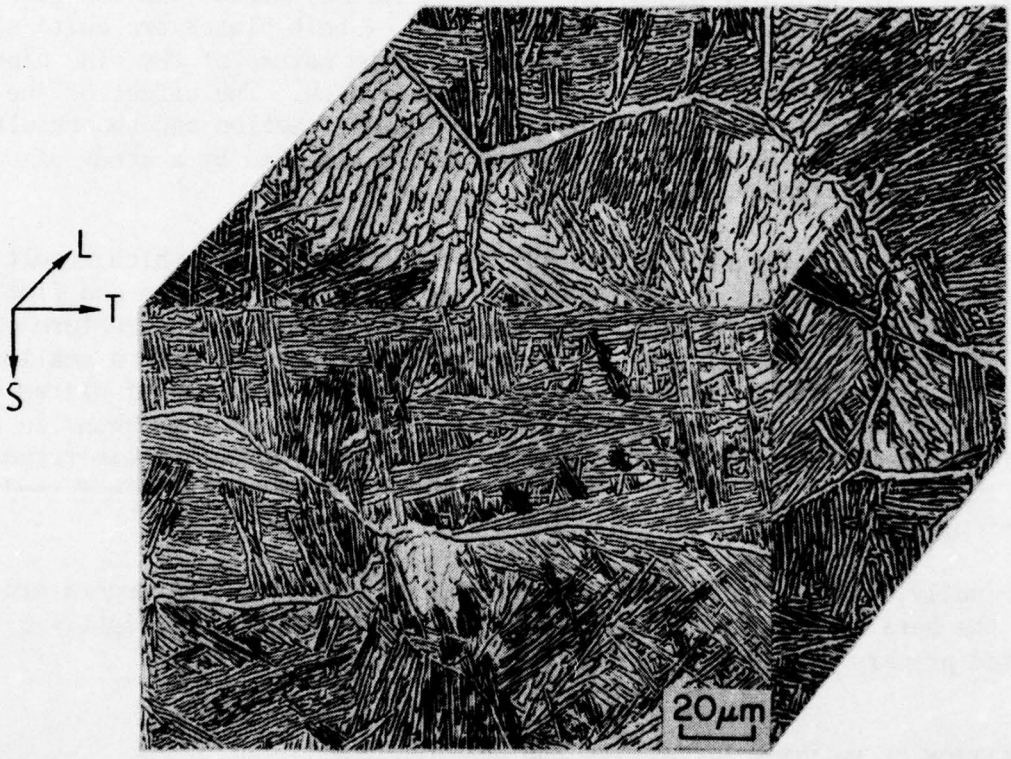

Figure 37. Microstructure of plate A, 500X - orientation, with respect to the rolling direction L, is shown using the convention of ASTM E399-74.

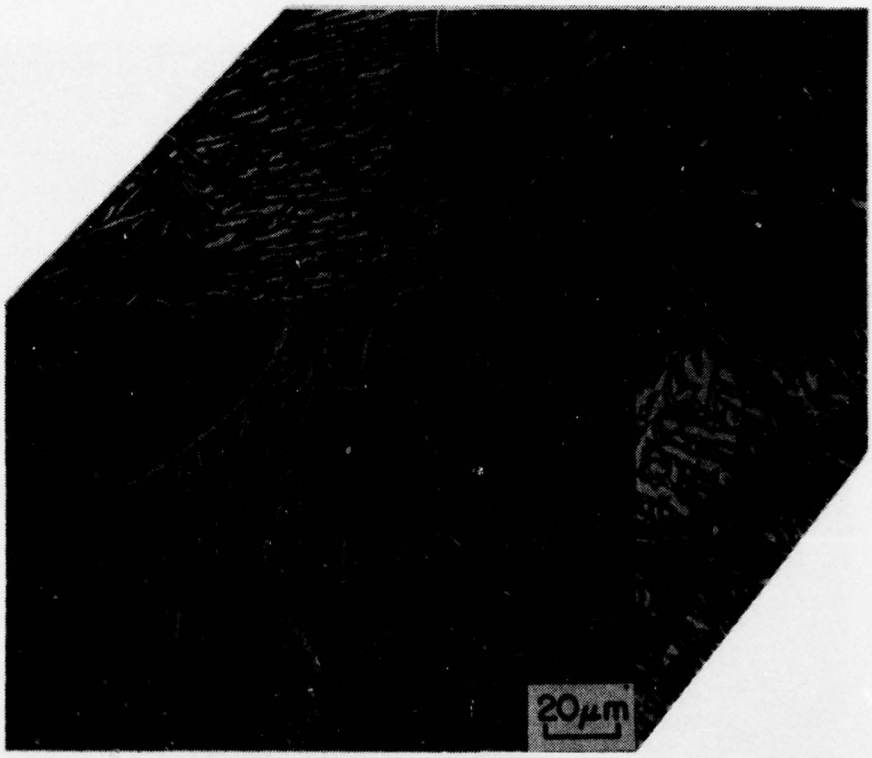

Figure 38. Microstructure of plate B, 500X.

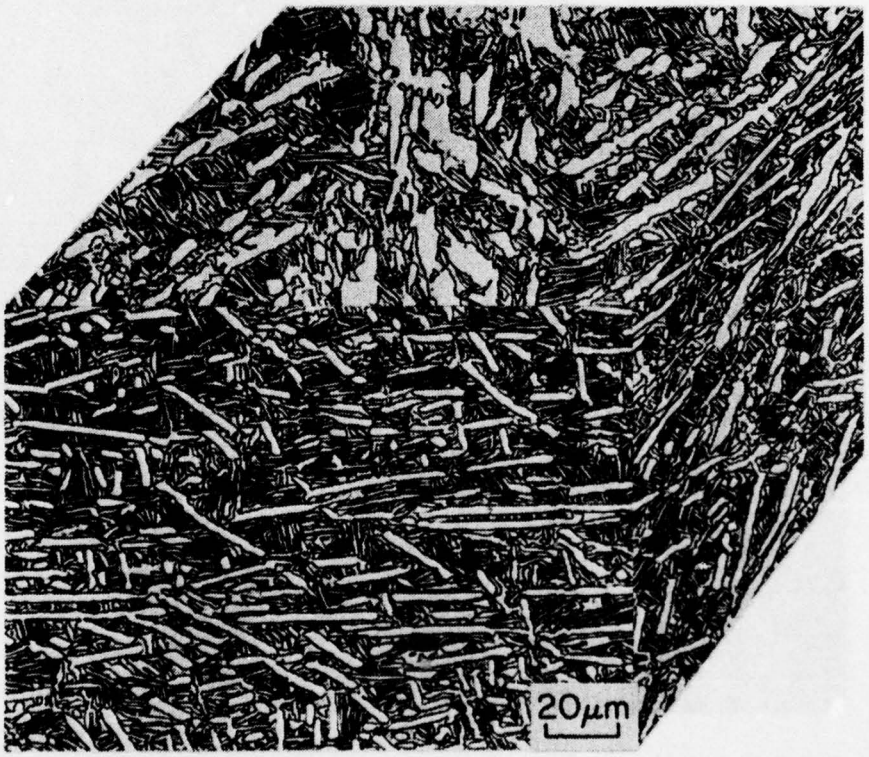

Figure 39. Microstructure of plate C, 500X.

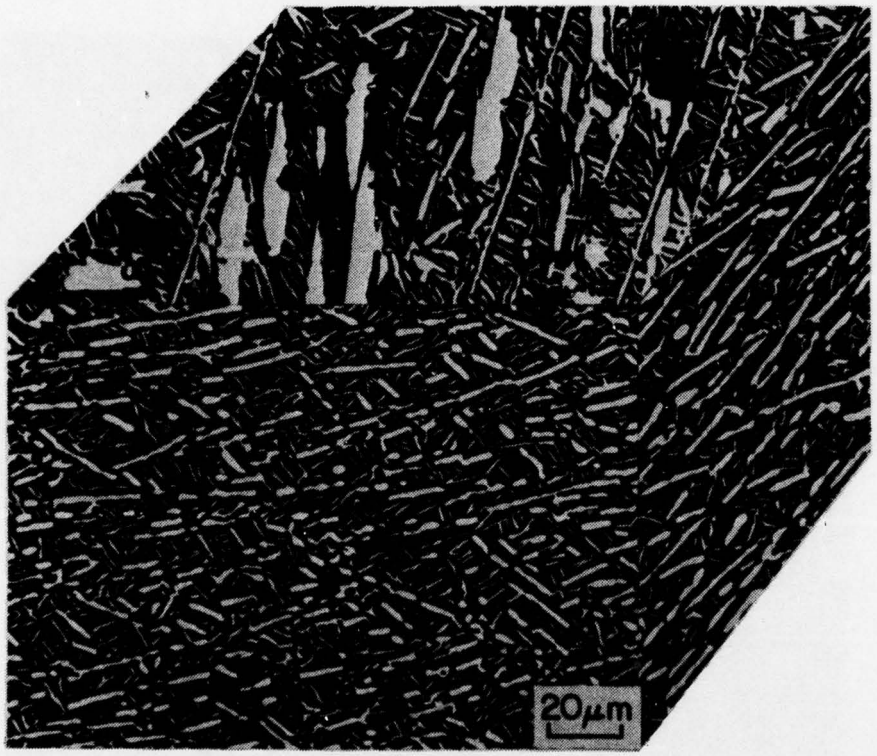

Figure 40. Microstructure of plate D, 500X.

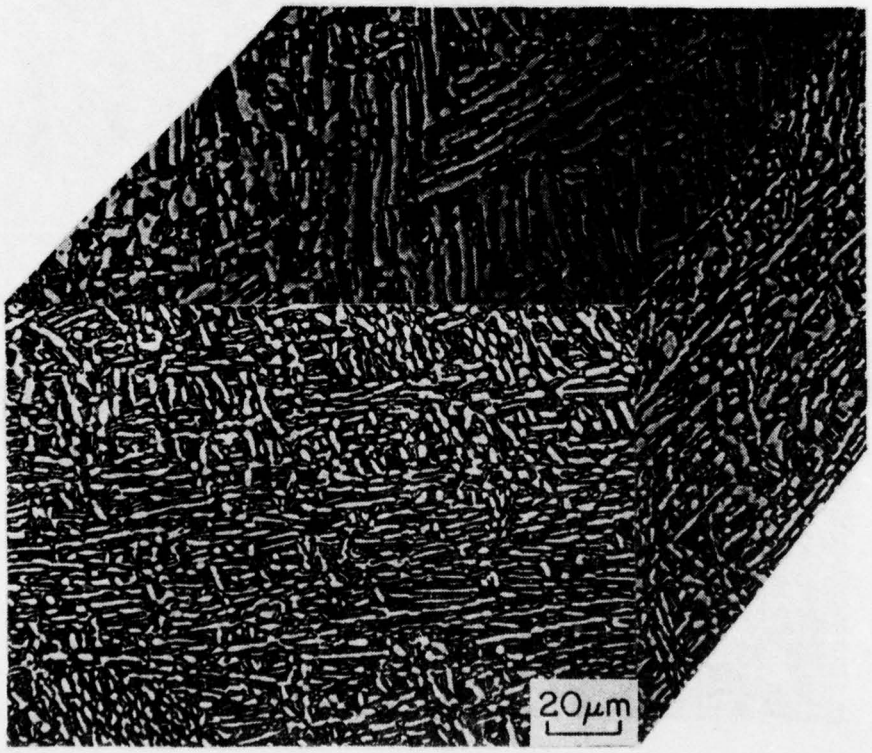

Figure 41. Microstructure of plate E, 500X.

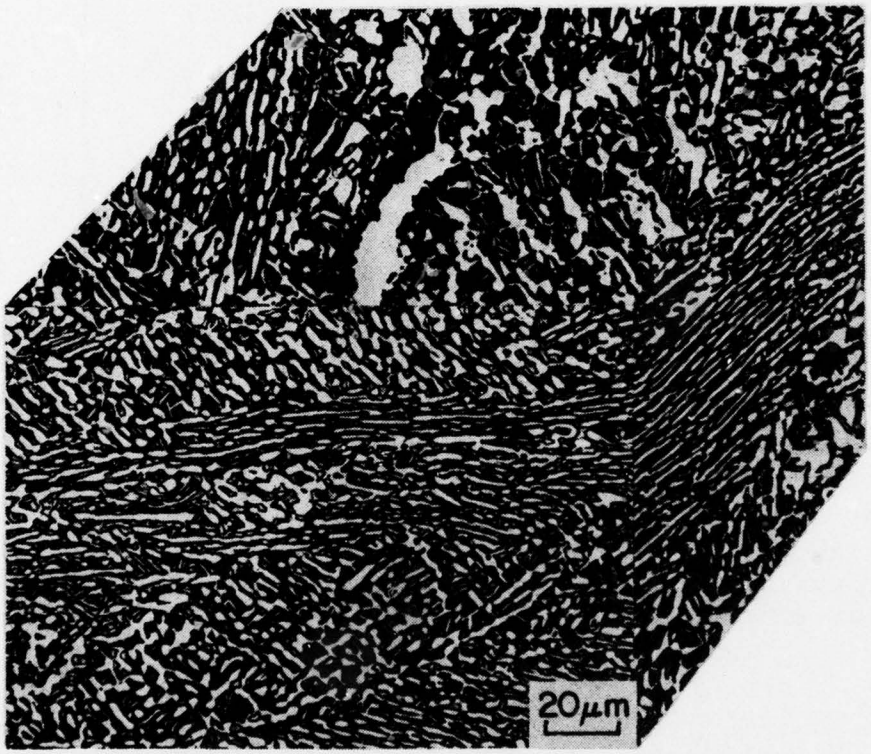

Figure 42. Microstructure of plate F, 500X.

AD-A067 785 ROCKWELL INTERNATIONAL EL SEGUNDO CA LOS ANGELES DIV F/G 11/6
FRACTURE TOUGHNESS IN TITANIUM ALLOYS.(U)
DEC 78 G R KELLER, J C CHESNUTT, F H FROES N00019-76-C-0427
UNCLASSIFIED NA-78-917 NL

2 OF 2
AD
A067 785

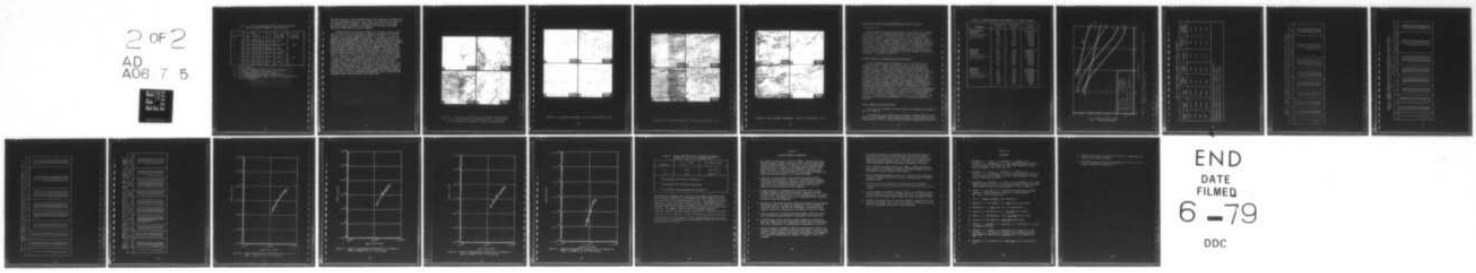

END
DATE
FILMED
6-79
DDC

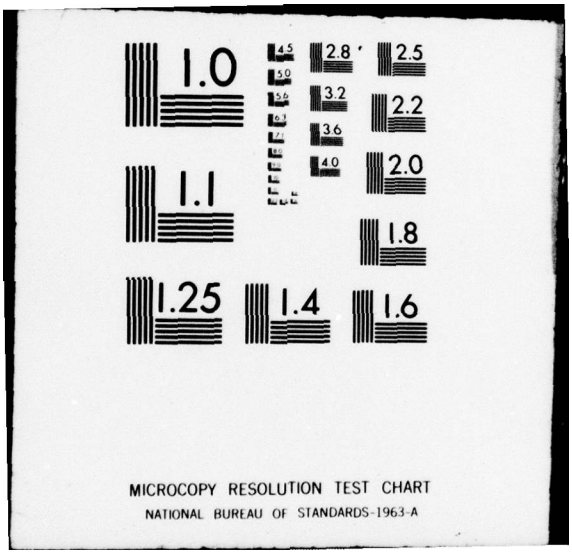
1.0
1.1
1.25
1.4
1.6
1.8
2.0
2.2
2.5
2.8
3.2
3.6
4.0
4.5
5.0
5.6
6.3
7.1
8.0
9.0
MICROCOPY RESOLUTION TEST CHART
NATIONAL BUREAU OF STANDARDS-1963-A

TABLE 20. TENSILE, FRACTURE TOUGHNESS, AND STRESS-CORROSION-CRACKING-THRESHOLD SUMMARY OF PRODUCTION PLATE

Plate (1)	UTS (2) ksi	TYS ksi	e %	RA %	K_{I_C} (K_Q) (3) ksi $\sqrt{in}$	$K_{I_{SCC}}$ (3) ksi $\sqrt{in}$
A	139	134	15.4	33.3	124.1	
B	150	140	13.0	26.9	(112.3) (4)	69.0
C	142	141	17.8	39.9	76.3	
D	159	154	12.4	35.4	(60) (5)	
E	140	139	18.3	50.1	88.6	68.1
F	162	157	11.9	37.2	53.6	

(1) Refer to Table 5.
(2) All tensile specimens in transverse (T) orientation.
(3) K_{I_C} and $K_{I_{SCC}}$ specimens in TL orientation.
(4) Failed precrack shape requirement of ASTM E399-74.
(5) Failed during precracking; value estimated from fracture surface and precrack loading.

existent since most of the elongated primary alpha particles are aligned with the crack propagation direction. This result is in contrast to the case in the forgings in which randomly oriented, high-aspect ratio primary alpha particles (Figure 9, Reference 3 and Figure 1(b), Reference 12) produce significant enhancement of fracture toughness.

Scanning election fractography (Figures 43, 44, and 45) further illustrate the effect of beta processing on toughness enhancement and show the similarities in fracture topography of plates C, D, E and F. For each K_{I_C} specimen, a pair of micrographs is presented. A low magnification micrograph of the fatigue precrack-to-overload (K_{I_C}) transition zone and a higher magnification micrograph of the overload region near the transition is presented for beta processed material in Figure 43. This illustrates the abrupt transition and the highly irregular fracture topography that occur in this processing mode, resulting in high fracture toughness. The remaining four plates (Figures 44 and 45) exhibited relatively smooth transitions and fine equiaxed, dimpled fracture consistent with moderate-to-low toughness conditions in this alloy. The $K_{I_{SCC}}$ values for plates B and E were 0.61 K_Q and 0.77 K_{I_C}, respectively. Fractographs of the two $K_{I_{SCC}}$ specimens are shown in Figure 46. Higher magnification micrographs of the stress-corrosion cracking region of the specimens (Figure 46, (b) and (d) show faceted-corrosion cracking similar to that observed in other titanium alloys. Some secondary cracking perpendicular to the plane of the fracture is observed in Figure 46, (a) and (c), which corresponds to cracking parallel to the LT plane in Figures 38 and 41. The plane could contain easy crack propagation directions as a result of elongated grain boundaries in the former case and elongated primary alpha particles in the latter case.

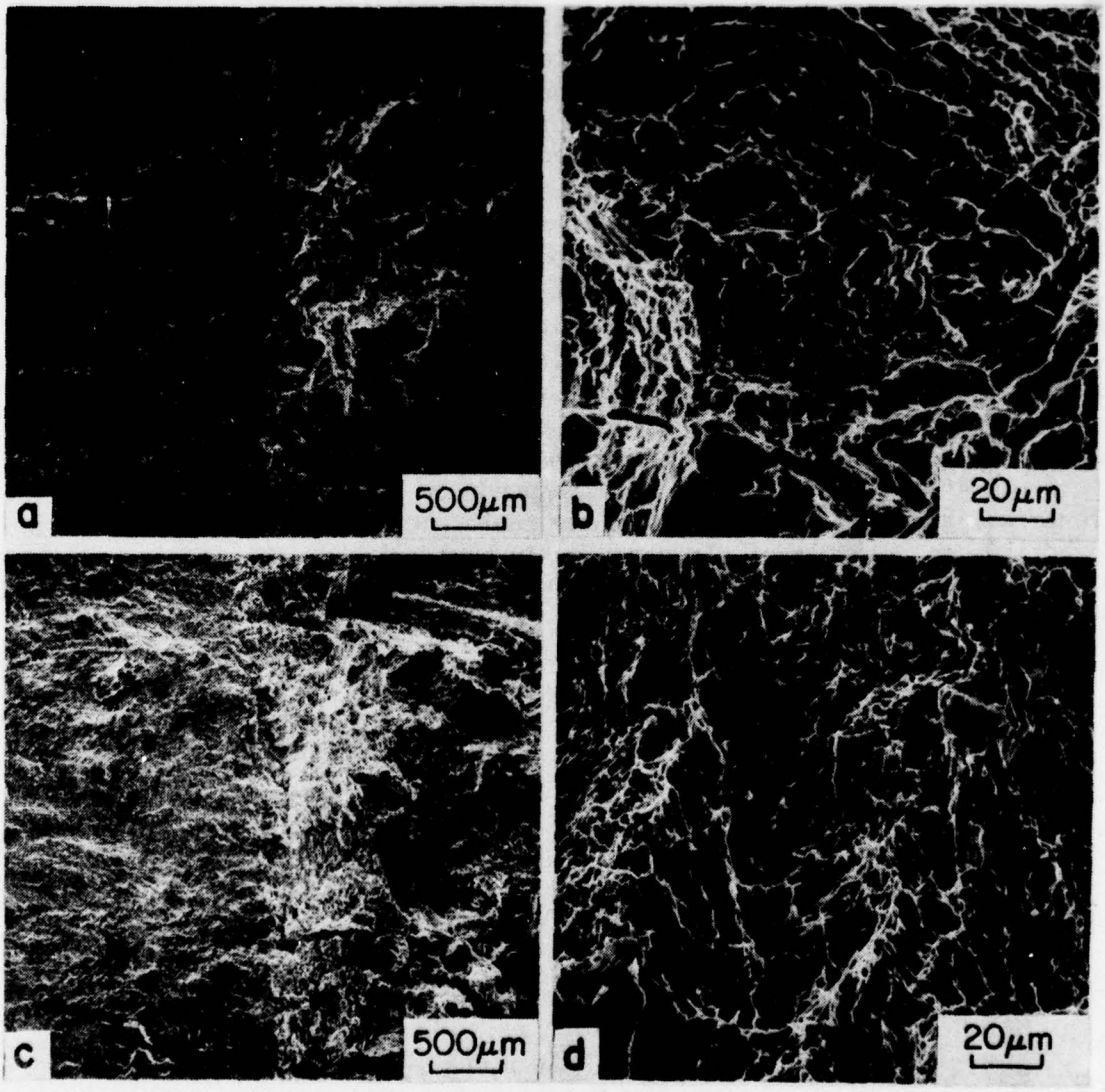

Figure 43. Fractographs (scanning election micrographs) of the fracture faces of K_{I_C} specimens plate A (a,b) and plate B (c,d) - the direction of crack propagation is from left to right in all micrographs.

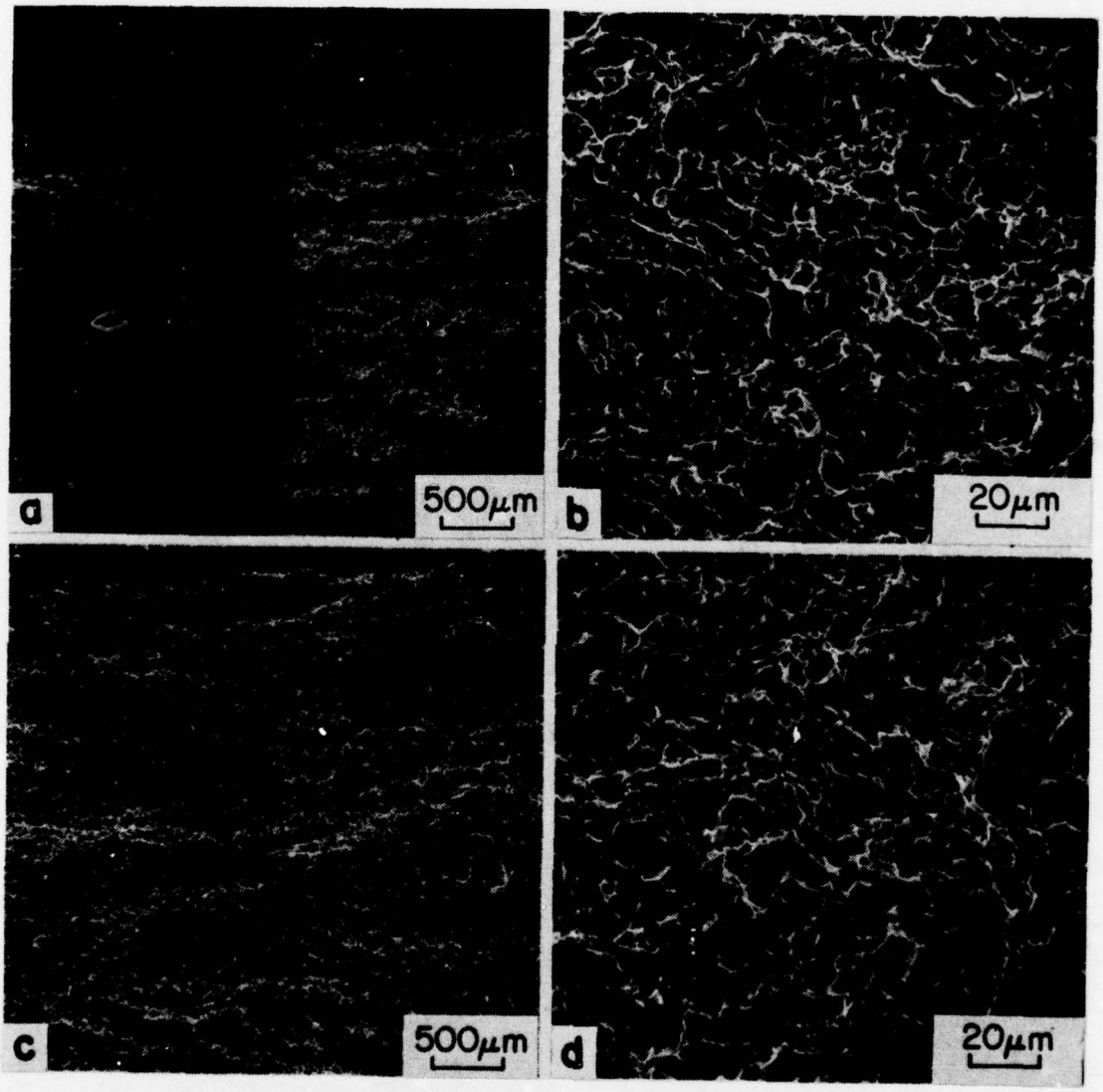

Figure 44. K_{IC} specimen fractographs - plate C (a,b) and plate D (c,d).

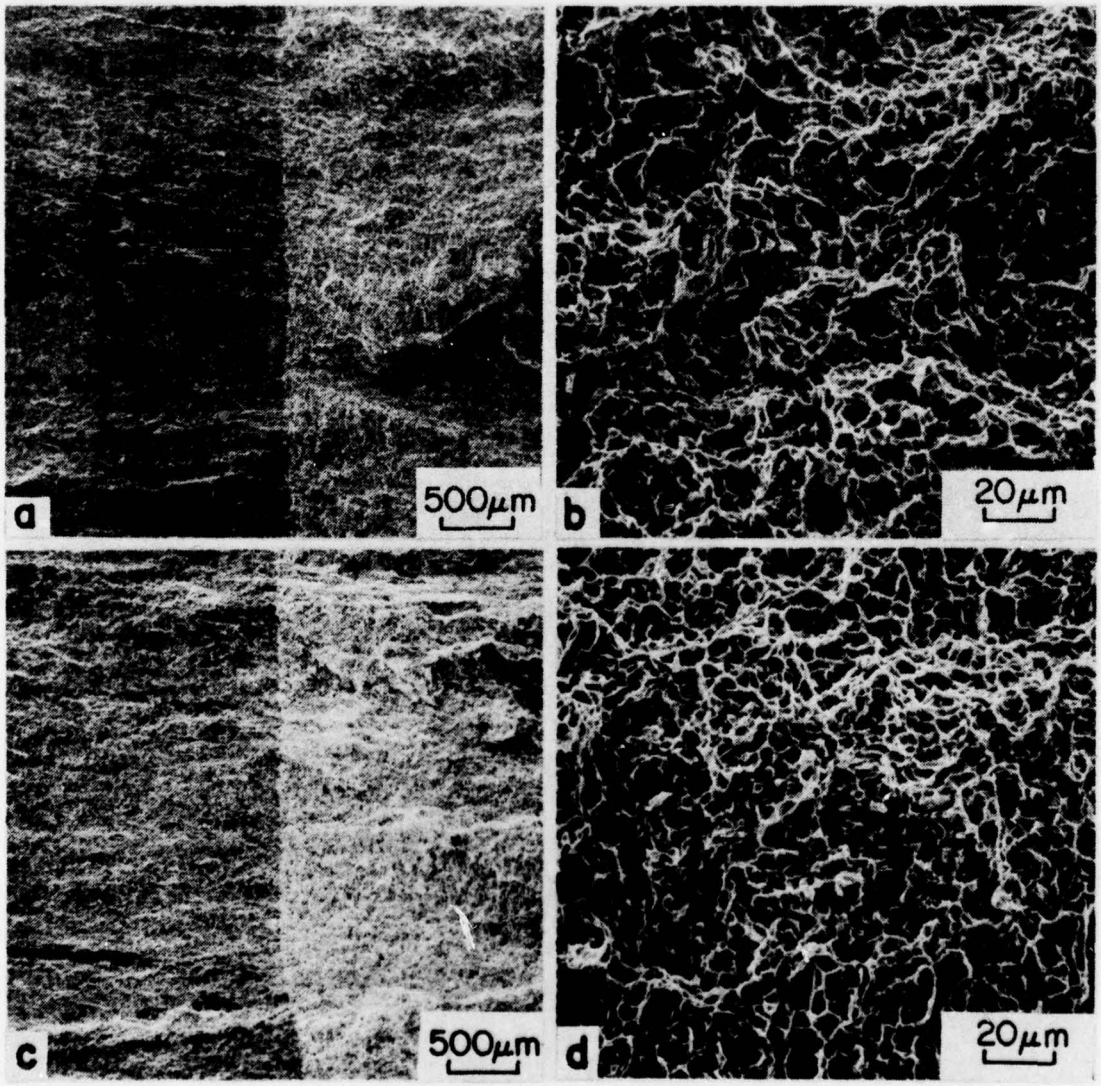

Figure 45. K_{IC} specimen fractographs - plate E (a,b) and plate F (c,d).

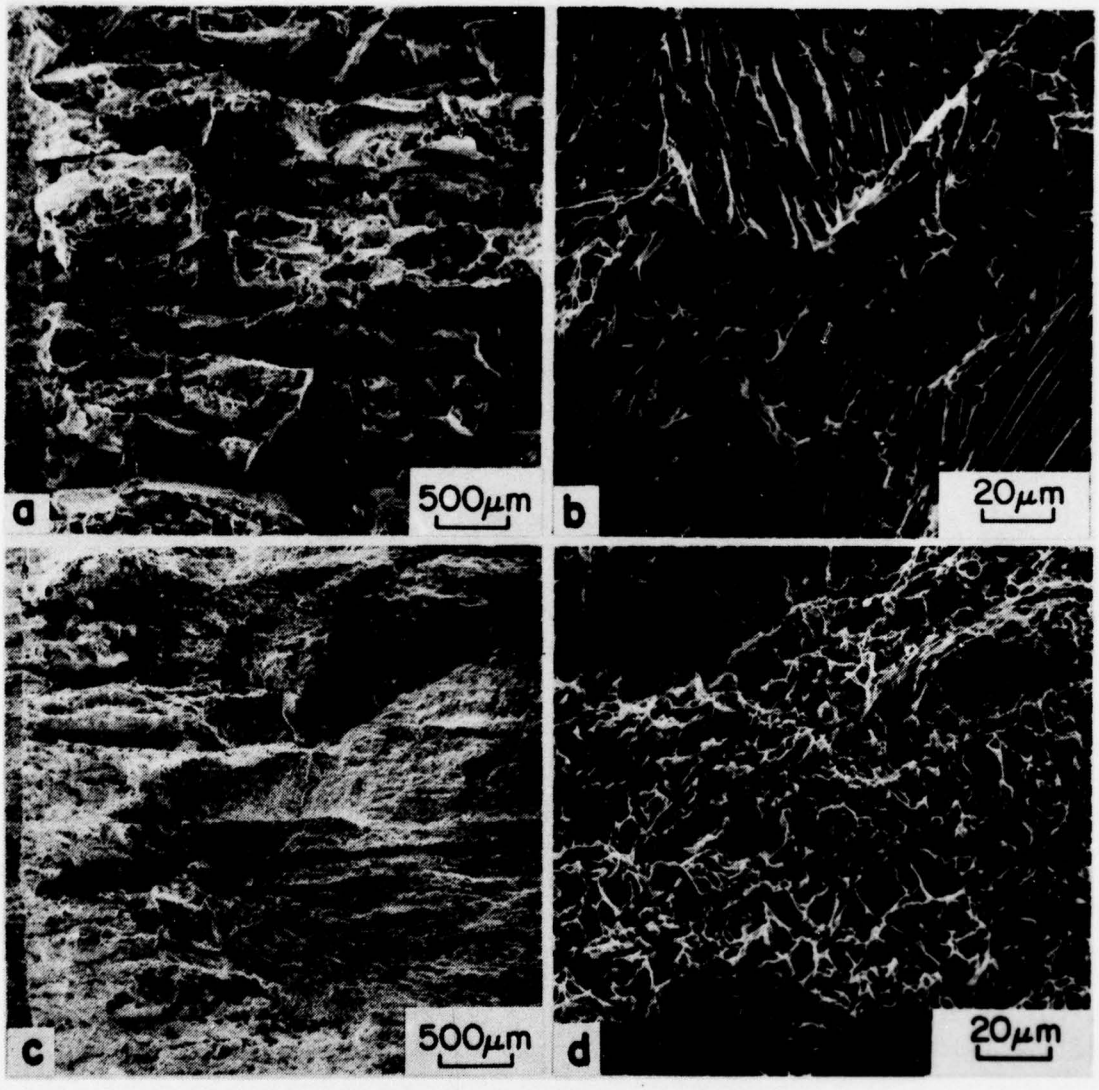

Figure 46. K_{ISCC} specimens fractographs - plate B (a,b) and plate E (c,d).

EVALUATION OF FORGINGS PRODUCED UNDER CONTRACT N00019-75-C-0208

FATIGUE PROPERTIES

Fatigue data for beta processed forging 5-2 heat treated to a nominal strength of 145 ksi (1,000 MPa) and for alpha beta processed forging 5-11 heat treated to 135 ksi (930 MPa) at two stress ratios are presented in Table 21 and Figure 47. Also shown in Figure 47 are typical S-N curves for cond RA Ti-6Al-4V for comparison purposes. The results indicate a significantly higher level of fatigue strength associated with alpha-beta processed material R = 0.5 than for the beta forged material. Decreasing the R factor to 0.1 produces a reduction in fatigue strength at cycles beyond 5×10^5; however, the latter compares favorably with the typical curve plotted for Ti-6Al-4V. This behavior is consistent with results recorded for production plate at Kt = 1 as shown in Figure 29.

FRACTURE TOUGHNESS AND FATIGUE CRACK PROPAGATION DATA

Fracture toughness data for forgings 5-1, 5-3, 5-5, and 5-12 are presented in Table 22 together with tensile data for the same specimen loading direction. Fatigue crack propagation data generated during precracking of the K_{I_C} specimens are presented in Tables 23 through 26 and Figures 48 through 51. The fracture toughness results reflect the influence of the primary alpha phase morphology produced by processing. Forgings 5-3 and 5-5 reveal a structure characterized by lenticular primary alpha with no continuous grain boundary alpha network. These forgings exhibited the highest toughness values. Somewhat lower toughness was produced in forging 5-1, which contained an acicular alpha Widmanstatten microstructure with continuous grain boundary alpha network. Comparatively low fracture toughness was obtained in forging 5-12 due to the formation of a nearly equiaxed globular alpha microstructure. In contrast, fatigue crack propagation results show no apparent sensitivity to changes in primary alpha morphology. A comparison of Figures 48 through 51 indicates nearly identical growth rates over the range of ΔK's from 15 to 40 ksi $\sqrt{in}$. (17 to 44 MPa$\sqrt{m}$). This suggests a matrix-controlled phenomenon for crack propagation under these conditions.

STRESS CORROSION CRACKING RESISTANCE

Stress corrosion cracking resistance results are presented for forgings 5-1 and 5-3 in Table 27.

One hundred-hour K_{Iscc} measurements were made on specimens taken from the compact tension specimens used to generate the fatigue-crack-growth-rate curves from forgings 5-1 and 5-3. These two microstructural conditions were chosen to

TABLE 21. ROOM TEMPERATURE FATIGUE PROPERTIES OF CORONA-5 FORGINGS

Condition	Max stress (ksi)	Max stress (% Ftu)	Cycles to failure
Beta processed	100	69.3	10,000,000 NF
forging 5-2	105	72.8	2,534,000
at R = 0.5, Kt = 1;	110	76.3	629,000
Ftu = 144.2 ksi	112	77.7	485,000
	115	79.8	182,000
	117.5	81.5	91,000
	120	83.2	50,000
	125	86.7	7,000
Alpha-beta	108	79.8	10,000,000 NF
processed	110	81.3	7,982,000
forging 5-11	115	85.0	4,460,000
at R = 0.5, Kt = 1;	120	88.7	1,869,000
Ftu = 135.3 ksi	122.5	90.5	1,938,000
	125	92.4	93,000
	127	93.9	107,000
	130	96.1	60,000
Alpha-beta	75	55.4	8,474,000
processed	85	62.8	10,000,000 NF
forging 5-11	100	73.9	1,630,000
at R = 0.1, Kt = 1;	110	81.3	1,249,000
Ftu = 135.3 ksi	120	88.7	682,000
	122.5	90.5	329,000
	125	92.4	64,000
	127.5	94.2	46,000

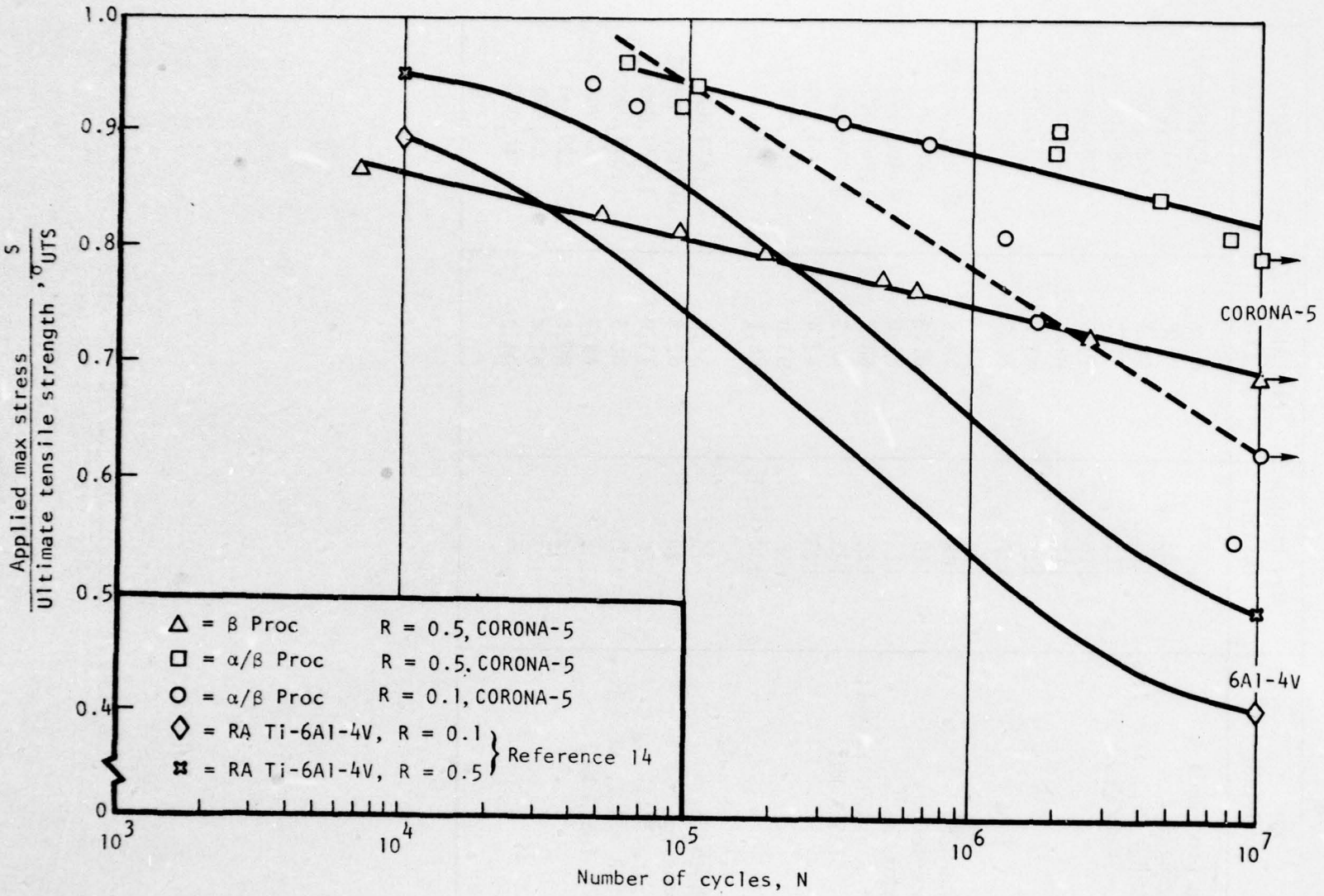

Figure 47. Comparison of room-temperature, normalized fatigue properties of CORONA-5 and Ti-6Al-4V at R = 0.1 and R = 0.5.

TABLE 22. FRACTURE TOUGHNESS PROPERTIES OF CORONA-5 FORGINGS[1]

Forging No.	Blocker temp	Finish temp	Ultimate strength (ksi)	Yield strength (ksi)	Elongation (%)	Reduction of area (%)	Fracture toughness (ksi $\sqrt{in.}$)
1[2]	1,750° F	1,750° F	136.4	123.4	12.0	20.8	121.6
3[2]	1,750° F	1,675° F	141.7	126.4	15.3	31.3	148.0
5[2]	1,750° F	1,600° F	145.2	129.3	13.4	20.0	145.9
12[3]	1,625° F	1,600° F	148.7	136.2	10.4	14.8	53.6

[1] All tests conducted in the transverse or WR grain direction.

[2] Annealed and aged 1,550° F/8 hr/AC + 1,3000° F/4 hr/AC.

[3] Annealed and aged, 1,475° F/16 hr/AC + 1,125° F/4 hr/AC.

TABLE 23. COMPUTER TABULATION OF FATIGUE CRACK PROPAGATION DATA FOR CORONA-5 FORGING 1 - 5NRW F-1, CORONA-5, FORGING 1, LA, RT, R = 0.08, 600 CPM, W = 4.20, H = 2.52, B = 2.105

	A	B	DA	DN	Max LD	Min LD	DA/DN (10^{-6} in./CY)	DK
1	1.349	1.384						
2	1.387	1.414	0.034	10000.0	10000.0	800.00	3.400	13242
3	1.418	1.454	0.036	15000.0	10000.0	800.00	2.367	13482
4	1.460	1.478	0.033	5000.0	12000.0	960.00	6.600	16475
5	1.506	1.514	0.041	9000.0	12000.0	960.00	4.556	16810
6	1.578	1.577	0.068	6000.0	14000.0	1120.00	11.250	20212
7	1.645	1.641	0.066	6000.0	14000.0	1120.00	10.917	20996
8	1.721	1.714	0.074	4000.0	16000.0	1280.00	18.625	25003
9	1.799	1.788	0.076	2500.0	18000.0	1440.00	30.400	29434
10	1.835	1.838	0.043	1000.0	20000.0	1600.00	43.000	33928
11	1.994	2.015	0.168	3500.0	20000.0	1600.00	48.000	36284
12	2.049	2.049	0.044	1000.0	20000.0	1600.00	44.499	38943
13	2.108	2.097	0.054	900.0	20000.0	1600.00	59.445	40285

TABLE 24. COMPUTER TABULATION OF FATIGUE CRACK PROPAGATION OF CORONA-5 FORGING 3 - 5NRW F-3, CORONA-5, FORGING 3, LA, RT, R = 0.08, 600 CPM, W = 4.20, H = 2.52, B = 2.104

	A	B	DA	DN	Max LD	Min LD	DA/DN (10^{-6} in./CY)	DK
1	1.293	1.365						
2	1.331	1.388	0.030	11500.0	10000.0	800.00	2.652	12979
3	1.357	1.406	0.022	10000.0	10000.0	800.00	2.200	13150
4	1.407	1.455	0.049	4000.0	15000.0	1200.00	12.375	20089
5	1.439	1.478	0.028	2000.0	15000.0	1200.00	13.750	20500
6	1.493	1.524	0.050	3000.0	17500.0	1400.00	16.667	24422
7	1.550	1.577	0.055	3000.0	17500.0	1400.00	18.333	25142
8	1.611	1.636	0.060	3000.0	17500.0	1400.00	20.000	25978
9	1.675	1.702	0.065	3000.0	17500.0	1400.00	21.667	26941
10	1.741	1.768	0.066	3000.0	17500.0	1400.00	22.000	28013
11	1.793	1.818	0.051	2000.0	17500.0	1400.00	25.500	29030
12	1.853	1.876	0.059	2000.0	17500.0	1400.00	29.500	30040
13	1.920	1.942	0.067	2000.0	17500.0	1400.00	33.250	31261
14	1.998	2.012	0.074	2000.0	17500.0	1400.00	37.000	32728
15	2.096	2.102	0.094	2200.0	17500.0	1400.00	42.727	34641

TABLE 25. COMPUTER TABULATION OF FATIGUE CRACK PROPAGATION DATA FOR CORONA-5 FORGING 5 - 5NRW F-5, CORONA-5, FORGING 5, LA, RT, R = 0.08, 600 CPM, W = 4.20, H = 2.52, B = 2.107

	A	B	DA	DN	Max LD	Min LD	DA/DN (10^{-6} in./CY)	DK
1	1.320	1.333						
2	1.358	1.384	0.044	7000.0	10000.0	800.00	6.357	13004
3	1.392	1.417	0.034	10000.0	10000.0	800.00	3.350	13262
4	1.430	1.466	0.043	15000.0	10000.0	800.00	2.900	13530
5	1.464	1.527	0.048	6000.0	12000.0	960.00	7.917	16637
6	1.524	1.589	0.061	9000.0	12000.0	960.00	6.778	17142
7	1.584	1.638	0.054	5000.0	14000.0	1120.00	10.900	20664
8	1.621	1.663	0.031	2000.0	14000.0	1120.00	15.500	21182
9	1.673	1.710	0.049	4000.0	14000.0	1120.00	12.375	21690
10	1.754	1.789	0.080	4000.0	16000.0	1280.00	20.000	25769
11	1.785	1.817	0.030	1000.0	18000.0	1440.00	29.500	29978
12	1.815	1.843	0.028	1000.0	18000.0	1440.00	28.000	30518
13	1.846	1.874	0.031	1000.0	18000.0	1440.00	31.000	31088
14	1.889	1.914	0.042	1000.0	20000.0	1600.00	41.500	35347
15	1.932	1.959	0.044	1000.0	20000.0	1600.00	44.000	36336
16	1.979	2.006	0.047	1000.0	20000.0	1600.00	47.000	37439
17	2.030	2.056	0.050	1000.0	20000.0	1600.00	50.500	38686
18	2.082	2.118	0.057	1000.0	20000.0	1600.00	57.000	40146

TABLE 26. COMPUTER TABULATION OF FATIGUE CRACK PROPAGATION DATA FOR CORONA-5 FORGING 12 - CORONA-5, 5NTSF-12, 68F, DRY AIR, 10HZ, R = 0.1, W = 2.00, H = 1.20, R = 1.000, AN = 12248.0, 0.474 INCHES

	AF (Fu)	AS (in.)	DA (in.)	DN (Cycles)	Max LD (lb)	Min LD	ABAR (in.)	DA/DN (in./CY)	DK (ksi $in.^{0.5}$)	K Max (ksi $in.^{0.5}$)
1	1.	0.595								
2	3775.	0.620	0.025	220000.0	2000.0	200.0	0.608	1.1311E-07	7.495	8.328
3	4481.	0.647	0.027	20000.0	2000.0	200.0	0.634	1.3661E-06	7.692	8.546
4	5203.	0.675	0.028	100000.0	2000.0	200.0	0.661	2.7941E-07	7.918	8.798
5	5985.	0.706	0.030	120000.0	2200.0	220.0	0.690	2.5220E-07	8.993	9.992
6	6774.	0.736	0.031	108000.0	2200.0	220.0	0.721	2.8273F-07	9.812	10.346
7	7663.	0.771	0.034	50000.0	2400.0	240.0	0.753	6.8809E-07	10.556	11.729
8	8430.	0.800	0.030	30000.0	2400.0	240.0	0.785	9.8943E-07	10.977	12.196
9	9197.	0.830	0.030	25000.0	2600.0	260.0	0.815	1.1873E-06	12.340	13.712
10	10057.	0.863	0.033	15000.0	2600.0	260.0	0.847	2.2188E-06	12.847	14.274
11	10915.	0.896	0.033	7500.0	2800.0	280.0	0.880	4.4273E-06	14.449	16.055
12	11650.	0.925	0.028	7000.0	2800.0	280.0	0.911	4.0635E-06	15.059	16.732
13	12530.	0.959	0.034	7000.0	3000.0	300.0	0.942	4.8651E-06	16.845	18.716
14	13643.	1.002	0.043	7000.0	3000.0	300.0	0.980	6.1533E-06	17.797	19.774

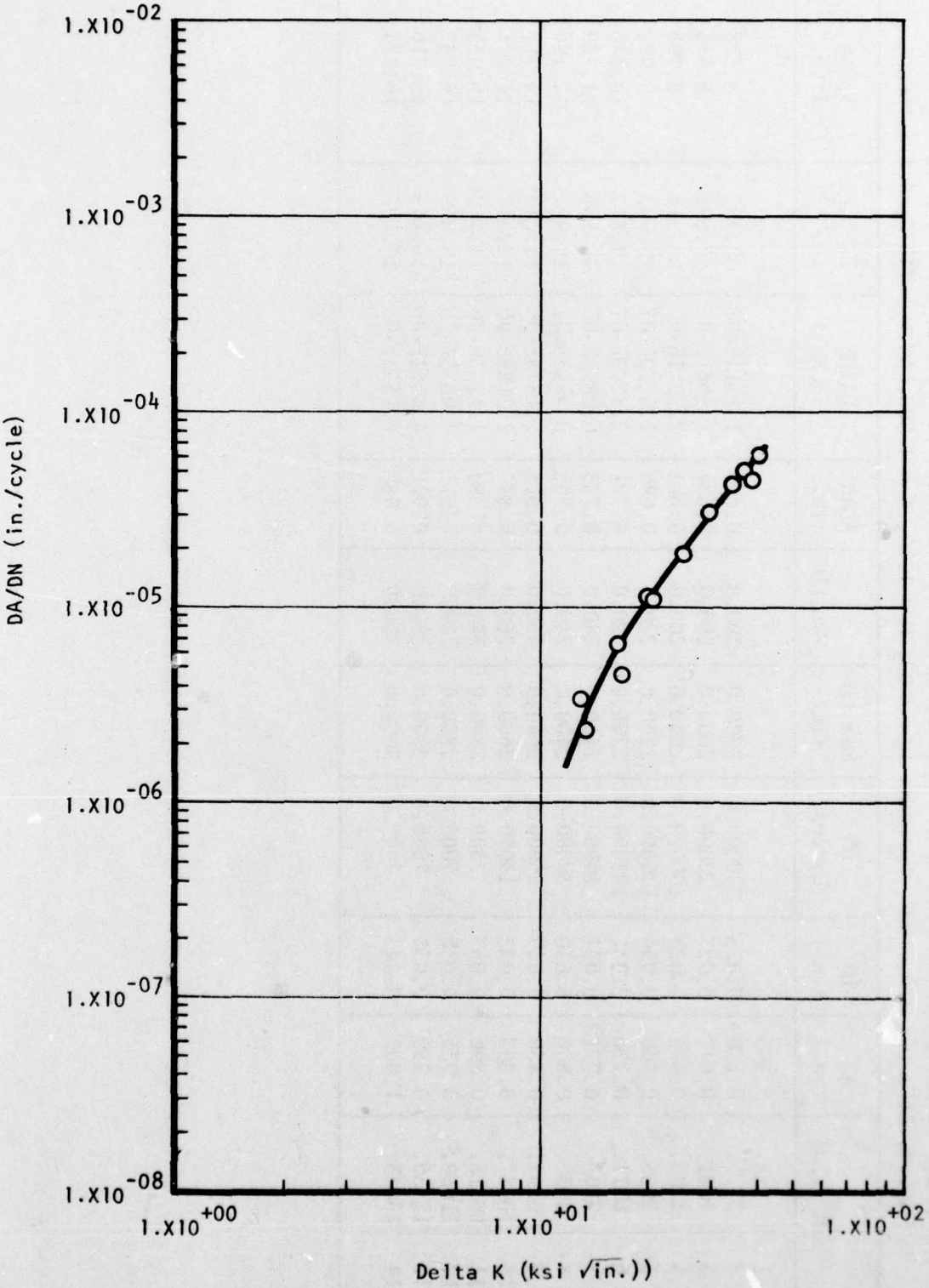

Figure 48. Fatigue crack propagation characteristics of forging 5-1, 5 NRW F-1, CORONA-5, RT, R = 0.08, 600 cpm.

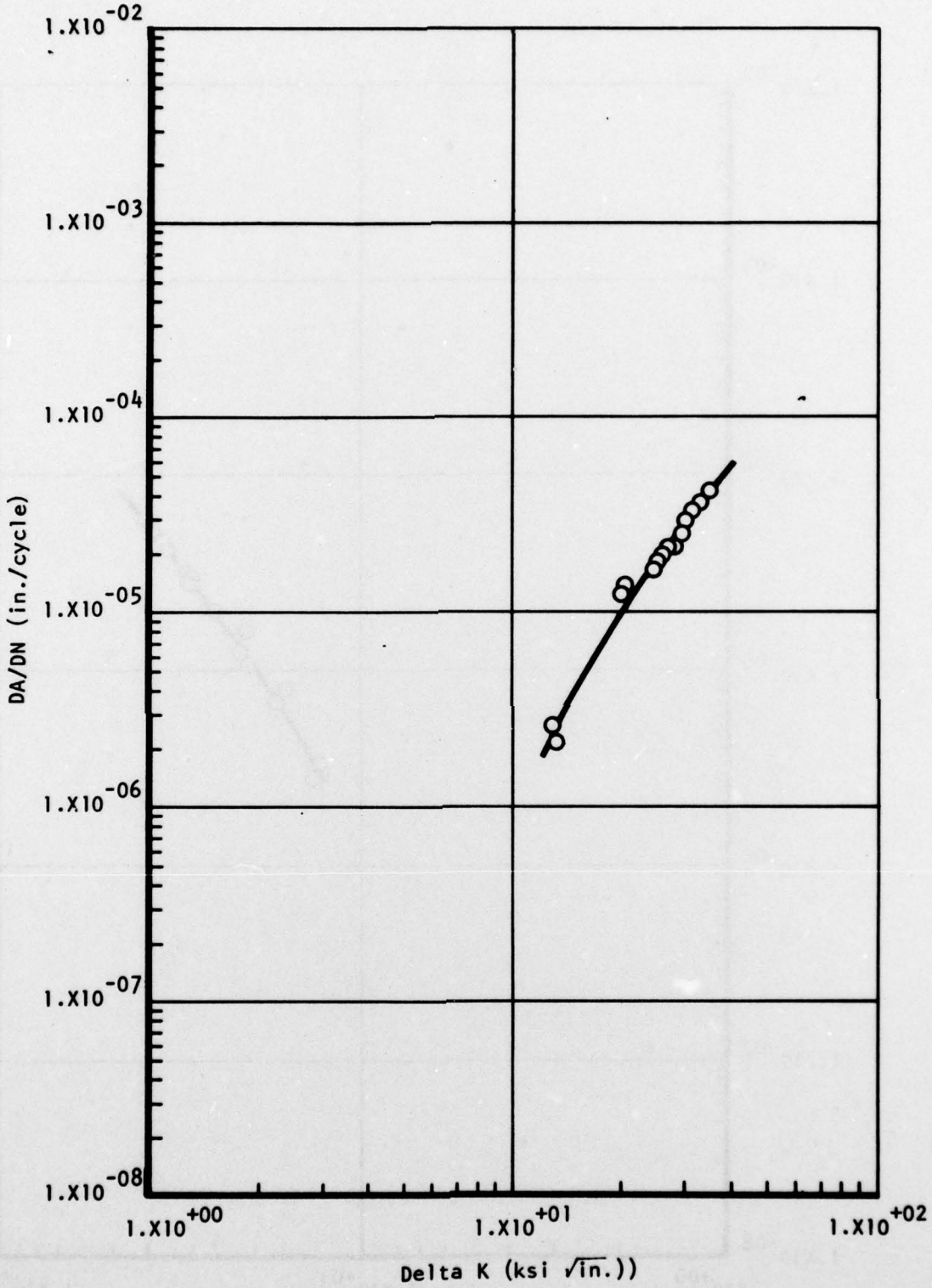

Figure 49. Fatigue crack propagation characteristics of forging 5-3, 5 NRW F-3, CORONA-5, RT, R = 0.08, 600 cpm.

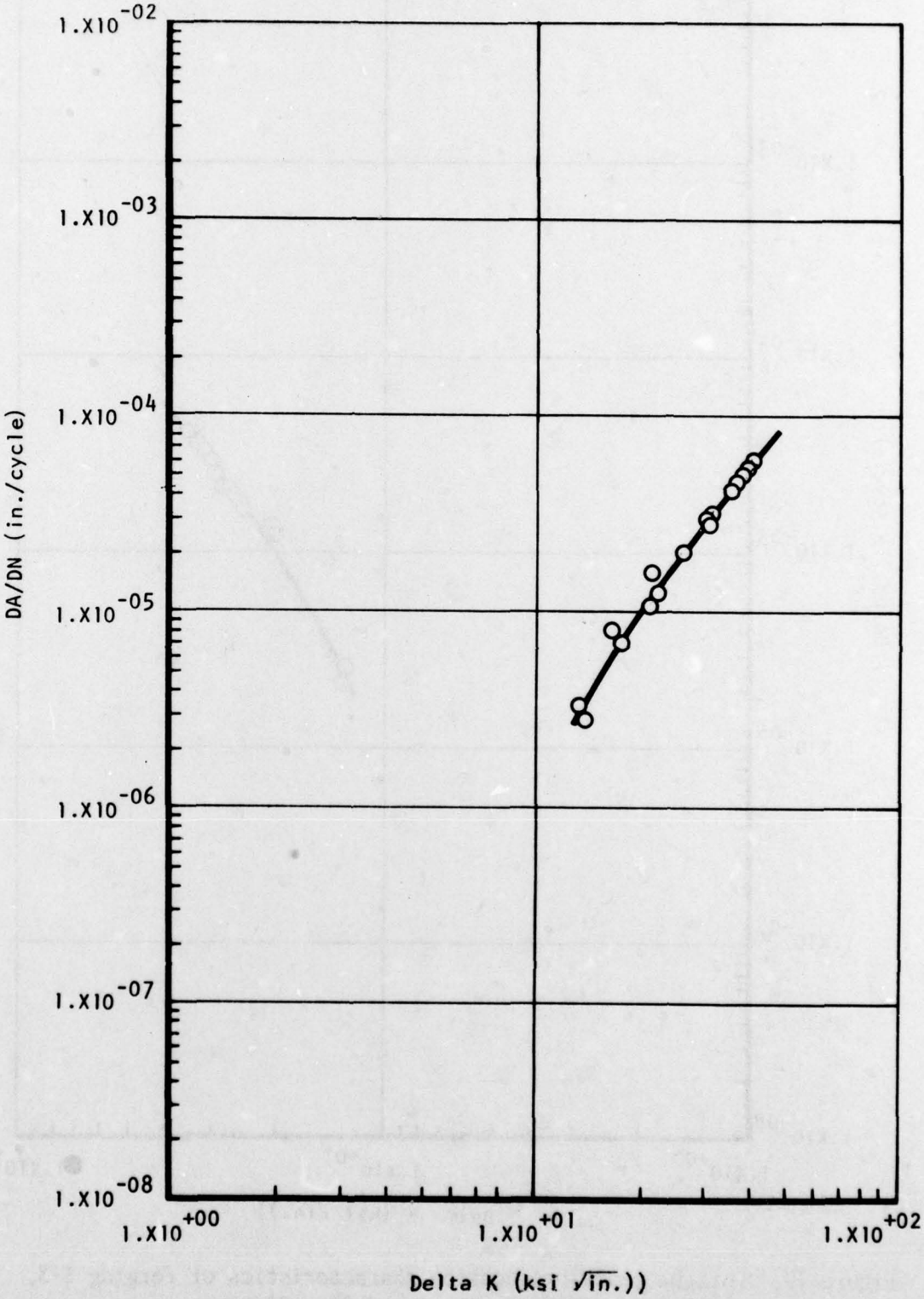

Figure 50. Fatigue crack propagation characteristics of forging 5-5, 5 NRW F-5, CORONA-5, RT, R = 0.08, 600 cpm.

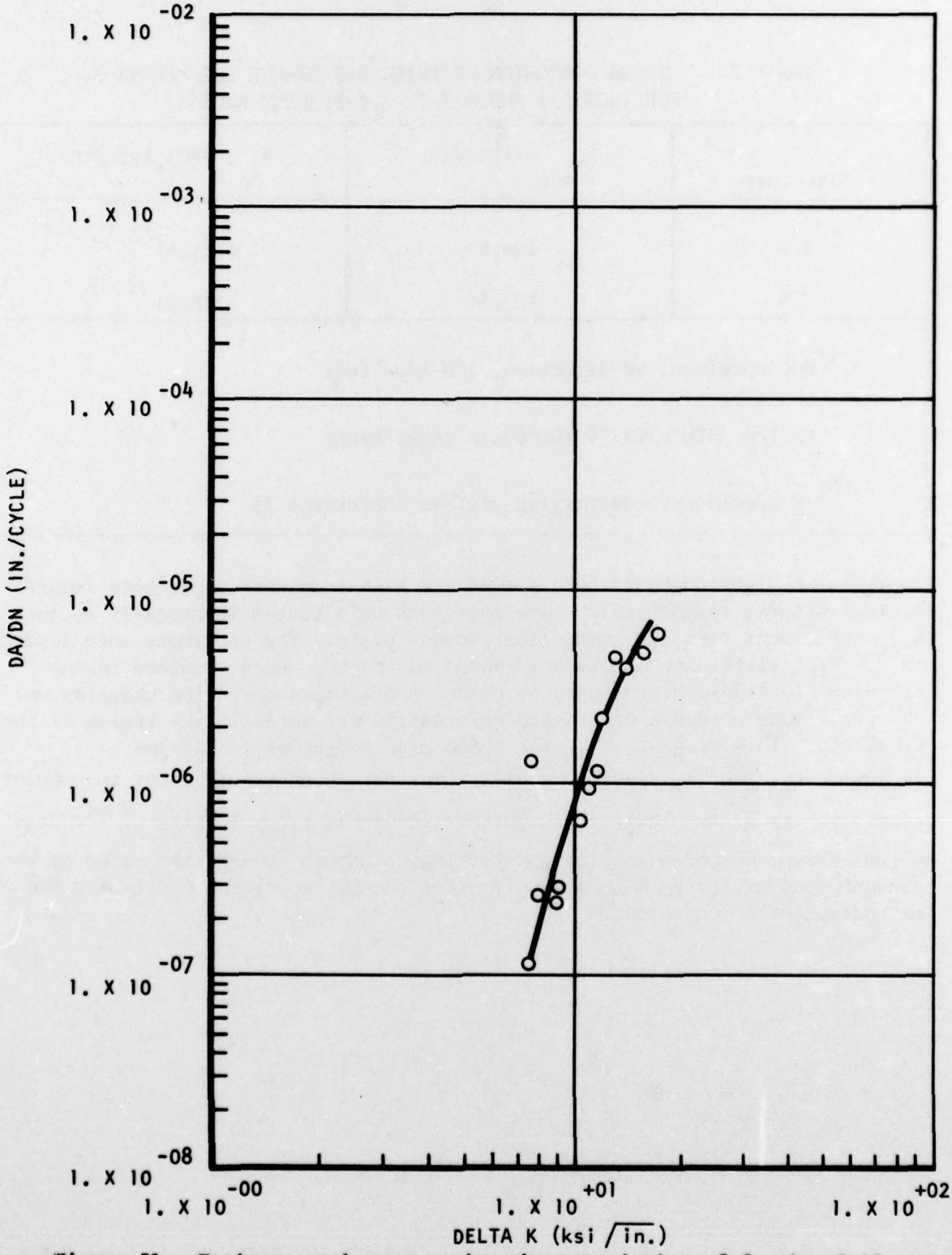

Figure 51. Fatigue crack propagation characteristics of forging 5-12, 5 NRW F-12, CORONA-5, RT, R = 0.08, 600 cpm.

TABLE 27. STRESS CORROSION CRACKING RESISTANCE FOR CORONA-5 FORGINGS 5-1 AND 5-3 IN 3.5-PERCENT NaCl[1]

Structure	$K_{I_{scc}}$, ksi $\sqrt{in.}$	K_{I_c}, (KQ) ksi $\sqrt{in.}$
5-1	106.6	(121.6)[2,3]
5-3	127.5	(148.0)[2,3]

[1] WOL specimen, WR direction, 100-hour test

[2] Failed ASTM E399-74 thickness requirement

[3] TS specimens from forging preform (Reference 3)

represent a high-toughness beta forged and high-toughness alpha-beta forged microstructure, respectively. The specimens were tested identically to the K_{ISCC} specimens from the production process plate. The specimens were loaded to 0.9 K_{IC}; little or no crack advanced was noted. When examined in the scanning electronic microscope, no evidence of stress corrosion cracking was observed; some evidence of plastic deformation was noted in the region of the crack tip. This suggests that for these high toughness conditions (K_{IC}>120 ksi $\sqrt{in.}$), specimen geometry may have been insufficient to prevent extensive crack tip plasticity. Further threshold K_{ISCC} testing of the da/dt versus K-type or corrosion-fatigue testing, although outside the scope of the present program, is recommended to confirm the WOL specimen results for these microstructural conditions.

Section VI

DETAILED TECHNICAL CONCLUSIONS

1. The primary microstructural feature in CORONA-5 contributing to high fracture toughness (namely, high-aspect-ratio lenticular alpha phase formed from the beta matrix) is achieved by several thermomechanical processing routes, including (1) beta annealing followed by a high alpha-beta anneal, (2) beta working followed by a high alpha-beta anneal, and (3) beta working followed by a high alpha-beta anneal plus alpha-beta working followed by a low alpha-beta anneal.

2. Alpha-beta working followed by high alpha-beta annealing tends to globularize the alpha phase, resulting in reduced fracture toughness. A subsequent lower temperature alpha-beta anneal produces lenticular alpha within the intergranular subgrain structure which has the potential of restoring high fracture toughness.

3. Through adjustment in thermomechanical processing, shifts in the strength-toughness trend line are produced to achieve a constant critical crack length equivalent to an alloy exhibiting K_{Ic} = 70 ksi/$\sqrt{in.}$ at 120 ksi TYS. The highest trend line is exhibited by beta finishing followed by alpha-beta annealing.

4. Mathematical expressions have been derived which define both the maximum and minimum times at the annealing temperature, for given amounts of alpha-beta reduction, required for achievement of the desired high-toughness lenticular microstructure in a family of Ti-Mo-Cr-Al alloys.

5. Tensile properties of production-processed CORONA-5 plate met target goals and exhibited good uniformity with respect to test direction.

6. Unnotched axial tension high-cycle fatigue properties of production-processed CORONA-5 plate are significantly higher than Ti-6Al-4V beyond 10^5 cycles. Notched K_t = 3.0 properties are equivalent to Ti-6Al-4V.

7. Fracture toughness of CORONA-5 production-processed plate reflects the influence of both microstructure and tensile strength. Lenticular alpha results in higher toughness, and globular alpha results in the opposite. For a given hot working process, toughness is higher at lower yield strength.

8. The range of fatigue crack propagation data from production-processed plate exceeds the range of values generated from all prior CORONA-5 programs, with slowest growth rates associated with beta-processed and alpha-beta-annealed production plate. The latter also represent the slowest growth rates generated throughout development of the alloy.

9. Stress corrosion cracking resistance of CORONA-5 production-processed plate tested in 3.5 percent NaCl aqueous environment compares favorably with Cond RA Ti-6Al-4V, based on limited data.

10. Optical and SEM metallography confirms the influence of microstructure on fracture toughness and stress corrosion cracking behavior of CORONA-5 production plate.

11. Unnotched axial tension high-cycle fatigue properties of CORONA-5 forgings are significantly higher than Ti-6Al-4V beyond 10^5 cycles at two R factors.

12. Fracture toughness of CORONA-5 forgings reflects the influence of microstructure similar to that seen in production plate; i.e., high toughness associated with lenticular primary alpha, and lower with globular alpha.

13. Fatigue crack propagation test results for CORONA-5 forgings fall on the low side (slow growth rate) of the scatter band for production plate and indicate no dependence upon primary alpha morphology.

Section VII

REFERENCES

1. Berryman, R. G., Froes, F. H., Chesnutt, J. C., Rhodes, C.G., Williams, J. C., and Malone, R. F., Final Engineering Report, Naval Air Systems Command Contract N00019-73-C-0355, "High Toughness Titanium Alloy Development," TFD-74-657, July 1974

2. Berryman, R. G., Froes, F. H., Chesnut, J. C., Rhodes, C. G., Williams, J. C., and Malone, R. F., Final Engineering Report, Naval Air Systems Command Contract N00019-74-C-0273, "High Toughness of Titanium Alloys," TFD-75-640, July 1975

3. Berryman, R. G., Chesnutt, J. C., Froes, F. H., and Rhodes, C. G., Final Engineering Report, Naval Air Systems Command Contract N00019-75-C-0208, "High Toughness Titanium Alloy Development," TFD-76-471, June 1976

4. Hirth, J. P., and Froes, F. H., "Interrelationships Between Fracture Toughness and Other Mechanical Properties in Titanium Alloys," Met. Trans., Vol 8A, p 1165, 1977

5. Seitz, F., Physics of Metals, 1943, McGraw-Hill

6. Holloman, J. H., and Jaffee, L. D., AIME Vol 162, p 223, 1945

7. Nehrenberg, A. E., Steel, Vol 127, p 72, October 1950

8. Larson, F. R., and Miller, I, Jr., Trans ASME, Vol 74, 1952

9. Fisher, J. C., and MacGregor, C. W., Trans ASME, Vol 67, 1945

10. Larson, F. R., and Salmas, V., Trans. ASM, Vol 46, 1954

11. Yolton, C. F., Chesnutt, J. C., Hamilton, C. H., and Froes, F. H., work in progress, 1977-1978

12. Chesnutt, J. C., Rhodes, C. G., Berryman, R. G., Froes, F. H., and Williams, J. C., "The Effect of Microstructure on Fracture of a New High Toughness Titanium Alloy", Fracture, 1977, Vol 2, pp 195-201, 1977

13. Williams, D. P., and Nelson, H. G., Met. Trans, Vol 3, pp 2107-2113, 1972

14. Rockwell International, Los Angeles Division, B-1 Airframe Material Fatigue Design Properties Manual

15. MCIC-HB-01, Damage Tolerant Design Handbook, Part 1, MCIC, Battelle Columbus Laboratories, December 1972